DESIGN AND IMPLEMENTATION OF A VOLTAGE SOURCE CONVERTER BASED HYBRID ACTIVE POWER FILTER

A THESIS SUBMITTED TO
THE GRADUATE SCHOOL OF NATURAL AND APPLIED SCIENCES
OF
MIDDLE EAST TECHNICAL UNIVERSITY

BY

ONUR UÇAK

IN PARTIAL FULFILLMENT OF THE REQUIREMENTS
FOR
THE DEGREE OF MASTER OF SCIENCE
IN
ELECTRICAL AND ELECTRONICS ENGINEERING

SEPTEMBER 2009

Approval of the thesis:

DESIGN AND IMPLEMENTATION OF A VOLTAGE SOURCE CONVERTER BASED HYBRID ACTIVE POWER FILTER

submitted by **ONUR UÇAK** in partial fulfillment of the requirements for the degree of **Master of Science in Electrical and Electronics Engineering Department, Middle East Technical University** by,

Prof. Dr. Canan Özgen _____
Dean, Graduate School of **Natural and Applied Sciences**

Prof. Dr. İsmet Erkmen _____
Head of Department, **Electrical and Electronics Engineering**

Prof. Dr. Muammer Ermiş _____
Supervisor, **Electrical and Electronics Engineering Dept., METU**

Prof. Dr. Işık Çadırcı _____
Co-Supervisor, **Electrical and Electronics Engineering Dept., Hacettepe University**

Examining Committee Members:

Prof. Dr. H. Bülent Ertan _____
Electrical and Electronics Engineering Dept., METU

Prof. Dr. Muammer Ermiş _____
Electrical and Electronics Engineering Dept., METU

Prof. Dr. Aydın Ersak _____
Electrical and Electronics Engineering Dept., METU

Assist. Prof. Dr. Ahmet M. Hava _____
Electrical and Electronics Engineering Dept., METU

Dr. Faruk Bilgin _____
TÜBİTAK-UZAY

Date: September 10, 2009

I hereby declare that all information in this document has been obtained and presented in accordance with academic rules and ethical conduct. I also declare that, as required by these rules and conduct, I have fully cited and referenced all material and results that are not original to this work.

Name, Last name : Onur UÇAK

Signature :

ABSTRACT

DESIGN and IMPLEMENTATION OF A VOLTAGE SOURCE CONVERTER BASED HYBRID ACTIVE POWER FILTER

Uçak, Onur

M.S., Department of Electrical and Electronics Engineering

Supervisor : Prof. Dr. Muammer Ermiş

Co-Supervisor : Prof. Dr. Işık Çadırcı

September 2009, 139 pages

This research work is devoted to the analysis, design and implementation of a shunt connected Hybrid Active Power Filter by the use of a lower rated voltage source PWM converter, and a series connected LC passive filter. In recent years, voltage and current harmonics have become a serious problem both in transmission and distribution systems, due to the widespread usage of non-linear loads such as diode/thyristor rectifiers, electric arc furnaces and motor drives. In order to obtain a better performance than those of the conventional passive filter solutions, active power filters (APF) have been worked on and developed. Among various configurations listed in the literature, conventional shunt connected voltage source active power filter is widely used in industrial applications. Unfortunately, for large power applications, the losses and the rating of the APF increase considerably. As a result, various hybrid filter topologies have been developed which combine the advantages of both passive and active filters.

In this thesis, a shunt connected hybrid active power filter is developed by combining a 4.7 kVA voltage source converter and a 30kVAR 7^{th} harmonic passive filter. The developed system has been implemented to eliminate the most dominant 5^{th}, 7^{th} and

11^{th} current harmonic components existing at 400V low voltage bus of TÜBİTAK-SPACE Technologies Institute. The theoretical and experimental results have shown that the DC link voltage of the converter and the rating of APF are minimized while keeping the filtering performance satisfactory.

Keywords: Active Power Filter, Hybrid Power Filter, Passive Filter, Voltage Source Converter, Current Harmonic

ÖZ

GERİLİM KAYNAKLI ÇEVİRGEÇ TABANLI MELEZ AKTİF GÜÇ FİLTRESİ TASARIMI VE UYGULAMASI

Uçak, Onur
Yüksek Lisans, Elektrik ve Elektronik Mühendisliği Bölümü
Tez Yöneticisi : Prof. Dr. Muammer Ermiş
Ortak Tez Yöneticisi : Prof. Dr. Işık Çadırcı

Eylül 2009, 139 sayfa

Bu araştırma çalışması, düşük anma değerli 3 faz gerilim kaynaklı çevirgeç ve seri pasif filtre bağlantısı ile oluşturulan şönt bağlı melez aktif güç filtresi, tasarımı ve uygulanmasına hasredilmektedir. Son yıllarda, diyot/tristör doğrultucular, ark ocakları ve motor sürücüler gibi doğrusal olmayan yüklerin yaygın kullanımı, gerilim ve akım harmoniklerinin dağıtım ve iletim sistemlerinde önemli bir problem haline gelmesine neden olmaktadır. Geleneksel pasif filtre çözümünün beraberinde getirdiği dezavantajları ortadan kaldırmak için aktif güç filtreleri (AGF) üzerinde çalışılmış ve geliştirilmiştir. Literatürde farklı topolojileri belirtilen AGF'ler arasında, şönt bağlı gerilim kaynaklı AGF'ler endüstriyel uygulamalarda kullanımı en yaygın olan yapı olarak göze çarpmaktadır. Ancak yüksek güç uygulamalarında, çevirgeç anma değeri ve kayıplar önemli ölçüde artmaktadır. Bu nedenle geleneksel aktif güç filtrelerini, pasif filtreler ile birleştiren ve her iki yapının da avantajlarını barındıran melez filtre yapıları geliştirilmiştir.

Bu tezde, 4.7 kVA anma değerli 3 faz gerilim kaynaklı çevirgeç ve 7inci harmoniğe ayarlı 30kVAR kapasitesindeki seri pasif filtre bağlantısı ile şönt bağlı melez aktif güç filtresi oluşturulmaktadır. Geliştirilen şönt bağlı melez filtre, TÜBİTAK-UZAY Teknolojileri Enstitüsünde 400V alçak gerilim seviyesinde mevcut olarak gözlemlenen, en baskın 5inci, 7inci ve 11inci akım harmoniklerini süzmek amacıyla uygulanmaktadır. Gerilim kaynaklı çevirgecin DA bağ geriliminin ve anma değerinin düşük seviyelerde tutularak filtre performansının tatmin edici seviyelerde olduğu benzetim çalışmaları ve deneysel sonuçlarla gösterilmektedir.

Anahtar Kelimeler: Aktif Güç Filtre, Melez Aktif Güç Filtre, Pasif Filtre , Gerilim Kaynaklı Çevirgeç, Akım Harmoniği

To My Wife

ACKNOWLEDGEMENTS

I would like to express my deepest gratitude and sincerest respects to my supervisor Prof. Dr. Muammer Ermiş for his guidance, advice, criticism, encouragements and insight throughout this research.

I would like to show my gratitude also to my co-supervisor Prof. Dr. Işık Çadırcı for her guidance, advice, criticism, encouragements and insight throughout this research.

I would like to express my special thanks to Alper Terciyanlı for his brilliant suggestions and contributions. His encouragement and continuous trust in me is the main reason for the success of this research work.

I would also like to acknowledge that, this study is fully supported by the Public Research Grant Committee (KAMAG) of TÜBİTAK within the scope of the National Power Quality Project (105G129).

I wish to express my special thanks to İlker Kocabaş for sharing his knowledge and experience on digital signal processors.

I would also like to thank my colleagues Tülay Avcı and Murat Göl for their support and contributions during my study.

Special appreciation goes to Faruk Bilgin, Adnan Açık and Nadir Köse for sharing their knowledge and valuable times with me during my studies.

Special thanks to Erinç Altıntaş and Özgür Ünsar, mobile power quality measurement team members of National Power Quality Project of Turkey

(ProjectNo: 105G129), in obtaining the electrical characteristics and power quality of TÜBİTAK-UZAY by field measurements.

The assistance of the valuable staff in Power Electronics Group of TÜBİTAK-UZAY is gratefully acknowledged. I am especially thankful to Mustafa Kılınç and Cihan Yavuz for their substantial technical assistance and companionship during installation of the laboratory prototype. I am also thankful to Seda Karatekin for her contribution to the pcb design.

I would like to express my deepest gratitude to my family, Hüseyin, Letafet and Ece Uçak for their unlimited support throughout my life. I also express my sincerest thanks to my family Recep, Zehra and Seren Kankılıç for their continuous morale support.

Finally and foremost, I would like to thank my lovely wife for her presence, patience and endless support during this heavy work.

TABLE OF CONTENTS

LIST OF TABLES

TABLES

LIST OF FIGURES

FIGURES

CHAPTER 1

INTRODUCTION

In recent years, improvements in power electronics devices and semi-conductor technology have increased the usage of non-linear loads. Widespread use of non-linear loads deteriorates the quality of power in both transmission and distribution systems. The ideal power quality is defined by electrical power energy with pure sinusoidal supply voltage waveform at a constant frequency and a specified constant magnitude [1]. Nowadays, the power quality is not only defined by the continuity of electricity but also characterized by its main parameters. The frequency and magnitude of the supply voltage, current and voltage harmonics, voltage sags, voltage swells, flicker and phase imbalances are the main parameters of the power quality [2]. In today's environment, electronic loads are very sensitive to harmonics, sags, swells and other disturbances. So, power quality has become as important as the continuity of the electricity.

Among these parameters, current and voltage harmonics have become a growing power quality concern when the undesirable effects on both utility and customer electronic equipments are considered. Arc furnaces, converters, adjustable speed drives, static VAR compensators, cylcloconverters, switch mode power supplies and PWM modulated drives are some of the non-linear loads that generate harmonics. Voltage distortion, excessive neutral return currents, reduction in equipment lifetime and overheating of cables, motors and transformers are some of the adverse effects of harmonics injected by these non-linear loads.

In order to overcome the harmonic related problems, passive filters consisting of capacitors, inductors and damping resistors have been used for a long time. However,

installing conventional passive harmonic filters provide limited solutions to many power quality problems. Moreover, the risk of the resonance with supply impedance of the passive filters has increased the attention to active solutions. As a result, active power filters in various topologies have been studied and reported in the literature [3].

1.1 Definition of Harmonic Problems

Electrical loads, drawing sinusoidal current from a sinusoidal voltage source, are called as linear loads. They consist of only resistive (R), inductive (L) and capacitive (C) passive elements. Whereas, non-linear loads draw non-sinusoidal current waveform, although they are fed from a sinusoidal voltage source. In order to indicate the undesirable effects and severity of these non-sinusoidal signals, harmonic terminology was introduced by Institute of Electrical and Electronics Engineers (IEEE) in 1981 for these non-sinusoidal signals which can be represented as the sum of the sinusoidal signals in different frequencies by Fourier series. According to IEEE Std. 519 [2] reported in 1981, "A sinusoidal component of a periodic wave or quantity having a frequency that is an integral multiple of the fundamental frequency is defined as harmonic".

The increase in the usage of non-linear loads which contain semiconductor switching devices, has resulted in distorted current and voltage waveforms at the point of common coupling (PCC) of industrial loads. Some of the most commonly used non-linear loads and the current drawn from the AC mains are shown below. In Fig 1.1, a single phase rectifier with smoothing capacitor which supplies most of the single phase devices (computers, printers, fluorescents, etc.) is indicated. The sharp rising and falling of line current introduces considerable amount of odd harmonics into the system.

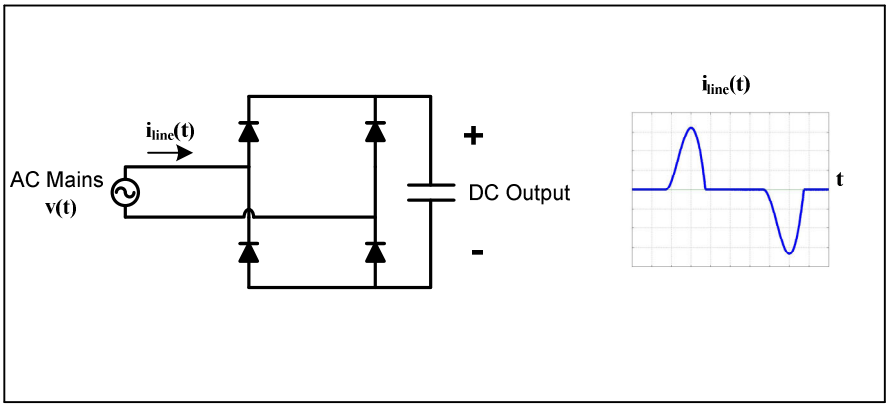

Fig 1.1 Single Phase Rectifier (with Smoothing Capacitor)

Moreover, six-pulse controlled or uncontrolled rectifiers are commonly used in AC/DC drives and Uninterruptable Power Supply (UPS) applications. Fig 1.2 and Fig 1.3 shows a six-pulse diode rectifier with a smoothing inductor and capacitor with their distorted current waveforms. The distorted current introduces harmonics of the order 5^{th}, 7^{th}, 11^{th}, 13^{th} and so on.

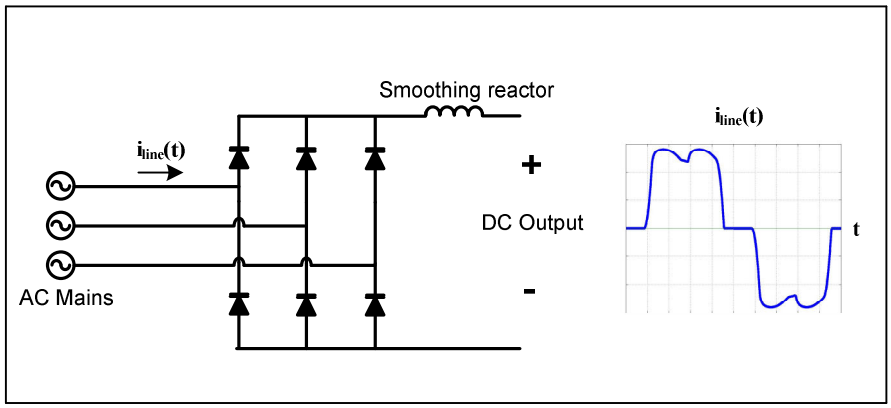

Fig 1.2 Three Phase Diode Rectifier (with Smoothing Reactor)

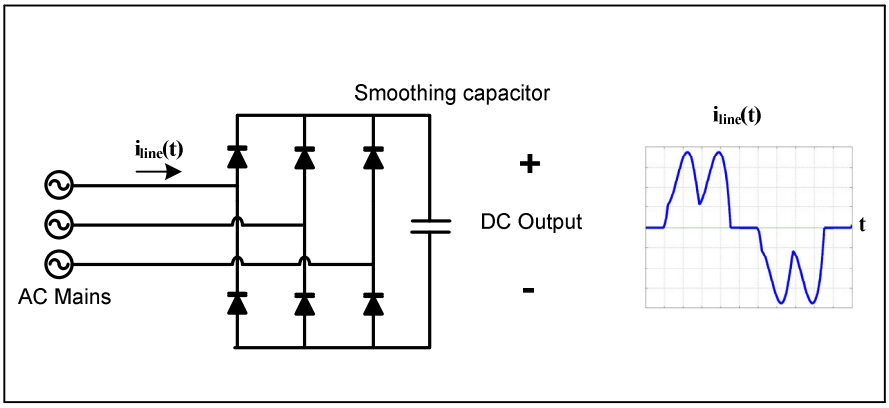

Fig 1.3 Three Phase Diode Rectifier (with Smoothing Capacitor)

In the vicinity of a distorted current produced by a non-linear load, the utility voltage is also distorted as the harmonic current interacts with the system impedance. The distortion in the utility voltage also affects the other loads which are connected to the same bus. However, other than the utility voltage distortion at PCC, harmonic pollution introduces a number of problems such as excessive losses on transformers and conductors, malfunctioning of electrical devices and power system equipments, over current/voltage problem due to resonance, over current at neutral conductors and interferences in communication systems [1].

Transformer losses are composed of core loss and winding losses. Core losses are formed by the magnetic flux when the transformer is excited by the terminal voltage. In fact, voltage harmonics are not a great concern for the core losses since the flux magnitude is inversely proportional with the harmonic order and in most power systems voltage harmonics are small enough when compared to fundamental component of the bus voltage [4]. However, winding losses, including eddy current and stray losses, are directly affected by the current passing through the transformer. Eddy current losses are directly proportional to the square of the harmonic order. Therefore, current harmonics result in additional losses and overheating on transformers which may cause electrical insulation failure and reduction in expected life time of the equipment [5].

Additional losses and overheating problems are also experienced by power cables of an electrical system due to the skin effect. If the cable is subjected to a current waveform with high frequency harmonics, the AC resistance of conductors increases with frequency, thus raising the I^2R losses. Moreover, unexpected trips on circuit breakers, malfunctioning of devices using utility voltage as reference, faulty readings of kWh meters and the telephone interference in communication systems are the common problems observed in the presence of the harmonics.

Hence, in order to set some practical limitations about harmonics and to offer some recommendations, a standard named [2] "Guide for Harmonic Control and Reactive Power Compensation of Static Power Converters" was revealed in 1981 by IEEE society. After the adverse effects of non linear loads on neighborhood loads had been discovered, in 1992 the standard was revised and updated [1]. The severity of the harmonic magnitude is indicated by some quantities such as harmonic factor (HF), Total Harmonic Distortion (THD), Total Demand Distortion (TDD).

Harmonic factor which is valid for both current and voltage is the ratio of the root sum square value of all harmonics to the root mean square value of the fundamental (1.1). It is also called as distortion factor (DF). Moreover, another quantity called Total Harmonic Distortion (THD) has been used in low-voltage, medium-voltage and high-voltage systems to extinguish the distortion factor of a voltage or a current waveform (1.2).

$$Harmonic\,Factor\,(Voltage)=\frac{\sqrt{\sum_{h=2}^{\infty}(V_h^{\,2})}}{V_1}$$
$$Harmonic\,Factor\,(Current)=\frac{\sqrt{\sum_{h=2}^{\infty}(I_h^{\,2})}}{I_1} \qquad (1.1)$$

$$Total\ Harmonic\ Distortion\ (THD_F) = \frac{\sqrt{\sum_{h=2}^{50}(V_h^2)}}{V_1} x100\ \% \tag{1.2}$$

V_1 : *RMS value of the fundamental voltage component*
I_1 : *RMS value of the fundamental current component*
V_h : *Amplitude of the voltage harmonic component of order* "h"
I_h : *Amplitude of the current harmonic component of order* "h"

Another THD definition different from statement (1.2) is used by Canadian Standards Association (CSA) and International Electrotechnical Commission (IEC) [6]. It defines the THD as a percentage of total RMS including the rms values of all harmonics (1.3).

$$Total\ Harmonic\ Distortion\ (THD_R) = \frac{\sqrt{\sum_{h=2}^{50}(V_h^2)}}{V_{RMS}} x100\ \%$$
$$V_{RMS} = \sqrt{\sum_{h=1}^{50} V_{hRMS}^2} \tag{1.3}$$

V_{RMS} : *Total RMS value*
V_{hRMS} : *Amplitude of the harmonic component of order* "h"

Table 1.1 shows the voltage distortion limit values recommended by IEEE 519-1992 at the point of common coupling (PCC). While the voltage distortion limitations are based on THD values, the current distortion limitations are based on a different variable as Total Demand Distortion (TDD) which is defined in (1.4).

$$Total\ Demand\ Distortion\ (TDD) = \frac{\sqrt{\sum_{h=2}^{50}(I_h^2)}}{I_L} x100\ \% \tag{1.4}$$

I_L : *Maximum demand load current*
I_h : *Amplitude of the harmonic current of order* "h"

Table 1.1 Voltage Distortion Limits

Bus Voltage at PCC	**Individual Voltage Distortion (%)**	**Total Voltage Distortion THD (%)**
69kV and below	3.0	5
69.001kV through 161kV	1.5	2.5
161kV and above	1	1.5
Note: High Voltage systems can have up to 2.0% THD where the cause is an HVDC terminal that will attenuate by the time it is tapped for a user		

The TDD limit defines how much a load can allocate the utility resource in terms of harmonic current, and it is directly proportional with the size of the load with respect to the capacity of the utility at PCC. The capacity of the utility is defined by the short circuit current I_{sc} at PCC, and the size of the load is the maximum demand load current calculated by the average of the last twelve monthly peak demand. Therefore, the load can inject harmonic current to the utility at higher percentages as the size of the load decreases with respect to the capacity of the system. In Table 1.2, current distortion limits for general distribution systems are shown [1].

The limitations on these quantities cover both the individual customers and the utility, to prevent a single user or a group of users connected to the same bus. In the light of the recommendations and limitations of IEEE Std. 519-1992, regulations about harmonics at different voltage levels were also announced by the Ministry of Energy and the Energy Market Regularity Authority (EMRA) in Turkey [7, 8].

Table 1.2 Current Distortion Limits for General Distribution Systems (120V through 69kV)

Individual Harmonic Order (Odd Harmonics), h						
I_{sc}/ I_L	Max. Harmonic Current Distortion for h					**TDD**
	h<11	**11≤h<17**	**17≤h<23**	**23≤h<35**	**35≤h**	
Below 20	4.0	2	1.5	0.6	0.3	5.0
Between 20-50	7.0	3.5	2.5	1.0	0.5	8.0
Between 50-100	10.0	4.5	4.0	1.5	0.7	12.0
Between 100-1000	12.0	5.5	5.0	2.0	1.0	15.0
Above 1000	15.0	7.0	6.0	2.5	1.4	20.0
Even Harmonics are limited to 25% of the odd harmonics limit above						
Current distortions that result in a dc offset, e.g., half wave converters, are not allowed						
* All power generation equipment is limited to these values of current distortion, regardless of actual I_{sc}/ I_L						
I_{sc}= Maximum short circuit current at PCC, I_L= Maximum demand load current (fundamental frequency component) at PCC						

1.2 Harmonic Mitigation Techniques

A number of solutions exist to reduce the undesirable effects of harmonics. The most common and the conventional method is installing passive harmonic filters to remove harmonic currents which present a low cost solution. However, passive filter implementations to filter out the harmonics have the following disadvantages:

- Possibility of resonances with the source impedance
- Supply impedance dependent system performance
- Fixed compensation characteristic and upgrade difficulty

Although enhancements in semiconductor device technology have led to an increase in the usage of modern harmonic polluter loads, they have also provided reliable solutions. In order to overcome the problems associated with traditional passive filters, active power filters (APF) have been worked on and developed in recent years in conjunction with the improvement in semiconductor switches. In this part, firstly traditional method of harmonic filtering is briefly discussed. Then, active power filter history, the basic operation principle of APFs and the classification in the literature are highlighted. Finally, the hybrid active power filter topology which is the main concern of this thesis is introduced.

1.2.1 Passive Filters

In order to solve the current harmonic related problems, passive filters consisting of capacitors, inductors and damping resistors have been used for a long time. They are used as either to inject a series high impedance to block the harmonic currents, or to create a shunt low impedance path to divert the harmonic currents path. So, passive filters are installed either in shunt connection or series connection. While shunt connected passive filters carry only a fraction of line current, series filters are subjected to full line current. Moreover, the reactive power compensation capability of shunt connected passive filters and the lower installation cost of shunt filters make series passive filters non preferable.

The shunt connected passive filters are classified as band-pass, high pass and C-type filters. Among these types, low pass and high pass filters are the most common types due to their design simplicity and low cost [9]. In Fig 1.4 most common types of shunt passive filters and their circuit configuration is represented.

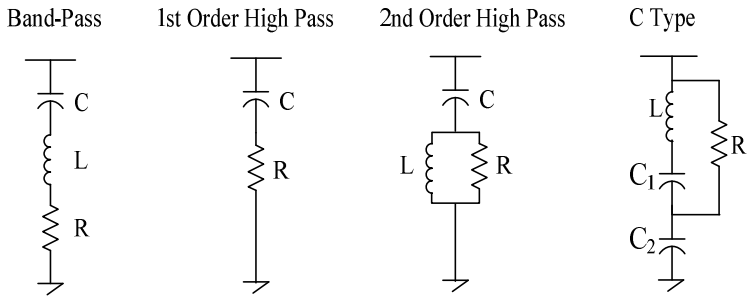

Fig 1.4 Shunt Passive Filters

One of the most commonly filter type used in industry for harmonic suppression is band-pass filters. Although sufficiently low impedance is obtained at a specific frequency, characteristics of the filter may considerably change with system parameters. A parallel resonance occurs at frequencies lower than the tuned frequency. As a result, undesirable harmonic currents can be magnified which decreases the performance of the overall system [10]. The impedance of a single tuned filter represented in Fig 1.4 is calculated as follows:

$$Z_{filter} = R + j\left[wL - 1/(wC)\right] \tag{1.5}$$

Tuning frequency of the filter is defined by the w that results in a zero imaginary part in (1.5). So the tuning frequency (f_{tuned}) of the filter is given in (1.6).

$$f_{tuned} = \frac{1}{2(\pi)(\sqrt{LC})} \tag{1.6}$$

The initial step for designing a single tuned filter is defining the size of the capacitor with a reasonable power factor at the operating line voltage. In (1.7), "kVAR filter" represents the reactive power capacity of the filter and V_{LL} represents the line to line rated voltage of the filter. Once the size of the capacitor is defined with a reasonable power factor at the operating line voltage, the reactance value can be calculated by (1.7).

$$X_c = \frac{V_{LL}^{\ 2}}{\text{kVAR filter}} \tag{1.7}$$

Another parameter included in the filter design is the quality factor (Q) which defines the sharpness of the filter [9]. The mathematical representation of quality factor given in (1.8) shows that the resistance value of the filter is based on Q value. Generally quality factor term is not adjusted to change the filtering characteristic because of the considerable increase in losses [10]. As a result, resistance value is chosen to be the internal resistance value of the filter reactor. Finally, the parallel resonance frequency which occurs lower than the tuning frequency is given by (1.9) where L_s is the corresponding inductance of the source. The frequency response of a typical band-pass filter tuned at 237 Hz is given in Fig 1.5 to clarify the parallel resonance risk phenomenon.

$$Q = \frac{\sqrt{LC}}{R} \tag{1.8}$$

$$f_{resonance} = \frac{1}{2\pi}\sqrt{\frac{1}{(L_s + L)\,C}} \tag{1.9}$$

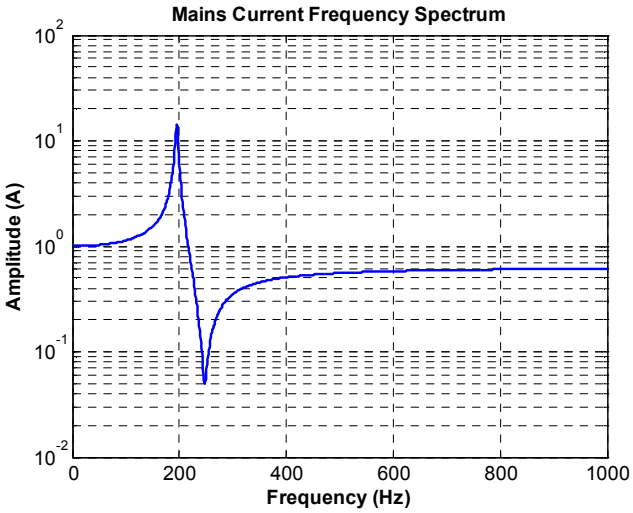

Fig 1.5 Typical Response of a Band-Pass Filter

Another most commonly used filter type for harmonic suppression is high pass filters. They provide low impedance above a corner frequency. However, the impedance obtained with a high pass filter in its passband can not be as low as an impedance value obtained by a single tuned filter at its tuned frequency. The harmonics of a system can be reduced with a definite percentage above the corner frequency but large rating of the filter results in high losses at fundamental frequency. First order high pass filters represented in Fig 1.4 shows higher losses at fundamental frequency, so first order type high pass filters are rarely used. In opposite to this, second order high pass filters show less losses at fundamental frequency when compared with the first order types. Although third order type filters are the most effective form in the loss performance, their filtering performance is inferior to that of the second order types.

There exist also C-type filter which is a variation of high pass filter, where the inductance L is replaced with a series LC circuit tuned at fundamental frequency (Fig 1.4). So, the resonant LC circuit bypasses the resistance at fundamental frequency thus reduces the losses. C-type filters are generally applied for compensating arc furnaces and cyclo converters.

Although passive filters have been used for harmonic related problems due to their installation simplicity, low cost and efficiency, there are some limitations, restrictions and undesirable effects on the overall system performance as stated below [11]:

- The system performance is greatly dependent on the supply impedance. Once passive filters are installed, it is not so easy to change their corner frequency or size in the vicinity of change in system conditions.
- Resonance may occur between the source impedance and the filter impedance which results in amplification of harmonics.
- Passive filters have fixed compensation characteristics.

- Aging, deterioration and temperature effects may change the tolerances of the filter components. Therefore, passive filters may result in detuning problem.

As a result, the preceding disadvantages of passive filters have increased the attention on active power filter solutions.

1.2.2 Active Power Filters

1.2.2.1 History of APFs

The concept of the Active Power Filter and its operation principles were firstly introduced by H. Sasaki and T. Machida in 1970s [12]. In 1982, an 800 kVA current source inverter based active power filter was implemented by using GTO thyristors for the first time in the world [13, 14]. For the proceeding 20 years, the control strategies of active power filters have been developed [15].

In the early stages of APF implementations, generally power MOSFETs and GTOs were utilized. However, the real improvement in APF technology has appeared with the introduction of insulated gate bipolar transistors (IGBTs). Moreover the progress in digital signal processors (DSPs), field programmable gate arrays (FPGAs) and availability of Hall Effect sensors and isolation amplifiers at low cost have forced researchers and designers to develop efficient control strategies for the APFs to solve harmonic related problems in the utility and industrial power systems.

The operation principle of APFs is basically canceling the distorting harmonic currents by measuring them and generating a harmonic current spectrum in opposite phase to the measured current. As shown in Fig 1.6, the parallel active power filter is considered as a current source injecting harmonic current into the ac system with the same amplitude and in anti-phase that of the load current to obtain an undistorted sinusoidal source current.

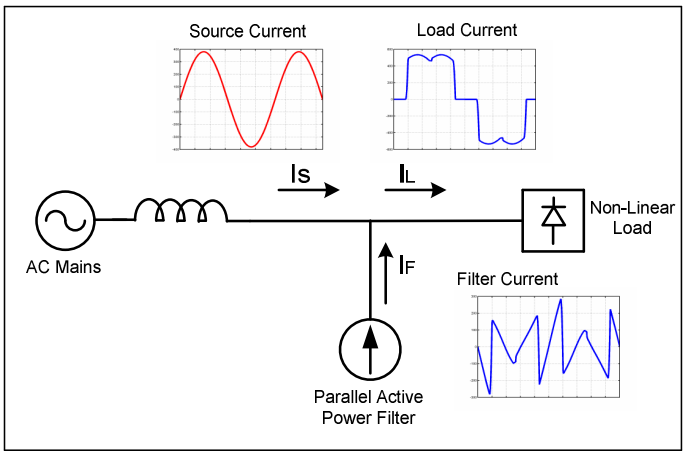

Fig 1.6 Main Principle of Active Filtering

The compensation currents are generated via a pulse width modulated (PWM) converter including a DC link energy storage element (DC Link Capacitor or DC Link Inductor) depending on the employed converter type. No additional DC supply is required for the DC link side; because a small amount of current at fundamental frequency is drawn from the supply to meet the APF losses so that the DC link voltage or current is kept constant. In addition to their basic principle of harmonic current compensation, active power filters are also used for elimination of voltage harmonics, reactive power compensation and load balancing depending on the type of the APF. There exist several active power filter types in the literature in accordance with their converter types, circuit topologies and number of phases [3].

1.2.2.2 Classification of Active Power Filters

Active power filters are divided into two groups according to their converter types used in the development of the power circuit, as Current Source Converter (CSC) and Voltage Source Converter (VSC) type active power filters. The main difference between these two topologies is the energy storage element at the DC link side of the converter.

In CSC type APF, the power circuit acts as a non sinusoidal current source with a DC link inductor (L_{dc}) as an energy storage element (Fig 1.7). The converter is formed by six controllable semiconductor switches and series diodes to each switch, in order to obtain reverse voltage blocking capability. The connection of APF to the AC mains side is made by a second order low pass filter formed by L_f and C_f. The second order filter suppresses the high frequency switching ripples formed by APF. However, it amplifies the harmonic contents around the resonance frequency of the filter. In order to damp the amplification due to the second order low pass filter, an appropriate current control method or damping resistors are used for CSC based APFs [16].

In VSC type APF, the power circuit has a DC link capacitor (Cdc) as an energy storage element (Fig 1.7) The inverter consists of six controllable semiconductor switches each of which should support the maximum filter current injected to the mains side. The APF is connected to the mains side through a filter inductor (Lf) to provide the controllability of active power filter current. The filter inductor also acts as a first order passive filter to suppress high frequency ripples generated by the converter.

For both type of APFs, the practical solution for the controllable semiconductor device selection is, choosing an insulated gate bipolar transistor (IGBT) which is superior to GTOs and MOSFETs if the allowable switching frequency, conduction/switching losses and power ranges of these devices are considered together. However, available IGBT modules, which are always fabricated with their antiparalel diodes in the market, are more convenient for voltage source type active power filters [17, 18]. Therefore, for current source converter topology additional series diodes are required to obtain a reverse voltage blocking capability which increases the cost, size and design level of the CSC type APFs. Moreover, using a reactor as a storage element at the DC link side, results in higher losses compared to voltage source converter type APFs [19]. Although CSC type active power filters present direct current control capability, high reliability and fast response, voltage source type active power filters have become more popular and preferable in

industrial applications due to their small size, lower initial cost and higher efficiencies.

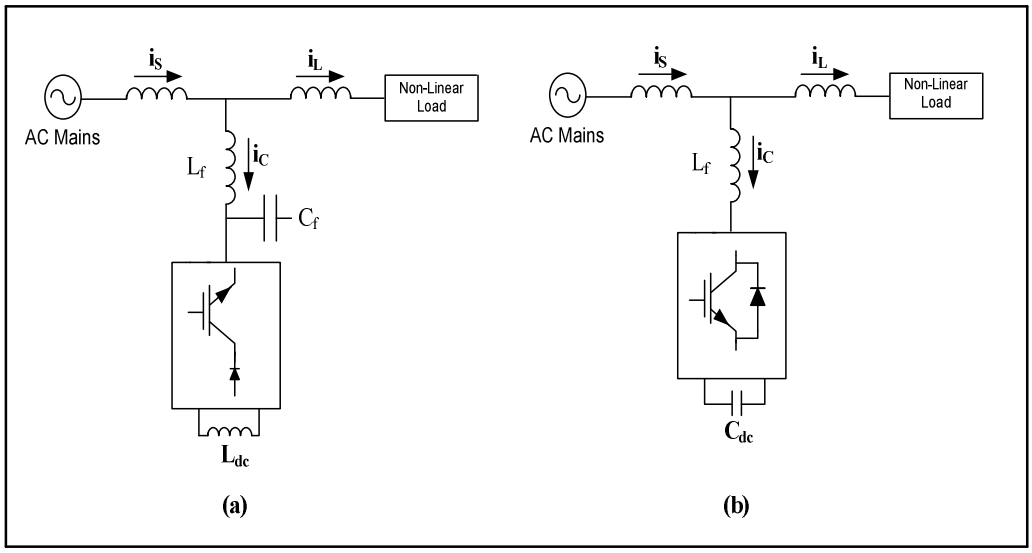

Fig 1.7 APF Converter Classification
(a) Current Source Converter type APF (b) Voltage Source Converter type APF

Active power filters are also classified as shunt (parallel) APF, series APF, unified power quality conditioners (UPQC) and hybrid filters according to their topologies [13]. Shunt APFs are widely used for eliminating load current harmonics and reactive power compensation. Both of the filters represented in Fig 1.7 are shunt active power filters.

Fig 1.8 shows the connection of a series APF which is usually used for eliminating voltage harmonics and regulating voltage at the load or line terminal [20]. The operation principle is the dual of the shunt connected active power filters (Fig 1.6). In this case, APF injects a voltage term (V_{AF}) in series with the utility voltage to operate as a harmonic isolator between the load and utility or to operate as a voltage regulator (Fig 1.9). Moreover, in many cases series active power filters are combined with shunt passive filters in order to decrease the rated power of the APF [21].

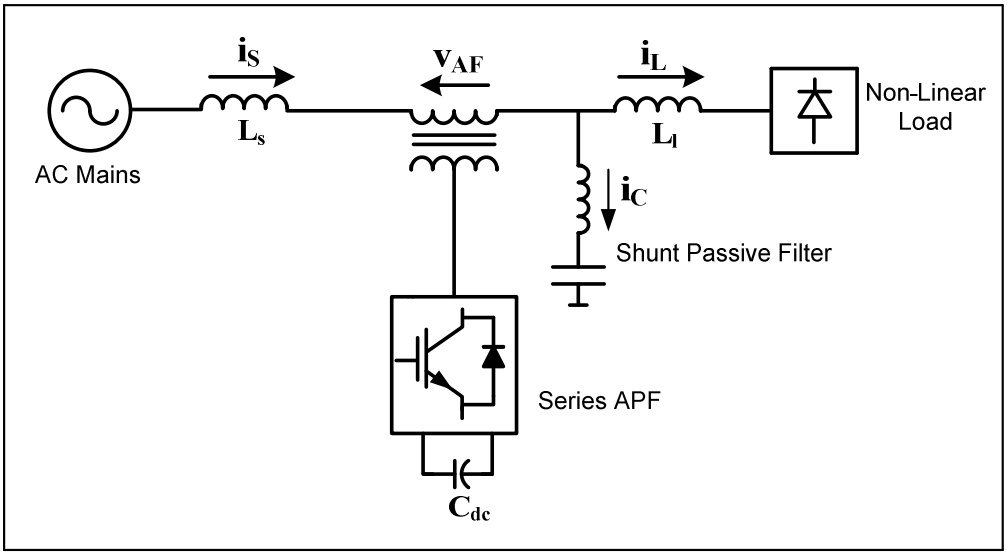

Fig 1.8 Series Active Power Filter

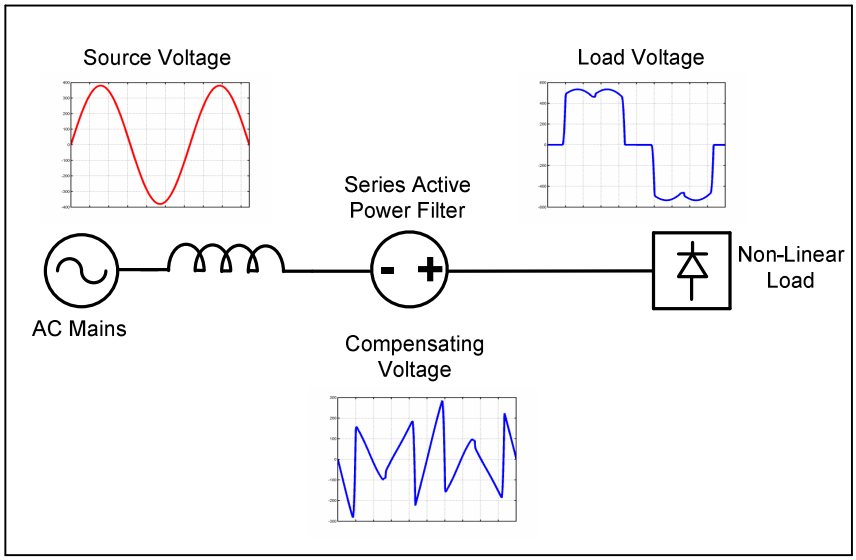

Fig 1.9 Operation Principle of Series APF

Another type of APF which combine the series and shunt active filters is developed as unified power quality conditioners (UPQC). As indicated in Fig 1.10**,** the shunt connected part is located at the load side and the series part is located at the source

side. Since the topology is the combination of a series APF and shunt APF with a common DC link, it can perform voltage harmonic filtering, voltage regulation as well as current harmonic filtering and reactive power compensation. Although UPQC is an ideal solution for most of the power quality problems, the complexity of their control strategies and the higher cost of their power stages confines their applications.

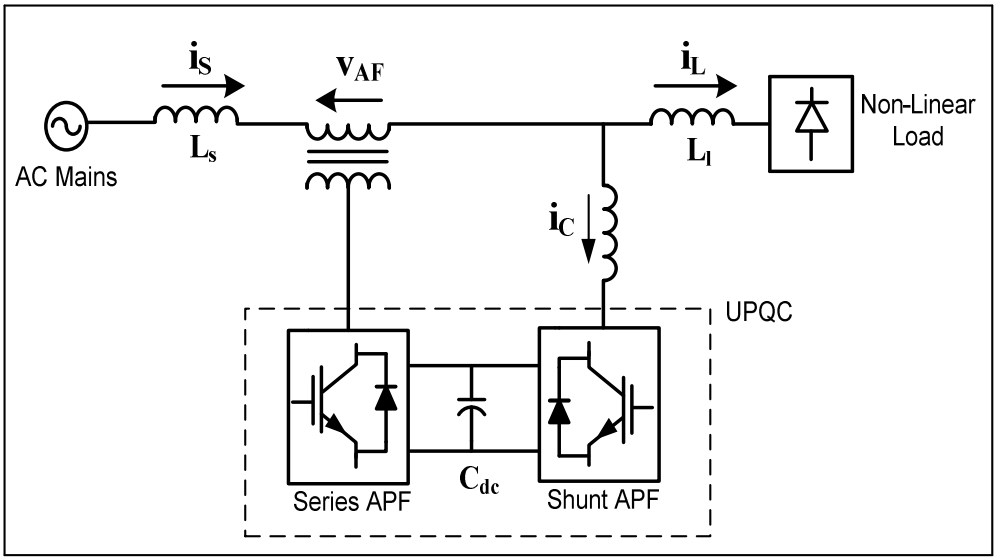

Fig 1.10 Unified Power Quality Conditioner

Adjustable speed drives (ASDs), uninterruptible power supplies (UPSs) are some of the non linear loads connected to three wire supply systems. However, there are many non linear single phase loads fed from a single phase or three phase four wire supply systems such as computers and commercial lighting. So, it is not amazing to classify APFs according to supply or the load system. As a result, APFs can be grouped as two-wire, three-wire and four-wire according to their number of phases [3]. According to the load conditions of the system, an appropriate APF topology should be selected to overcome the harmonic related power quality problems. For instance: an excessive amount of single phase loads, supplied from a three phase

supply with neutral conductor, will result in over current in neutral conductor, harmonic and unbalance. In order to diminish these problems, four-wire APFs should be adopted.

Among these topologies described above, shunt connected voltage source Active Power Filters have been mostly developed and put into practical usage on the market. Toshiba [22], ABB [23], Fuji [24] are some of the companies which offer APF products rated from 10kVA to several MVAs [25].

1.2.3 Hybrid Power Filters

Although an increased attention has been paid to the active power filters, some problems about APFs have also been discovered as the active power filters are put into practical usage. For large power applications, it is difficult to implement a low loss and a low cost PWM converter. Moreover, currents injected by APF may be absorbed by passive filters which are previously installed into the AC system. As a result, various hybrid filter topologies which combine the traditional harmonic filtering method of passive filters, and active power filters have been developed**.**

In 1988, a series active filter connected via a matching transformer was combined with a shunt connected passive filters (Fig 1.11). In this topology active power filter does not compensate the load harmonic content but it operates as a harmonic isolator between the source and the load [26]. So, performing as an isolator instead of performing a full compensation reduces the rating of the series active filter. However, in this topology the protection of the APF is crucial as it is connected to the supply in series. The series connection of APF decreases the reliability of this topology.

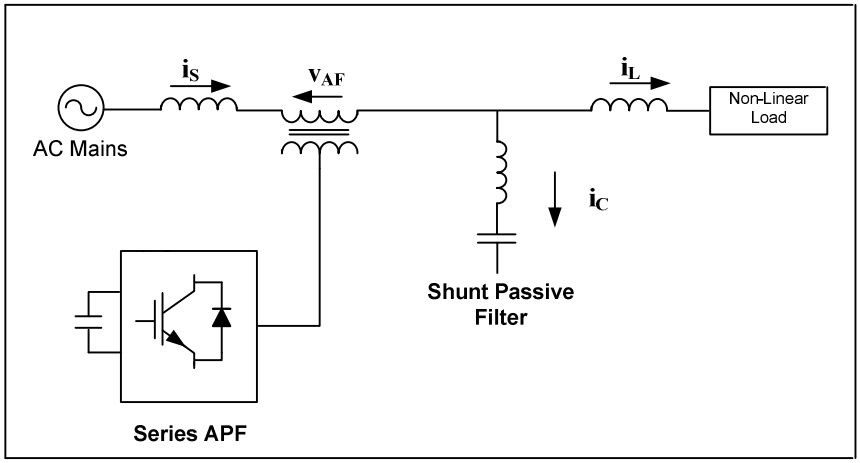

Fig 1.11 Combination of Series APF and Shunt Passive Filter

Another hybrid filter topology proposed in 1990 was formed by connecting active power filter in series with the passive filter (Fig 1.12). In the series connection, three current transformers were used to match the VA rating of the APF and the passive filter. Parallel and series resonance risk of the passive filter is damped by utilizing the active filter. The compensation principle of the system is investigated deeply in [27].

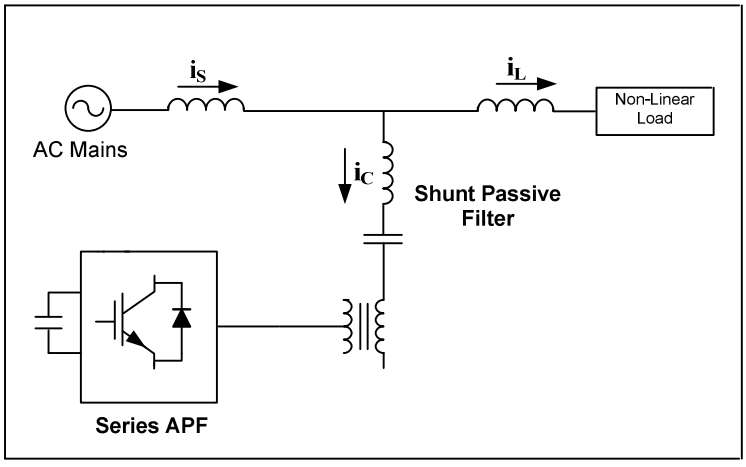

Fig 1.12 Series APF connected in series with Shunt Passive Filter

Both of the topologies represented in Fig 1.11 and Fig 1.12 include an active power filter, passive filter and a three phase transformer. Comparison between their compensation performance, filtering characteristics and reliabilities can be found in [28]. Existence of a transformer in the circuit topology inevitably increases the cost of the system which makes the topology non preferable. As a result, a shunt hybrid power filter topology named transformerless hybrid filter was proposed which uses a single LC passive filter for each phase and a small rated voltage source converter based active power filter [29]. The series connection between the LC passive filter and the voltage source converter is completed without using any matching transformer (Fig 1.13).

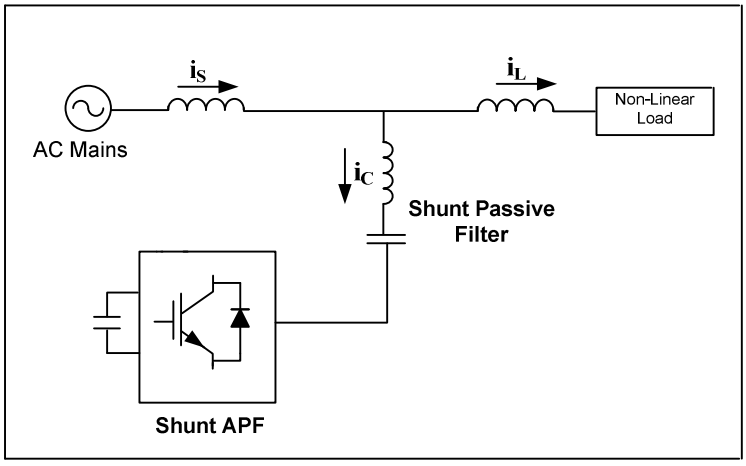

Fig 1.13 Transformerless Shunt Hybrid Power Filter

1.3 Scope of the Thesis

In recent years, harmonic pollution has become a growing problem in transmission and distribution systems, due to the non-linear loads used in industrial and domestic applications. So far, shunt passive filters have been preferred to suppress harmonics due to their low cost and efficiency. However, resonance risk with the supply

impedance, source impedance dependent performance, fixed compensation characteristics of passive filters discourage their applications. As a result, active power filters have been developed by utilizing PWM converters in various configurations and topologies to overcome the drawbacks of passive filters.

In addition to elimination of current and voltage harmonics, APFs have reactive power compensation and load balancing capabilities depending on the utilized topology. Among the topologies listed in the literature, conventional shunt connected voltage source converter type APF is widely used in industrial applications. However, for high power applications the rating and the losses of power converter increase considerably. Furthermore, in order to connect the APF system to the utility, a step down transformer is required which increase the initial cost of the system. Therefore another approach called Hybrid Active Power Filters to mitigate harmonics has been developed. Hybrid power filter topologies are formed by using a low cost passive filter and a low rated APF. In fact, hybrid power filters are used to improve the compensation characteristics of passive filters. The approach eliminates the drawbacks of pure active power filters and pure passive filters while keeping the advantages of both.

In this thesis, a shunt connected transformerless Hybrid Power Filter formed by the use of a low rated three phase voltage source PWM converter and a series connected LC passive filter, is designed and implemented. The laboratory prototype is designed to eliminate the most dominant harmonics existing at TÜBİTAK-SPACE Technologies Institute 400V bus. The existing 5^{th}, 7^{th} and 11^{th} harmonics are greatly reduced to satisfy the IEEE Std.519 current distortion limits. It is shown that the required DC link voltage for the system is quite low when compared with a pure voltage source type Active Power Filter. However, the usage of series connected passive filter in the hybrid filter topology results in unavoidable fundamental leading current flow. Furthermore, the reactive power compensation capability of the implemented hybrid power filter is fixed due to its topology which is the main disadvantage of the implemented system.

Moreover, the effectiveness of the control method given in [29] for the transformerless hybrid power filter is investigated. The undesirable effects of the supply side voltage harmonics are stated and a contribution to the control method by utilizing supply voltage is presented by simulation results. Actually, the current harmonic content of the experimental load includes not only 5^{th}, 7^{th} and 11^{th} harmonics but also unbalanced 3^{rd} harmonic due to the fluorescent lamps and single phase rectifiers. So, current references obtained in the indicated control method [29] also includes 3^{rd} harmonic. However, the designed hybrid power filter system has a 3 phase-3 wire connection and it is not possible to eliminate these 150Hz components with this configuration [3, 30-31]. In fact, the existence of third harmonics and its undesirable effects on conventional control method are discovered during the experimental tests of this thesis work. Since the power stage of the prototype has been already designed and mounted, a neutral point connection modification could not be performed. As a result, the problem is solved by modifying the current harmonic reference calculation method. The most dominant harmonic content of the load is calculated individually for each harmonic frequency but by excluding 3^{rd} harmonic component. The advantages of the designed system and the proposed current reference calculation methods are verified by both simulation and experimental results. The outline of the thesis is as given below:

In Chapter 2, circuit topology and the operating principle of the transformerless hybrid power filter is described. First, circuit configuration of the system and the principles of harmonic filtering are stated. Then, methods utilized in the control system for the calculation of current references are described. Thirdly, the most common control method preferred for transformerless hybrid power filter is introduced and analyzed. The undesirable effects of the supply side voltage harmonics are stated and a feed forward control loop is proposed. Finally, in order to exclude the 150Hz components of the load current from the compensation current references of the active filter, the proposed reference generation method is described. The applied modulation method to obtain the appropriate switching signals of semiconductor devices is also presented at the end of this Chapter.

In Chapter 3, the design procedure of the hybrid active power filter system is given, by means of simulation results. After showing the measurement results, obtained at 400V low voltage bus of TÜBİTAK, the non-linear load model of the system is obtained. Then, the circuit elements of the system are designed and selected in terms of their current and voltage ratings. After defining the system parameters, the theoretical results and the performance of the system are shown for the conventional control method and the proposed reference generation method by utilizing EMTDC/PSCAD program.

In Chapter 4, the implementation of 4.7 kVA hybrid active power filter and experimental results are presented. First, the power stage of the laboratory prototype which includes power converter, DC link side and passive filter elements are given. Secondly, control and protection circuits of the system are stated. After discussing the software structure of the implemented system, effectiveness of the proposed control method is confirmed by experimental results.

General conclusions are given in Chapter 5. In the same chapter further work proposals are also discussed.

In Appendix A, electrical characteristics of the Intelligent Power Module (IPM), technical specifications of the utilized DC link capacitor and passive filter reactor are given. Moreover, laminated bus bar design of the power converter is demonstrated in this part.

In Appendix B, technical data of the employed AC current sensor, the voltage transducer, 220VAC/24VDC power supply and the digital signal processor (DSP) are presented.

In Appendix C, flowchart of the developed DSP software is given.

CHAPTER 2

TRANSFORMERLESS SHUNT HYBRID POWER FILTER

2.1 Circuit Topology

Shunt hybrid power filter which is the main concern of this research work is formed by the use of a three phase voltage source PWM converter, and a series connected LC passive filter. The series connection between the passive filter and the voltage source converter is made directly, without using a transformer (Fig 2.1). The series connected LC filter is tuned to dominant harmonic component of the load. It absorbs the current harmonics arising from the non-linear load; however, the filtering characteristic of just the passive filter itself is not satisfactory. Hence, active power filter is used to improve the filtering performance of the overall system and to suppress the resonance risk of the passive filter.

The power circuit of the inverter includes an energy storage element of a DC link capacitor and controllable semiconductor switches with their antiparalel diodes. Active power filter injects compensation currents by operating as a current controlled voltage source. In conventional voltage source active power filter topology (Fig 1.7), the DC link capacitor voltage is required to be higher than the peak value of the utility voltage; otherwise the generated compensation currents cannot be injected to the mains [32, 33]. However, the presence of filter capacitor in this topology (Fig 2.1) ensures a reduced DC link voltage and a low rated voltage source converter at the expense of additional fundamental current, passing through the converter [34]. As a result, for low voltage applications, PWM converter can be formed by power MOSFETs instead of using IGBTs. So that, the initial cost of the converter can be

decreased by using MOSFETs instead of IGBTs. Similar to conventional VSC based APFs; hybrid power filter does not require a DC power supply for its DC link voltage regulation. The required voltage can build up with an appropriate control which is discussed in Section 2.2.2.1.3.

In order to clarify the compensation characteristic of the shunt Hybrid Power Filter, the system can be simplified by obtaining its single phase equivalent circuit as indicated in (Fig 2.2) where Z_s represents the source impedance and Z_f represents the passive filter impedance. The non linear load is shown as an ideal current source (I_l), and the APF is considered as a voltage source.

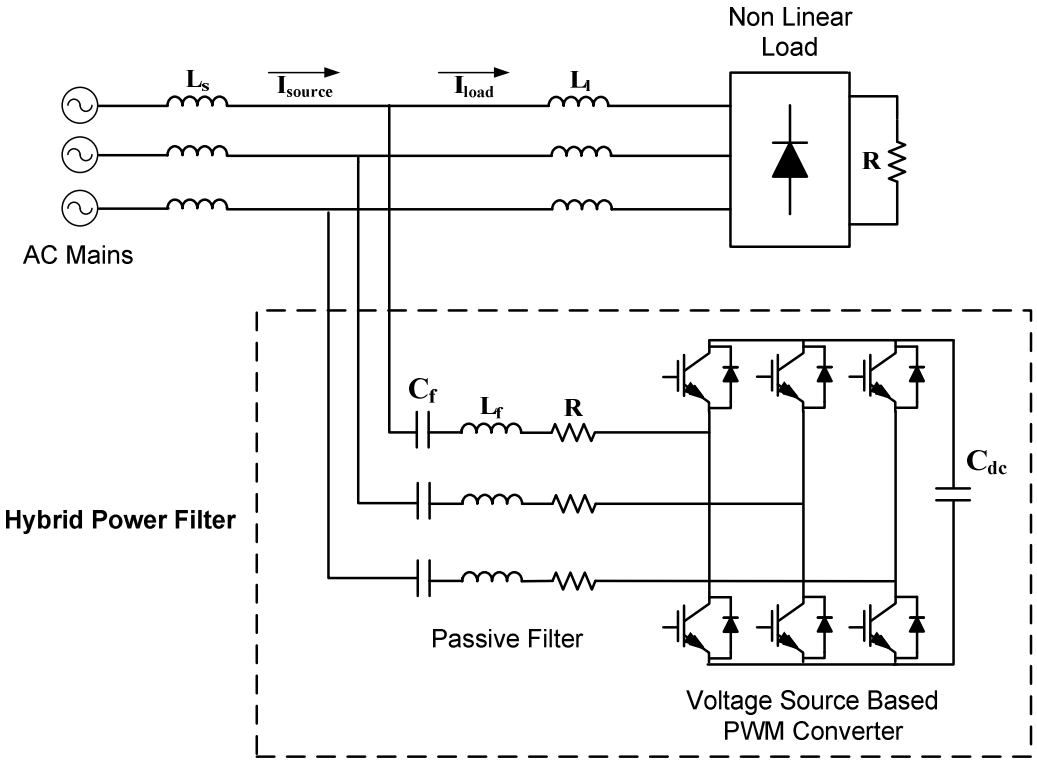

Fig 2.1 Transformerless Shunt Hybrid Power Filter

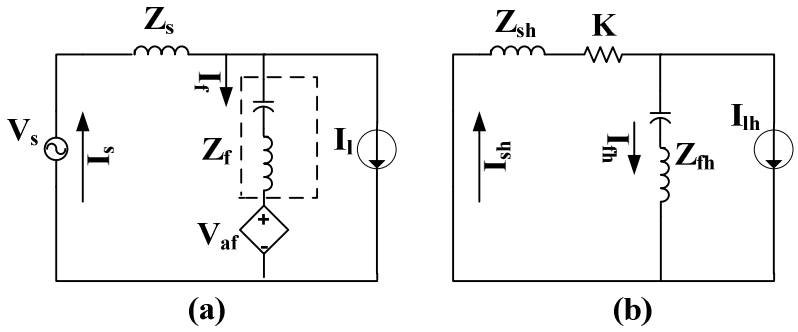

Fig 2.2 (a) Single Phase Equivalent Circuit (b) Harmonic Equivalent Circuit

If the active power filter terminal voltage is assumed to have no fundamental component, voltage across the PWM inverter can be represented as K x I_{sh} at harmonic frequencies where 'h' stands for the harmonic components and K represents the feedback gain which is described in Section 2.2.2.1.1. Hence, assuming the source voltage to be pure 50Hz and considering the current directions as in Fig 2.2, the following equations can be obtained by applying Kirchhoff's voltage law.

$$V_{sh} - I_{sh} Z_{sh} - I_{fh} Z_{fh} - V_{af} = 0$$

where ; (2.1)

$V_{sh} = 0$ and $V_{af} = KI_{sh}$

$$I_{sh} = I_{lh} + I_{fh} \tag{2.2}$$

Combine (2.1) and (2.2);

$$I_{sh} = \frac{Z_{fh}}{Z_{fh} + Z_{sh} + K} \tag{2.3}$$

Equation (2.3) indicates that as the active power filter is connected to the system, feedback gain K acts as a damping resistor which suppresses the resonance between the supply and the passive filter. Theoretically, as K approaches to infinity, the

harmonic content of the source current goes towards zero. However due to stability problems in the control loop, the gain K should be limited to certain values [29, 35].

Hence the design procedure of transformerless shunt hybrid filter can be divided into 2 groups as the design of the passive filter and the design of the active filter part. The design of the passive filter is mainly identifying the L_f, C_f parameters considering the harmonic content of the load. It is clear that, tuning frequency of the passive filter is chosen to be the most dominant harmonic component of the non linear load. Today's industrial loads generally consist of three phase diode rectifiers as AC/DC converters instead of PWM converters due to their low cost and efficiencies. As a result, in the case of a diode rectifier, the passive filter should be adjusted to eliminate the 5^{th} or 7^{th} harmonic current content.

Although the 5^{th} harmonic current content of a diode rectifier is higher than its 7^{th} harmonic components, it is more reasonable to tune the passive filter around 350Hz. An LC filter tuned at 350 Hz shows lower impedance at 550Hz and 650 Hz than a passive filter tuned at 250 Hz. So it has better filtering characteristics when 11^{th} and 13^{th} harmonics are taken into account. Moreover, for the same value of a filter inductor (L_f), the capacitor required for a 7^{th} harmonic filter is less bulky than that of a 5^{th} harmonic filter. An LC passive filter tuned at 350 Hz amplifies the 5th harmonic current components at the mains side; however, it can be suppressed by the active power filter with the applied feedback and feedforward control explained in Section 2.2.2.1 [29, 34-35].

2.2 Control Techniques and Modulation Methods

In transformerless hybrid filter topology, PWM converter generates compensation voltages by operating as a current controlled voltage source. So, the performance of the system is highly dependent on the accurate measurement and the calculation of the compensation current references. Once the current references are obtained,

voltage reference for each phase is produced by an appropriate control method in which the gate signals of semiconductor switches are also produced in modulation part.

2.2.1 Calculation of Current References

Current reference generation methods are classified as time domain or frequency domain methods in the literature [36-42]. Discrete Fourier Transform (DFT), Fast Fourier Transform (FFT), Recursive Discrete Fourier Transform (RDFT), Kalman filter are the methods developed in frequency domain. Before 1990's, FFT is the most popular method which defines the amplitude and the phase information of the sampled current/voltage over a period. However, as the order and the number of harmonics to be compensated increases, the number of calculations increases as well. Therefore, increased computational requirement and the longer response time have turned the attention towards time domain calculations.

Instantaneous reactive power (p-q) theory and synchronous reference frame (SRF) method are the most common and widely used time domain methods for current reference calculations. They have faster responses to rapid changes in power system, and require less computation as compared with the frequency domain methods. Moreover, the development in digital signal processors allows designers to make easy and effective implementations. In this thesis, both in simulation and implementation procedures of 400V Hybrid Power Filter prototype, synchronous reference frame method is utilized to extract the harmonic content of the load. In this section instantaneous reactive power theory is also described.

2.2.1.1 Instantaneous Reactive Power (p-q) Theory

Early calculations related with the power flow of electrical systems were based on the average power or rms values of voltage and current. In 1982, a new concept was

defined by H. Akagi, called instantaneous reactive power (p-q) theory in the journal transactions of IEEE Japan [43]. Then the new concept had also been verified experimentally that the theory is suitable and efficient to design controllers for the power conditioners including power electronic devices [44, 45].

The p-q theory is based on the definitions of instantaneous active and reactive powers in the time domain by using instantaneous voltage and current components on αβ0 coordinates. So the p-q theory first utilizes Clarke Transformation to map three phase instantaneous voltages and line currents into αβ0 axes. Transformation matrices C and C^{-1} for Clarke transformation and inverse Clarke transformation are given respectively in (2.4) and (2.5).

$$\begin{bmatrix} V_0 \\ V_\alpha \\ V_\beta \end{bmatrix} = C \begin{bmatrix} V_a \\ V_b \\ V_c \end{bmatrix} = \sqrt{\frac{2}{3}} \begin{bmatrix} \frac{1}{\sqrt{2}} & \frac{1}{\sqrt{2}} & \frac{1}{\sqrt{2}} \\ 1 & -\frac{1}{2} & -\frac{1}{2} \\ 0 & \frac{\sqrt{3}}{2} & -\frac{\sqrt{3}}{2} \end{bmatrix} \begin{bmatrix} V_a \\ V_b \\ V_c \end{bmatrix} \tag{2.4}$$

$$\begin{bmatrix} V_a \\ V_b \\ V_c \end{bmatrix} = C^{-1} \begin{bmatrix} V_0 \\ V_\alpha \\ V_\beta \end{bmatrix} = \sqrt{\frac{2}{3}} \begin{bmatrix} \frac{1}{\sqrt{2}} & 1 & 0 \\ \frac{1}{\sqrt{2}} & -\frac{1}{2} & \frac{\sqrt{3}}{2} \\ \frac{1}{\sqrt{2}} & -\frac{1}{2} & -\frac{\sqrt{3}}{2} \end{bmatrix} \begin{bmatrix} V_0 \\ V_\alpha \\ V_\beta \end{bmatrix} \tag{2.5}$$

Equations are given for voltage vectors but they are also valid for current vectors. The subscript "0" denotes the zero sequence components either in current or voltage. In a three phase three wire system, no zero sequence current can flow and if the phase voltages are balanced, no zero sequence voltage can exist even if the system is three phase four wire. For simplicity, the zero sequence terms in (2.4) and (2.5) are eliminated to show the α-β axes mapping of a three phase balanced linear system.

Instantaneous phase voltages and line currents in abc axes are given in (2.6) and (2.7).

$$\begin{aligned} V_a(t) &= \sqrt{2}\ V\cos(wt + \phi_V) \\ V_b(t) &= \sqrt{2}\ V\cos(wt + \phi_V - \frac{2\pi}{3}) \\ V_c(t) &= \sqrt{2}\ V\cos(wt + \phi_V + \frac{2\pi}{3}) \end{aligned} \tag{2.6}$$

$$\begin{aligned} i_a(t) &= \sqrt{2}\ I\cos(wt + \phi_I) \\ i_b(t) &= \sqrt{2}\ I\cos(wt + \phi_I - \frac{2\pi}{3}) \\ i_c(t) &= \sqrt{2}\ I\cos(wt + \phi_I + \frac{2\pi}{3}) \end{aligned} \tag{2.7}$$

Substitute (2.6) and (2.7) in (2.4);

$$\begin{aligned} V_\alpha &= \sqrt{\frac{2}{3}}\,(\sqrt{2}V\cos(wt+\phi_V) - \frac{\sqrt{2}}{2}V\cos(wt+\phi_V - \frac{2\pi}{3}) - \frac{\sqrt{2}}{2}V\cos(wt+\phi_V + \frac{2\pi}{3})) \\ &= \sqrt{3}V\cos(wt+\phi_V) \end{aligned} \tag{2.8}$$

$$\begin{aligned} V_\beta &= \sqrt{\frac{2}{3}}\,(\frac{\sqrt{3}}{2}V\cos(wt + \phi_V - \frac{2\pi}{3}) - \frac{\sqrt{3}}{2}V\cos(wt + \phi_V + \frac{2\pi}{3})) \\ &= \sqrt{3}V\sin(wt + \phi_V) \end{aligned} \tag{2.9}$$

Similarly,

$$\begin{aligned} i_\alpha &= \sqrt{3}I\cos(wt + \phi_I) \\ i_\beta &= \sqrt{3}I\sin(wt + \phi_I) \end{aligned} \tag{2.10}$$

Then, a voltage vector ‘e’ and a current vector ‘i’ (2.11) are defined on α-β reference frames using (2.8), (2.9), and (2.10). So, the graphical representations after abc to α-β transformation for the obtained voltage and current vectors in α-β reference frames are as indicated in Fig 2.3.

$$e = V_\alpha + jV_\beta = \sqrt{3}V\,(\cos(wt+\phi_V) + j\sin(wt+\phi_V) = \sqrt{3}V\,e^{j(wt+\phi_V)}$$
$$i = i_\alpha + ji_\beta = \sqrt{3}I\,(\cos(wt+\phi_I) + j\sin(wt+\phi_I) = \sqrt{3}I\,e^{j(wt+\phi_I)} \quad (2.11)$$

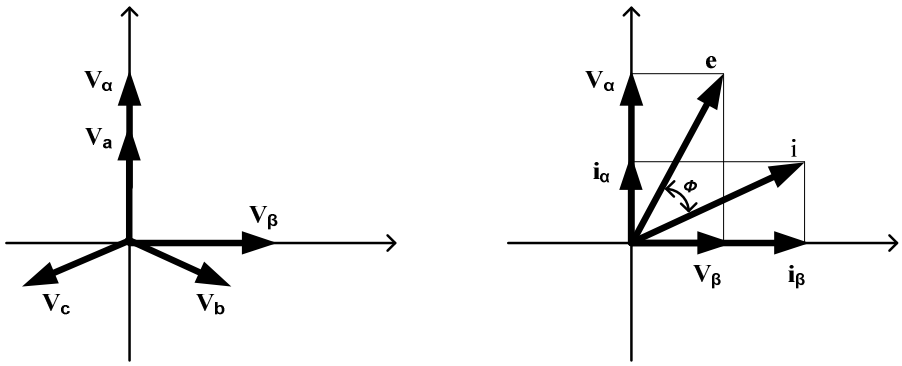

Fig 2.3 Clarke Transformation and Vector Representation in α-β Frames

Instantaneous complex power (S) is defined as the multiplication of the voltage vector 'e' and the complex conjugate of the current vector 'i^*' as given in (2.12).

$$S = e \cdot i^* = (V_\alpha + jV_\beta)\,(i_\alpha - ji_\beta)$$
$$= \underbrace{(V_\alpha i_\alpha + V_\beta i_\beta)}_{\mathbf{p}} + j\underbrace{(V_\beta i_\alpha - V_\alpha i_\beta)}_{\mathbf{q}} \quad (2.12)$$

A matrix form of (2.12) can be obtained as follows:

$$\begin{bmatrix} p \\ q \end{bmatrix} = \begin{bmatrix} V_\alpha & V_\beta \\ V_\beta & -V_\alpha \end{bmatrix} \begin{bmatrix} i_\alpha \\ i_\beta \end{bmatrix} \quad (2.13)$$

Rearranging (2.13);

$$\begin{bmatrix} i_\alpha \\ i_\beta \end{bmatrix} = \frac{1}{V_\alpha{}^2 + V_\beta{}^2} \begin{bmatrix} V_\alpha & V_\beta \\ V_\beta & -V_\alpha \end{bmatrix} \begin{bmatrix} p \\ q \end{bmatrix} \quad (2.14)$$

$$\begin{aligned} p &= \bar{p} + \tilde{p} \\ q &= \bar{q} + \tilde{q} \end{aligned} \tag{2.15}$$

Where p is the instantaneous real power, q is the imaginary reactive power. The real and imaginary power terms include only constant values for the derivations indicated above. However if the load is non-linear, the current vector will include not only the fundamental frequency component but also the harmonics, depending on the order. Then the instantaneous real and imaginary powers will have a dc component and an oscillating component as decomposed in (2.15). The average (dc) components of both active and reactive power terms in the system are represented with an over bar sign (-) and the oscillating parts are represented by an over tilde (~) sign. The oscillating part of the active power ($\tilde{p}$) which has a zero mean is an additional power flow without a contribution to the energy transfer from source to load. Moreover, the oscillating part of the imaginary power ($\tilde{q}$) stands for the power exchanged between the phases which has no effect on the energy transfer between the source and the load.

However if zero sequence terms exist in the system, simplified transformations and equations are not applicable. If zero sequence voltage and current both appear, another instantaneous power term p_0 (zero sequence power) is introduced. Assume three phase voltages and currents consist of positive and zero sequence terms (2.16), (2.17).

$$\begin{aligned} V_a(t) &= \sqrt{2}\, V_+ \sin(wt + \phi_V) + \sqrt{2}\, V_0 \sin(wt + \phi_{V0}) \\ V_b(t) &= \sqrt{2}\, V_+ \sin(wt + \phi_V - \frac{2\pi}{3}) + \sqrt{2}\, V_0 \sin(wt + \phi_{V0}) \\ V_c(t) &= \sqrt{2}\, V_+ \sin(wt + \phi_V + \frac{2\pi}{3}) + \sqrt{2}\, V_0 \sin(wt + \phi_{V0}) \end{aligned} \tag{2.16}$$

$$
\begin{aligned}
i_a(t) &= \sqrt{2}\ I_+ \sin(wt + \phi_I) + \sqrt{2}\ I_0 \sin(wt + \phi_{I0}) \\
i_b(t) &= \sqrt{2}\ I_+ \sin(wt + \phi_I - \frac{2\pi}{3}) + \sqrt{2}\ I_0 \sin(wt + \phi_{I0}) \\
i_c(t) &= \sqrt{2}\ I_+ \sin(wt + \phi_I + \frac{2\pi}{3}) + \sqrt{2}\ I_0 \sin(wt + \phi_{I0})
\end{aligned}
\tag{2.17}
$$

Applying C matrix given in (2.4);

$$
\begin{aligned}
V_\alpha &= \sqrt{3}V_+ \sin(wt + \phi_{V+}) \\
V_\beta &= \sqrt{3}V_+ \cos(wt + \phi_{V+}) \\
V_0 &= \sqrt{6}V_0 \sin(wt + \phi_{V0})
\end{aligned}
\tag{2.18}
$$

$$
\begin{aligned}
i_\alpha &= \sqrt{3}I_+ \sin(wt + \phi_{i+}) \\
i_\beta &= \sqrt{3}I_+ \cos(wt + \phi_{i+}) \\
i_0 &= \sqrt{6}I_0 \sin(wt + \phi_{I0})
\end{aligned}
\tag{2.19}
$$

By utilizing (2.12), real, imaginary and zero sequence power terms are obtained as given in (2.20) and (2.21).

$$
\begin{bmatrix} p_0 \\ p \\ q \end{bmatrix} = \begin{bmatrix} V_0 & 0 & 0 \\ 0 & V_\alpha & V_\beta \\ 0 & V_\beta & -V_\alpha \end{bmatrix} \begin{bmatrix} i_0 \\ i_\alpha \\ i_\beta \end{bmatrix} \tag{2.20}
$$

$$
p_0 = 3V_0 I_0 \cos(\phi_{V0} - \phi_{i0}) - 3V_0 I_0 \cos(2wt + \phi_{V0} + \phi_{i0}) = \bar{p}_0 + \tilde{p}_0 \tag{2.21}
$$

Real and imaginary powers indicated in (2.21) are similar to previous analysis described above since they depend only on positive sequence components of voltage and the current. The zero sequence power (p_0) has an average value and an oscillating part at twice the line frequency. It has no contribution to the real power p or the imaginary power q. The average value of the zero sequence power represents a unidirectional energy flow and oscillating part is responsible for instantaneous energy transfer.

It can be concluded that; p-q theory is based on the definitions of real, imaginary and zero sequence power terms by using instantaneous voltage and current components on αβ0 coordinates. The three phase instantaneous active power which corresponds to the total energy flow per unit time is the sum of the real power p and the zero sequence power p_0. However, imaginary power does not contribute to the energy transfer; it represents the energy being exchanged between the phases of the system.

It is reasonable to select the undesirable power components for compensators by using p-q theory. In the case of a non-linear load, the compensating current references of an active filter can be produced by selecting the appropriate power references after utilizing the instantaneous power theory [46]. For instance, if the active power filter is to be designed only for harmonic current compensation without any reactive power compensation, the oscillating parts of p and q should be selected as a power reference. The oscillating parts can be extracted with a high pass filter (HPF) and utilizing equation (2.13), (2.14) and inverse Clarke transformation respectively yields the desired compensation current references (i_{Ca}^*, i_{Cb}^*, i_{Cc}^*) in abc coordinates (Fig 2.4).

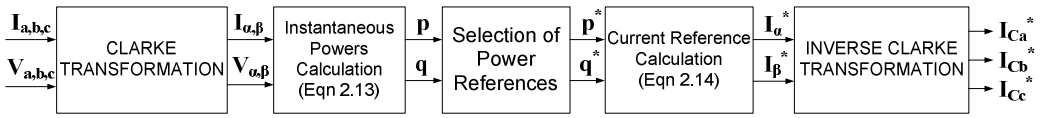

Fig 2.4 Current Reference Calculation based on p-q Theory

2.2.1.2 Synchronous Reference Frame Method

Synchronous reference frame method is based on the transformation of vectors into synchronously rotating direct (d), and quadrature axis (q) reference frames. In order to calculate the harmonic components of the mains current, initially three phase supply current vectors are mapped into stationary α-β axes by utilizing Clarke

Transformation (2.4). Then, vectors in stationary reference frame are transformed into synchronously rotating reference frame by utilizing Park transformation. Transformation matrices $\boldsymbol{P}$ and $\boldsymbol{P^{-1}}$ for Park transformation and inverse Park transformation are given respectively in (2.22) and (2.23). The phase angle θ represented in Park transformation defines the fundamental frequency phase information of the utility voltage and it is obtained from a phase locked loop circuit which is investigated in 2.2.2.1.1.

$$\begin{bmatrix} i_d \\ i_q \end{bmatrix} = P \begin{bmatrix} i_\alpha \\ i_\beta \end{bmatrix} = \begin{bmatrix} \cos(\theta) & -\sin(\theta) \\ \sin(\theta) & \cos(\theta) \end{bmatrix} \begin{bmatrix} i_\alpha \\ i_\beta \end{bmatrix} \tag{2.22}$$

$$\begin{bmatrix} i_\alpha \\ i_\beta \end{bmatrix} = P^{-1} \begin{bmatrix} i_d \\ i_q \end{bmatrix} = \begin{bmatrix} \cos(\theta) & \sin(\theta) \\ -\sin(\theta) & \cos(\theta) \end{bmatrix} \begin{bmatrix} i_d \\ i_q \end{bmatrix} \tag{2.23}$$

Once the current vectors are transformed into synchronously rotating d-q reference frame, the fundamental component of the mains current turns out to be a DC signal, and the harmonic components which are still AC signals are rotating with a corresponding angular frequency.

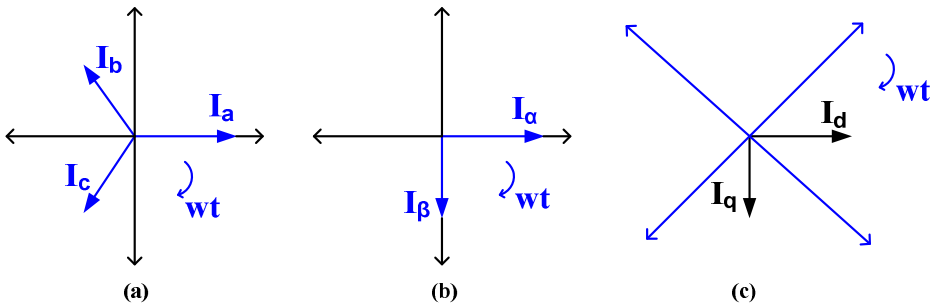

Fig 2.5 (a) Three Phase Current Vectors (b) Clarke Transformation (c) Park Transformation

For instance; 5^{th} and 7^{th} harmonic components of a distorted source current turns out to be a 300Hz signal for a 50Hz AC mains. Since the rotation angle of the reference frame is positive, positive and negative sequence harmonic components are transformed to 300Hz and its multiples in synchronous d-q reference frame [40-42, 47, 48]. Therefore, the method is specifically named as positive sequence SRF method.

AC signals are extracted via a high pass filter (HPF) or by subtracting the DC quantity obtained from a low pass filter (1-LPF). Low pass filters with low cut off frequencies (20Hz-30Hz) are sufficient to extract the DC component. Since the extracted signal is a DC quantity, SRF method is insensitive to phase errors introduced by the filters. Inverse transformation of the obtained AC signals reproduces the supply harmonic current components in stationary abc frame.

If the supply voltage is not balanced and the source current contains fundamental negative sequence component, it turns out to be a 100Hz component in synchronous d-q reference frame, and it is not extracted by the LPF. Therefore, fundamental negative sequence component appears in the references of the active power filter. However, utilizing negative sequence SRF method, in which the vectors are produced by $-\theta$, prevents the appearance of fundamental negative sequence component in the reference currents of the APF [47]. The method is similar to the positive sequence SRF. The current vectors are transformed into negative sequence d-q reference frame. In this case fundamental negative sequence current component turns out to be a DC signal and extracted via a LPF. The extracted DC signal is back transformed into stationary α-β reference frame, and subtracted from the references of the positive sequence SRF method in α-β reference frame. Current reference calculation including positive and negative sequence SRF method is summarized in Fig 2.6.

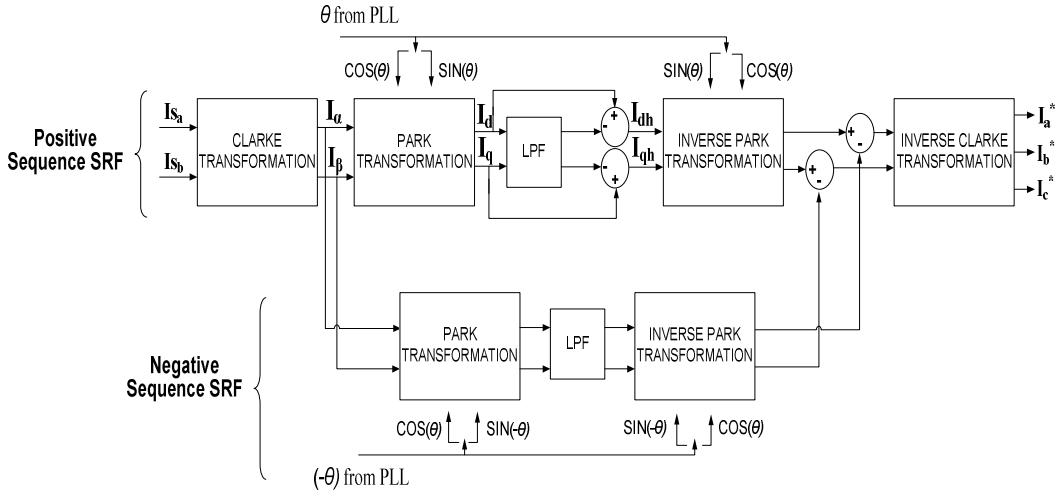

Fig 2.6 Current Reference Calculation Based on SRF Method

2.2.2 Control and Waveform Modulation Methods

The control methods used for VSC based Hybrid Power Filters are based on the generation of voltage references. Firstly the conventional control method which is proposed by H. Akagi is described. Then, the proposed voltage feedforward control which can be combined with the conventional control method is presented. Finally, the proposed voltage reference generation method which is used to exclude the 150Hz current harmonic components of the load is explained.

The conventional method is based on the calculation of voltage reference by utilizing the source current harmonic references. In this method, 50Hz component of the source current is extracted and the remaining oscillating part in d-q reference frame is treated as reference compensation currents. The conventional control method introduced by H. Akagi [34] is divided into three sub control methods; feedback control, feedforward control and DC Link Voltage Control.

Measurement results given in Section 3.1 show that there exist also unbalanced 3rd harmonic component in the supply current waveform. Theoretically, the topology

used in this thesis is not suitable to eliminate these components without the neutral wire connection [3, 30-31]. So, a reference generation method which is based on the calculation of voltage reference for each dominant harmonic frequency individually is proposed. Finally, the obtained voltage references are compared with a carrier wave to obtain the gate signals of the semiconductors.

2.2.2.1 Conventional Control Method

2.2.2.1.1 Feedback Control

In feedback control, synchronous reference frame method is used to calculate the harmonic components of the mains current. Three phase supply current vectors are transformed into d-q frames rotating at the fundamental frequency w1 by applying Clarke and Park transformations as described in Section 2.2.1.2 (Fig 2.5). In Park transformation, the phase angle (θ) of the supply voltage is required which affects the performance of the control method. Hence, an accurate phase tracking system is the key point of the control method to transform the measured current vectors into synchronously rotating d-q reference frame. In this research work, a phase locked loop system given in (Fig 2.7) is utilized both in theoretical and experimental works [49, 50].

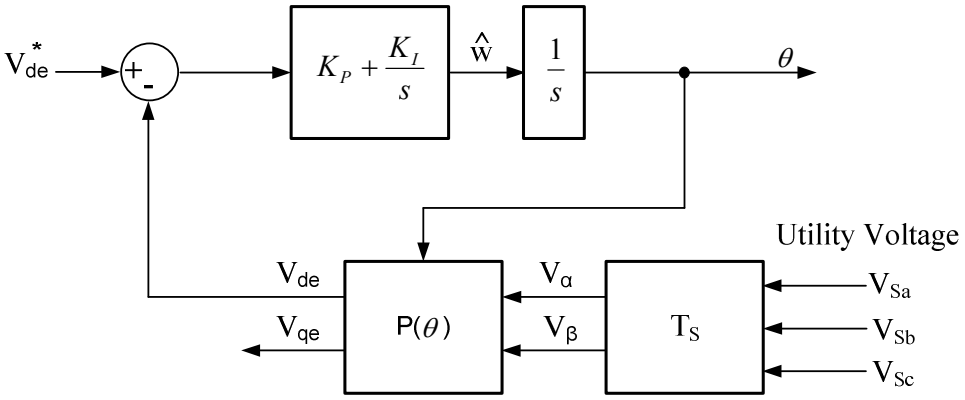

Fig 2.7 Block Diagram of the Phase Locked Loop

The phase tracking system indicated above includes the transformation of utility voltages into d-q reference frame and a PI controller. The system is a closed loop controller in which the transformation of the utility voltage is performed by using the θ output of the PI controller.

Assume that, the three phase balanced utility voltages are as follows:

$$\begin{bmatrix} V_{SA} \\ V_{SB} \\ V_{SC} \end{bmatrix} = V_M \begin{bmatrix} \sin(\varphi) \\ \sin(\varphi - \frac{2\pi}{3}) \\ \sin(\varphi + \frac{2\pi}{3}) \end{bmatrix} \tag{2.24}$$

Applying T_S and P (θ), utility voltage can be expressed in stationary (α-β) and synchronous (d-q) reference frames respectively as given in (2.25) and (2.26)

$$\begin{bmatrix} V_\alpha \\ V_\beta \end{bmatrix} = T_S \begin{bmatrix} V_{SA} \\ V_{SB} \\ V_{SC} \end{bmatrix} = \begin{bmatrix} V_{SA} \\ \frac{(V_{SC} - V_{SB})}{\sqrt{3}} \end{bmatrix} \tag{2.25}$$

Where, $T_S = \frac{2}{3}\begin{bmatrix} 1 & \frac{-1}{2} & \frac{-1}{2} \\ 1 & \frac{-\sqrt{3}}{2} & \frac{-\sqrt{3}}{2} \end{bmatrix}$

$$V_{de} = \cos(\theta) \times V_{SA} - \sin(\theta) \times \frac{(V_{SC} - V_{SB})}{\sqrt{3}} = V_M \sin(\varphi - \theta)$$
$$V_{qe} = \sin(\theta) \times V_{SA} + \cos(\theta) \times \frac{(V_{SC} - V_{SB})}{\sqrt{3}} = V_M \cos(\varphi - \theta) \quad (2.26)$$

If the output of the PLL (θ) is equal to phase angle of the utility (φ) without an error, $V_{de} = 0$ and $V_{qe} = V_M$. Hence, giving a zero reference to the V_{de}^* reference of the PI controller, assures locking onto utility voltage. The phase angle of the PLL system is finally obtained by integrating the error compensation output of the PI controller. The disturbances at utility voltage directly affect the PLL output so that the proportional and the integral constants (K_P, K_I) of the PI controller should be properly selected. The steady state output of the implemented PLL system is presented in Section 3.4.

As given in the block diagram of the feedback control method (Fig 2.9), the harmonic content of the source current is calculated by utilizing synchronous reference frame method. Firstly, three phase source currents are transformed into d-q reference frame by employing the phase angle output of the PLL where $w_1=\theta$. I_d represents the instantaneous reactive current and I_q represents the instantaneous active current component. The fundamental component of the mains current turns out to be a DC signal, and the harmonic components which are still AC signals are rotating with respect to the reference frame. Harmonic current components I_{dh} and I_{qh} can be extracted by a high pass filter with a low cut off frequency. Another approach to extract harmonic components is applying 1-LPF (Low pass filter) operation. The digital implementation of low pass filters in this thesis is performed by calculating the mean of the I_d and I_q components in 20ms window.

After obtaining the oscillating parts of the source current ($I_{dh,}$ I_{qh}) in rotating d-q reference frame, inverse Clarke and inverse Park transformations are applied to reproduce the harmonic current components in stationary abc frames. Each harmonic component is amplified by a feedback gain of "K" to obtain a voltage reference for each phase (V_{afb}^{*}, V_{bfb}^{*} and V_{cfb}^{*}) [29, 35]. Thus hybrid power filter is controlled to produce a voltage at its terminals (V_{AF}) which can be simplified as given in (2.27).

$$V_{AF} = K \times I_{sh} \tag{2.27}$$

Thus, single phase equivalent of the hybrid power filter at harmonic frequencies can be represented as indicated in Fig 2.8.

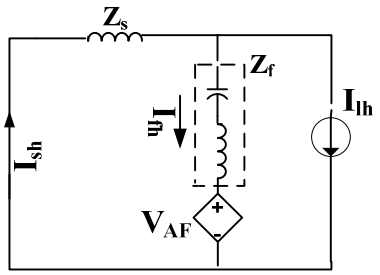

Fig 2.8 Single Phase Equivalent Circuit of Hybrid Power Filter (Feedback Control Applied)

So, harmonic content of the source current can be calculated as follows:

$$I_{sh} = I_{lh} + I_{fh} \tag{2.28}$$

$$V_{AF} + Z_f I_{fh} + Z_s I_{sh} = 0 \tag{2.29}$$

Combine (2.27), (2.28) and (2.29) to represent I_{sh} in terms of I_{lh} (2.30).

$$I_{sh} = \frac{Z_f}{K + Z_f + Z_s} \times I_{lh} \tag{2.30}$$

As can be deduced from (2.30), when the feedback control is applied, active power filter behaves as a pure resistor which is connected in series with the source impedance (Z_s). Hence, the feedback gain K suppresses the resonance between the supply and he passive filter. Therefore, the amplification phenomenon of the passive filter is diminished. Theoretically as K goes to infinite values, the harmonic content of the source current disappears totally. However, the feedback gain K is limited to the certain values due to the stability problems of the system.

In order to increase the filtering performance of the hybrid power filter, an additional feedforward control loop can be utilized. In Fig 2.9 a current feedforward control loop is also presented for the elimination of the 5^{th} harmonic current component.

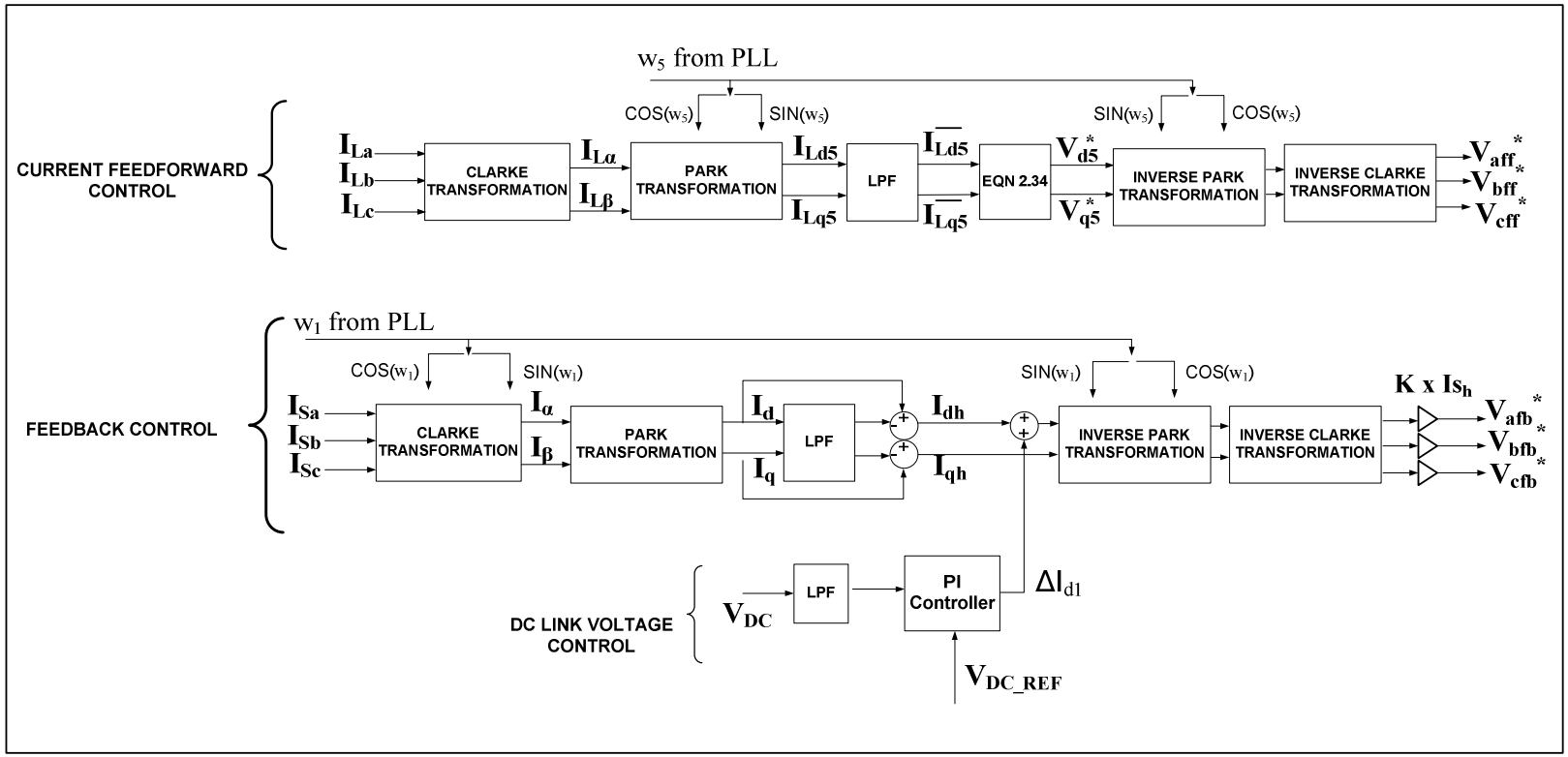

Fig 2.9 Conventional Control Method

2.2.2.1.2 Feedforward Control

Feedforward control presented in this part is introduced for the most dominant 5th harmonic current. The aim of the sub control method is to make the LC filter absorb all the fifth harmonic current component of the load. In this case, three phase load currents are transformed into d_5q_5 reference frame rotating at fifth harmonic frequency. So the 250Hz components of the load current in this frame (2.31) are obtained by utilizing low pass filters (Fig 2.9).

$$\overline{Il}_{dq5} = \overline{Il}_{d5} + \overline{Il}_{q5} \tag{2.31}$$

The impedance of the LC passive filter (Z_F) on α-β stationary frame and d_5q_5 rotating reference frame is indicated respectively in (2.32) and (2.33).

$$Z_F(s) = R_F + sL_F + \frac{1}{sC_F} \tag{2.32}$$

$$Z_{Fdq5}(s) = R_F + (s + jw_5)L_F + \frac{1}{(s + jw_5)C_F} \tag{2.33}$$

Then, the reference voltages in the feedforward control in steady state are obtained as given in (2.34) [51]. Finally, inverse transformation yields the voltage references of the feedforward control (V_{aff}^*, V_{bff}^* and V_{cff}^*).

$$\begin{bmatrix} V_{d5}^* \\ V_{q5}^* \end{bmatrix} = \begin{bmatrix} R_F & -w_5L_F - \frac{1}{w_5C_F} \\ w_5L_F - \frac{1}{w_5C_F} & R_F \end{bmatrix} \begin{bmatrix} \overline{Il}_{d5} \\ \overline{Il}_{q5} \end{bmatrix} \tag{2.34}$$

2.2.2.1.3 DC Link Voltage Control

DC link voltage control is maintained by a proportional plus integral (PI) regulator (Fig 2.9). DC link capacitor voltage is build up and regulated without any external power supply. In order to meet the loss inside the active power filter, an amount of active power is required and generated by producing a fundamental ac voltage controlled by the active filter.

Since a fundamental leading current flows through the LC passive filter, the active filter should generate a fundamental voltage that is in phase with this leading current. As a result, the current reference (ΔI_{d1}) obtained in this control loop is added to the reactive current component Id_h [29].

2.2.2.2 Proposed Voltage Feedforward Control Method and Proposed Voltage Reference Generation Method to Exclude 3rd Harmonics

2.2.2.2.1 Voltage Feedforward Control Method

The conventional control method including feedback control and feedforward control is effective to eliminate the current harmonics of a three phase diode rectifier load. Theoretical results shown in Section 3.4.1 are obtained by assuming the supply voltage is pure 50 Hz. However, existence of voltage harmonics at the mains side affects the performance of the feedback and feedforward control loops. In the vicinity of voltage harmonics at the utility, the single phase equivalent of the hybrid power filter is redrawn as given in Fig 2.10.

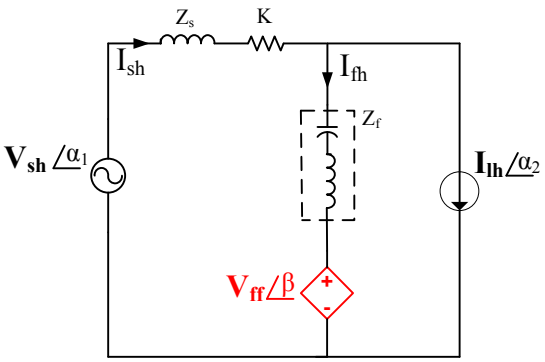

Fig 2.10 Single Phase Equivalent of Hybrid Power Filter
(Supply Side Voltage Harmonics are existing)

In previous single phase analysis, utility voltage is assumed to be pure 50 Hz. In this case a voltage harmonic component (V_{sh}) is introduced with zero phase angle. The harmonic components of the source current can be represented as given in (2.35)

$$I_{sh} = \frac{V_{sh}\angle\alpha_1}{K + Z_f + Z_s} + \frac{Z_f}{K + Z_f + Z_s} \times (I_{lh}\angle\alpha_2) \tag{2.35}$$

Assume no feedback control is applied (K=0);

$$I_{sh} = \underbrace{\frac{V_s\angle\alpha_1}{Z_f + Z_s}}_{I_{add}} + \underbrace{\frac{Z_f}{Z_f + Z_s}}_{I_{prev}} \times (I_{lh}\angle\alpha_2) \tag{2.36}$$

It is shown in (2.36) that, I_{add} is the additional harmonic current flow at the source side due to the existence of utility voltage harmonic. The resultant effect between these two current vectors (I_{add}, I_{prev}) can be either additive or subtractive which is determined by the their phase angles (α_1, α_2). In order to diminish this additional current flow, a voltage term (V_{ff}) should be generated at the output of the active power filter (2.37).

$$I_{sh} = \frac{V_{sh}\angle\alpha_1 - V_{ff}\angle\beta}{Z_f + Z_s} + \frac{Z_f}{Z_f + Z_s} \times (I_{lh}\angle\alpha_2) \tag{2.37}$$

If the generated voltage term is equal to the existing voltage harmonics in both magnitude and phase ($V_{ff} = V_{sh,}$ $\beta = \alpha_1$), additional current flow is prevented. As a result, the voltage feedforward control method given in Fig 2.11 is proposed. It mainly depends on extracting the supply voltage harmonic component and isolating the hybrid power filter from any harmonic current flow [52].

Since the 5th voltage harmonic is the most probable component that may appear on the utility, the block diagram of the control method (Fig 2.11) is given to isolate 5th voltage harmonic. Similar to feedback control method, synchronous reference frame method is utilized. Three phase utility voltages, which are already sampled for PLL (Section 2.2.2.1.1), are also transformed into d_5-q_5 reference frame which is rotating with an angular frequency of w_5 ($5w_1$). The angle used in the Park transformation (w_5) can be easily obtained by a simple multiplication and mod operation of the PLL output (w_1). After applying the park transformation, 250 Hz components of the utility voltage which are DC quantities with respect to d_5-q_5 reference frame, are obtained by employing LPFs.

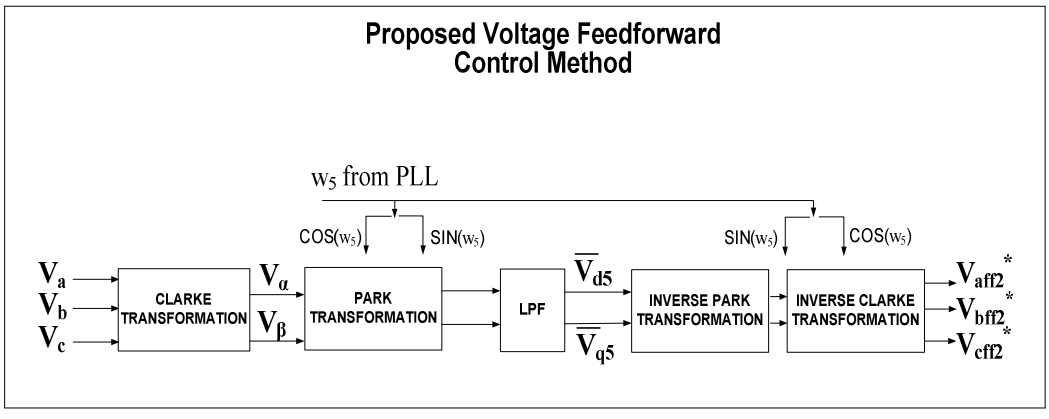

Fig 2.11 Proposed Voltage Feedforward Control Method

Finally, similar to feedback control, the voltage references of the proposed control method (V_{aff2}^*, V_{bff2}^*, V_{cff2}^*) are obtained by utilizing Inverse Park and Inverse Clarke Transformations respectively. Obtained voltage references should be added with the voltage references obtained in Section 2.2.2.1.1 and 2.2.2.1.2. The interaction between the existing voltage harmonics at the mains side and the current harmonics of the load is given by simulation results in Section 3.4.2.

2.2.2.2.2 Proposed Voltage Reference Generation Method to Exclude 3rd Harmonics

The performance of the conventional control method applied for the transformerless hybrid power filter is quite satisfactory as given in Section 3.4.1**.** However, if the harmonic content of the non-linear load includes unbalanced 3rd harmonic components, it is not possible to compensate these components without a neutral conductor. Therefore, 3rd harmonic should be excluded during the current reference calculations. However, in the conventional control method, 50 Hz component of the source current is extracted and the remaining part is treated as the harmonic current reference of the system. In the proposed control method, the harmonic content of the load is calculated for each dominant harmonic frequency by using synchronous reference frame method.

The load current (I_L) and the hybrid power filter current (I_F) can be represented in α-β stationary reference frame as follows:

$$I_L(\alpha,\beta)=\begin{pmatrix} I_{L\alpha} \\ I_{L\beta} \end{pmatrix}=\begin{pmatrix} (I_{L\alpha 1}\sin(w_1 t+\lambda_1)+\sum_{k=2}^{n} I_{L\alpha k}\sin(w_k t+\lambda_k)) \\ (I_{L\beta 1}\cos(w_1 t+\lambda_1)+\sum_{k=2}^{n} I_{L\beta k}\cos(w_k t+\lambda_k)) \end{pmatrix} \tag{2.38}$$

$$I_f(\alpha,\beta)=\begin{pmatrix} I_{F\alpha} \\ I_{F\beta} \end{pmatrix}=\begin{pmatrix} (I_{F\alpha 1}\sin(w_1 t+\psi_1)+\sum_{k=2}^{m} I_{F\alpha k}\sin(w_k t+\psi_k)) \\ (I_{F\beta 1}\cos(w_1 t+\psi_1)+\sum_{k=2}^{m} I_{F\beta k}\cos(w_k t+\psi_k)) \end{pmatrix} \quad (2.39)$$

Where subscript "k" and "m" denote the order of the harmonics, and subscript "1" stands for the fundamental component. Actually, the filter current includes not only the harmonic content of the load but also the high frequency ripple components seen at switching frequency. However, in hybrid power filter topology; these high frequency components are already suppressed by the existing LC passive filter. For the rest of the derivations filter current is assumed to be ripple free. So, it is clear from (2.39) that, the filter current contains the unavoidable fundamental current resulting from the LC filter and the compensation current harmonic components.

If the fundamental components of both the filter and the load current are removed from (2.38) and (2.39), an error signal can be obtained by subtracting the actual filter current from the measured load current for desired harmonic frequencies. The proposed method mainly depends on generating a voltage reference by converting the obtained error signal into a voltage reference signal by a proportional control [18]. In Fig 2.12, the proposed control method is given for suppressing the most dominant 5^{th}, 7^{th} and 11^{th} harmonics of a three phase uncontrolled rectifier.

Firstly, three phase load currents are mapped into α-β stationary reference frame. Then, the orthogonal load current vectors of $I_{L\alpha}$ and $I_{L\beta}$ are transformed into rotating frames with angular frequencies equal to that of the harmonic order. So, the PLL system given in 2.2.2.1.1 should not only generate 50 Hz phase information but also 250 Hz, 350 Hz and 550 Hz phase information. After transforming $I_{L\alpha}$ and $I_{L\beta}$ into rotating reference frames (d_5-q_5, d_7-q_7, d_{11}-q_{11}), the harmonic content of the vectors are obtained by applying low pass filters individually for each vector. Then, each current harmonic reference ($I_{L\alpha 5}$, $I_{L\alpha 7}$, $I_{L\alpha 11}$, $I_{L\beta 5}$, $I_{L\beta 7}$, and $I_{L\beta 11}$) is produced by

applying inverse park transformation. Thus, (2.38) can be modified to produce the current harmonic references as indicated in (2.40).

$$\begin{pmatrix} I_{L\alpha}{}^{*} \\ I_{L\beta}{}^{*} \end{pmatrix} = \begin{pmatrix} I_{L\alpha 5}\sin(w_5 t+\lambda_5)+I_{L\alpha 7}\sin(w_7 t+\lambda_7)+I_{L\alpha 7}\sin(w_7 t+\lambda_7) \\ I_{L\beta 5}\cos(w_5 t+\lambda_5)+I_{L\beta 7}\cos(w_7 t+\lambda_7)+I_{L\beta 7}\cos(w_7 t+\lambda_7) \end{pmatrix} \quad (2.40)$$

After transforming the hybrid power filter current into the same reference frame, the error signal is obtained by subtracting it from the reference current vectors ($I_{L\alpha}{}^{*}$, $I_{L\beta}{}^{*}$). Even though the compensating current references only include harmonics, the error signal still contains the 50 Hz component of the filter current. Hence, the unavoidable 50 Hz component is eliminated from the error signal by applying another Park Transformation and HPF operation respectively. As a result, the error signal ($error_{dh}$, $error_{qh}$) which contains only the oscillating harmonic components are obtained.

Similar to feedback control described in Section 2.2.2.1.1, DC link voltage control is obtained by a proportional plus integral (PI) regulator. The output reference of the PI controller (ΔI_{d1}) should be added to the reactive current component to generate a fundamental voltage in phase with the leading current of the passive filter. However, it is not applicable to add "ΔI_{d1}" to "$error_{dh}$" on the rotating reference frame.

Finally, the error signals "$error_{dh}$ and $error_{qh}$", obtained in d-q reference frame, are transformed into α-β reference frame and amplified with a proportional constant of "K" to obtain a compensating voltage reference. The compensating voltage and the DC link references are eventually added and transformed into stationary abc reference frame ($V_a{}^{*}$, $V_b{}^{*}$, $V_c{}^{*}$) which are modulated to obtain the gate pulses of the semiconductor switches.

The proposed method assures removing the 150Hz components from the compensation references of the hybrid power filter and given for 5^{th}, 7^{th} and 11^{th} harmonics (Fig 2.12). It is clear that, obtaining the current harmonic references in α-β

reference frame for each harmonic frequency increases the computation load of the control system. In the digital implementation of the proposed method, 40us sampling time is sufficient to perform all these calculations. However, if the number of the dominant harmonics to be compensated increase, the indicated sampling time may be insufficient thus decreases the system performance. It can be concluded that, the proposed voltage reference generation method is applicable to eliminate few critical harmonics of the load.

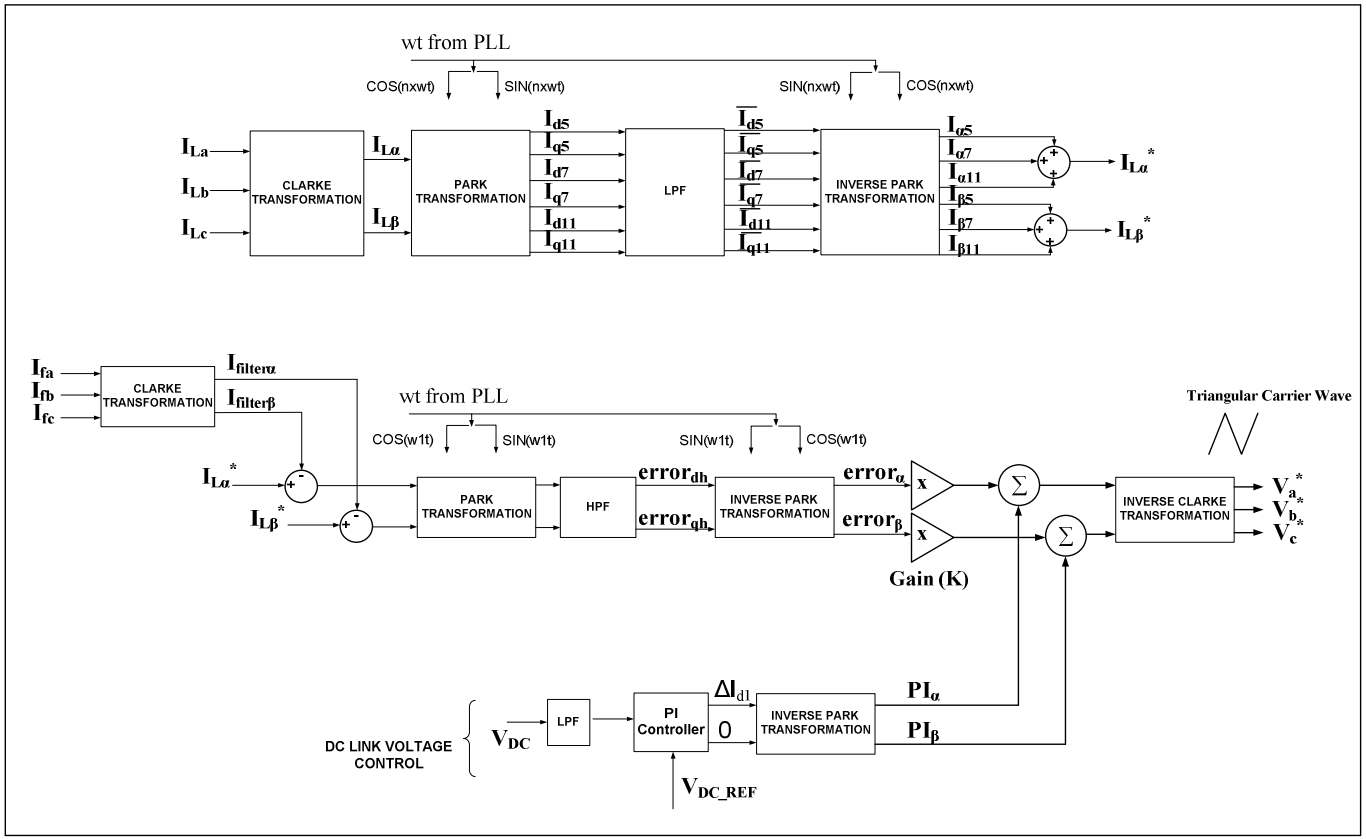

Fig 2.12 Proposed Voltage Reference Generation Method to Exclude 3rd Harmonics

2.2.2.3 Waveform Modulation Method

The voltage references (Va*, Vb*, Vc*) of both conventional and proposed method are modulated in the same way. In order to obtain the gate signals of the semiconductors Sinusoidal Pulse Width Modulation is utilized (Fig 2.13). PWM switching patterns are obtained by comparing the reference signals with the triangular carrier wave at a high frequency (generally 10-15 kHz).

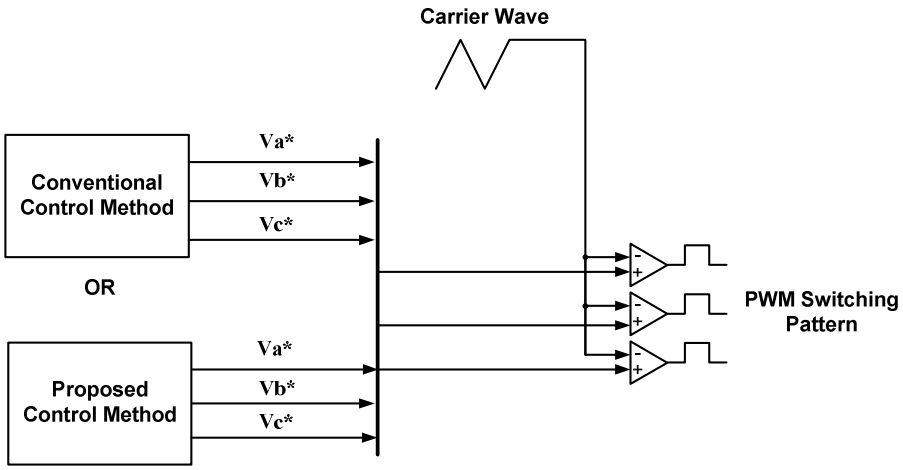

Fig 2.13 Waveform Modulation Method

In Section 3.4.2, it is shown that the performance of the conventional control method can be increased by combining the proposed voltage feedforward control. Moreover, in Section 3.4.3, the system is simulated for conventional and proposed control methods in the existence of 3rd harmonics respectively for the same DC link voltage level. It is shown that, the existence of third harmonics causes over modulation with the conventional method and an increase on DC link voltage is required.

CHAPTER 3

CIRCUIT DESIGN FOR HYBRID POWER FILTER PROTOTYPE

3.1 Harmonic Content of the Load Obtained by Measurement Results

In TÜBİTAK Space Technologies Institute, presence of diode rectifier loads (including especially the personal computer loads) results in distorted current at 400V low voltage side. In order to determine the capacity of the hybrid power filter, measurements are performed as a preliminary design work. In this Section, the measurement results are given to show the amount of distortion at supply current. Three phase current and voltage raw data are stored during 6 hours period with a sampling rate of 6400 sample/sec. The raw data are processed with 10 cycle resolution and values are restored as 3 second averages as indicated in the harmonic standard [8]. Distorted line current waveforms for each phase are given in Fig 3.1, Fig 3.2 and Fig 3.3 respectively. In order to show the amount of the distortion in the current, harmonic components are represented in terms of maximum demand load current (I_L). As described in Section 1.1, maximum demand load current is calculated by the average of the last twelve monthly peak demand. However, since the measurement duration is 6 hours, peak demand is taken as the maximum of the fundamental current component of 15 minutes averages (Fig 3.4, Fig 3.5). Odd harmonics of each phase are shown in terms of both magnitude and percent of I_L (Fig 3.6 to Fig 3.14). Limit value defined in IEEE 519 standards is drawn with a red line for each harmonic component.

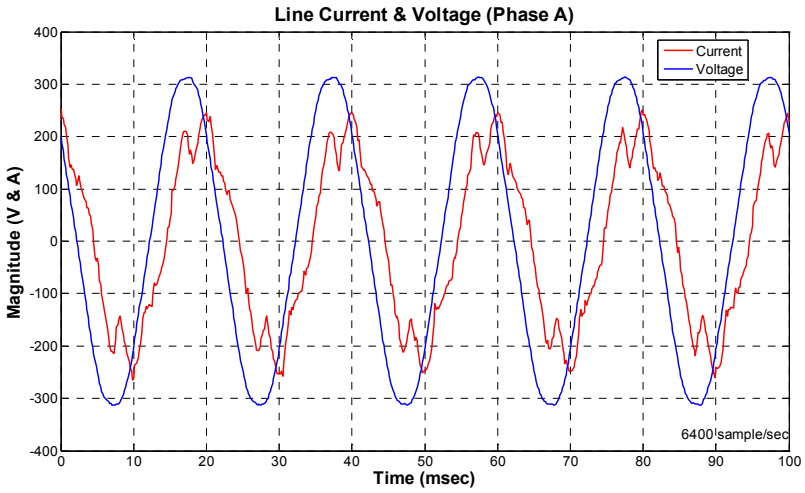

Fig 3.1 Line Current and Voltage (Phase A)

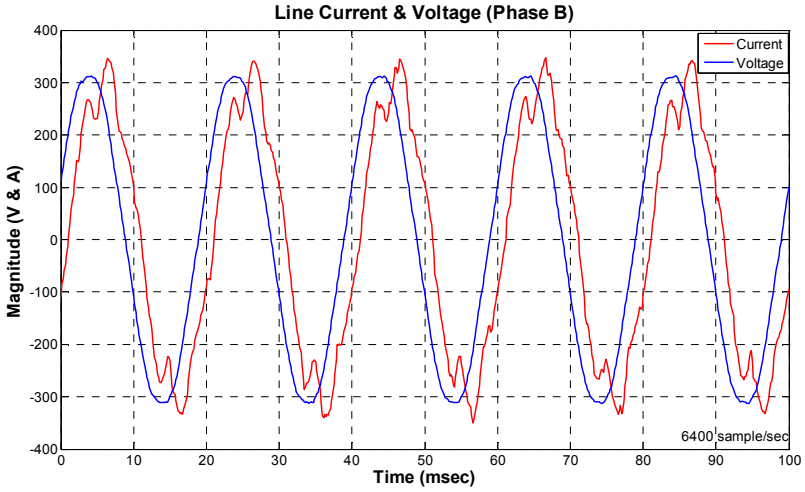

Fig 3.2 Line Current and Voltage (Phase B)

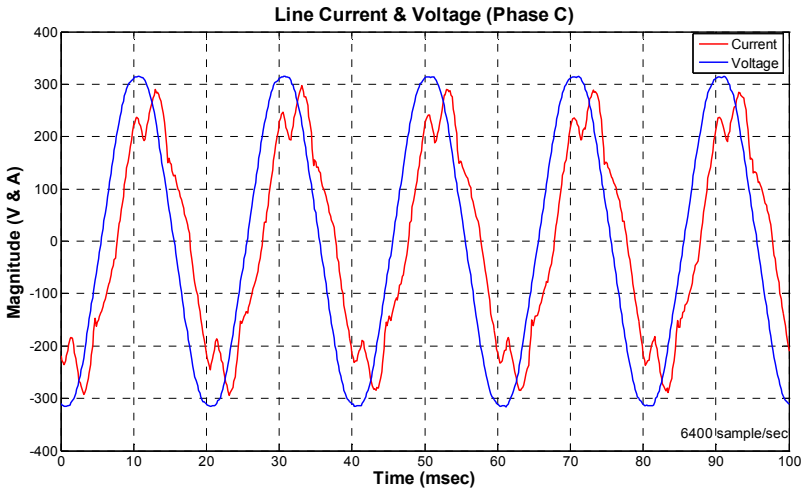

Fig 3.3 Line Current and Voltage (Phase C)

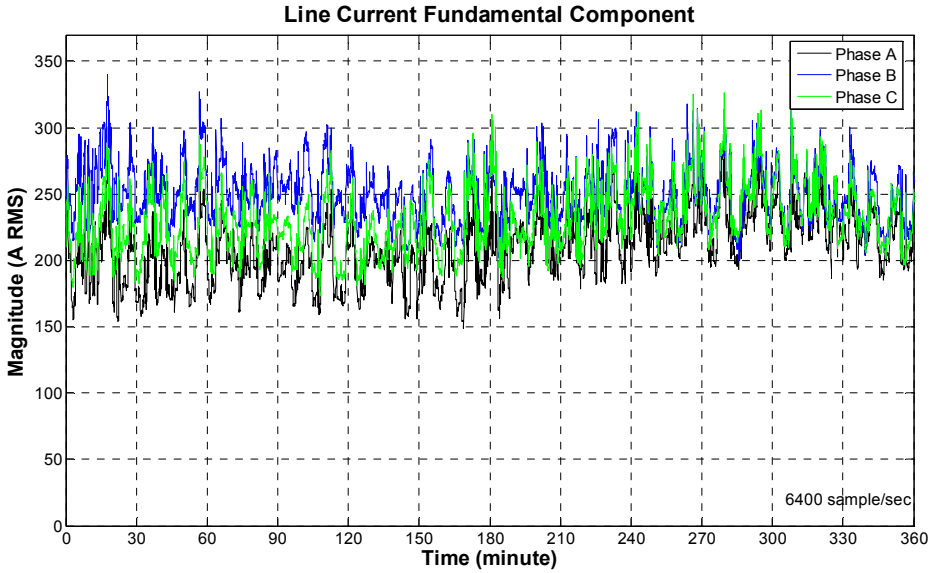

Fig 3.4 Fundamental Component of Line Current (3 sec. average, Field Data)

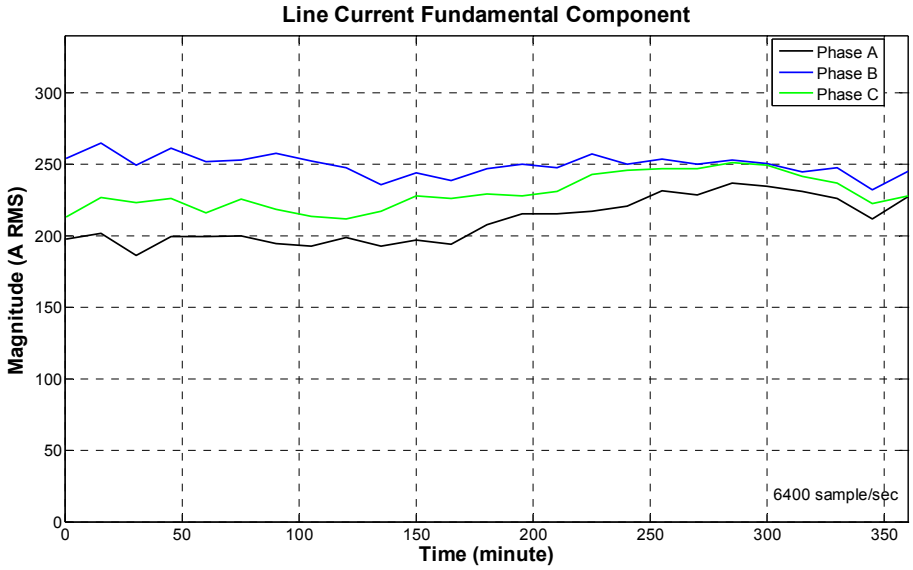

Fig 3.5 Fundamental Component of Line Current (15 min. average, Field Data)

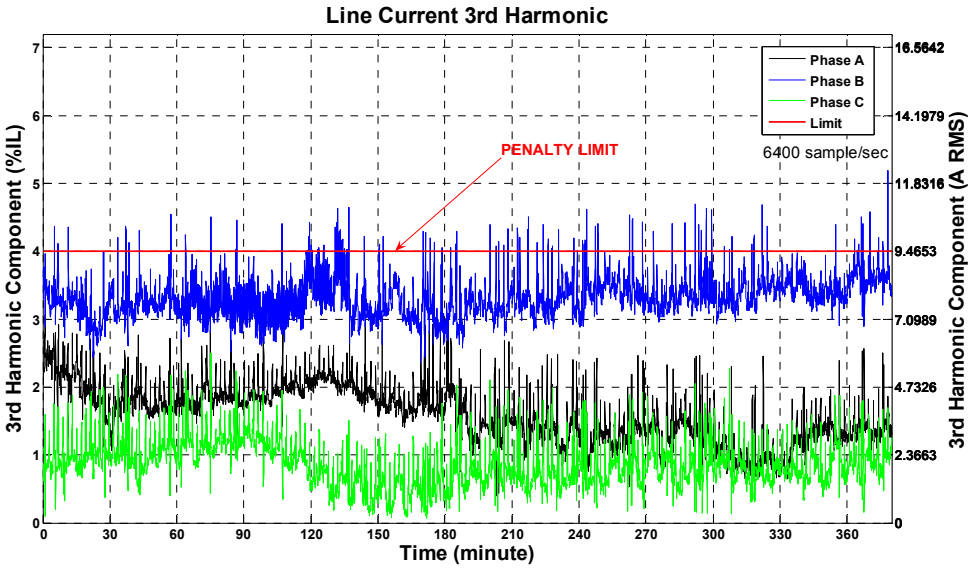

Fig 3.6 3rd Harmonic Component of Line Current (3 sec. average, Field Data)

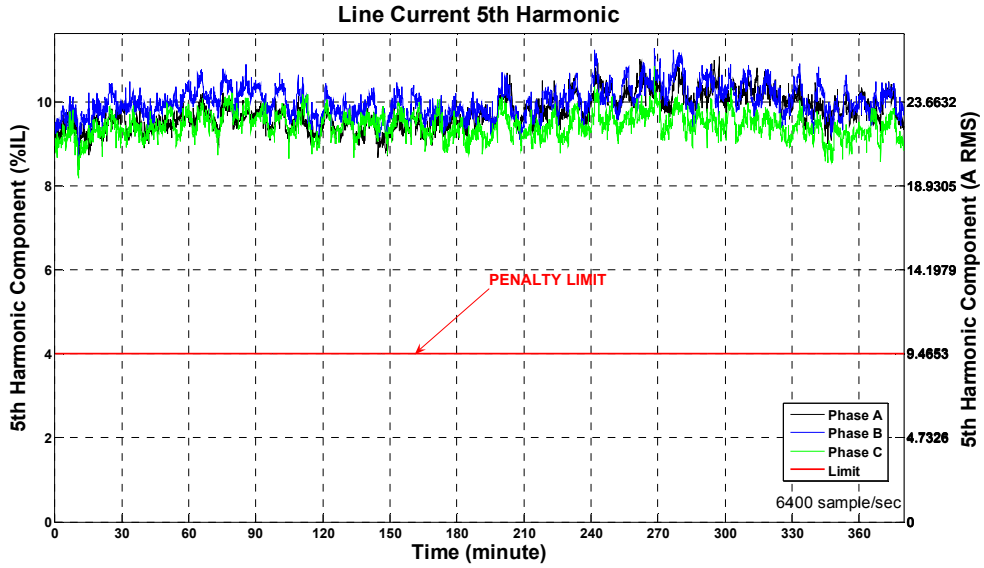

Fig 3.7 5th Harmonic Component of Line Current (3 sec. average, Field Data)

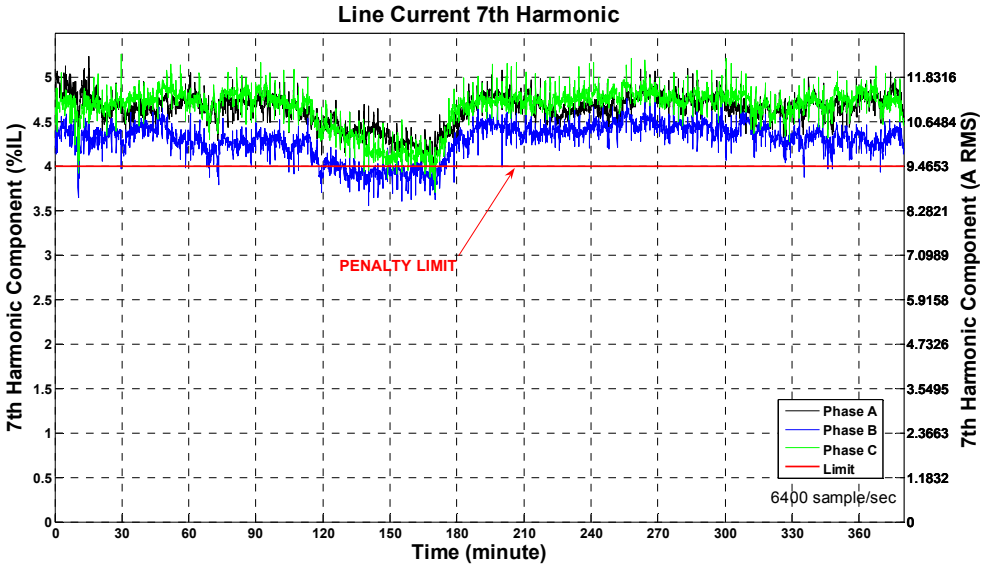

Fig 3.8 7th Harmonic Component of Line Current (3 sec. average, Field Data)

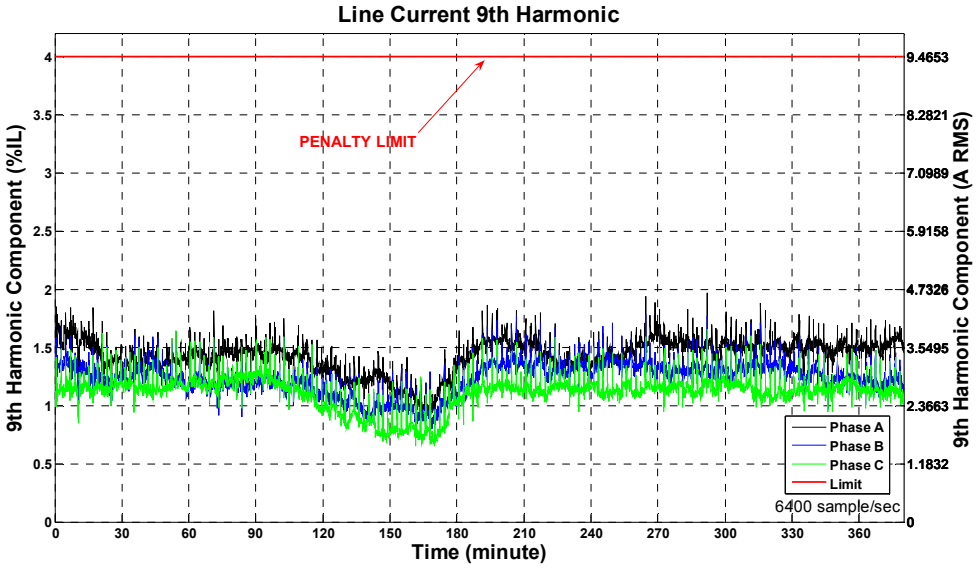

Fig 3.9 9th Harmonic Component of Line Current (3 sec. average, Field Data)

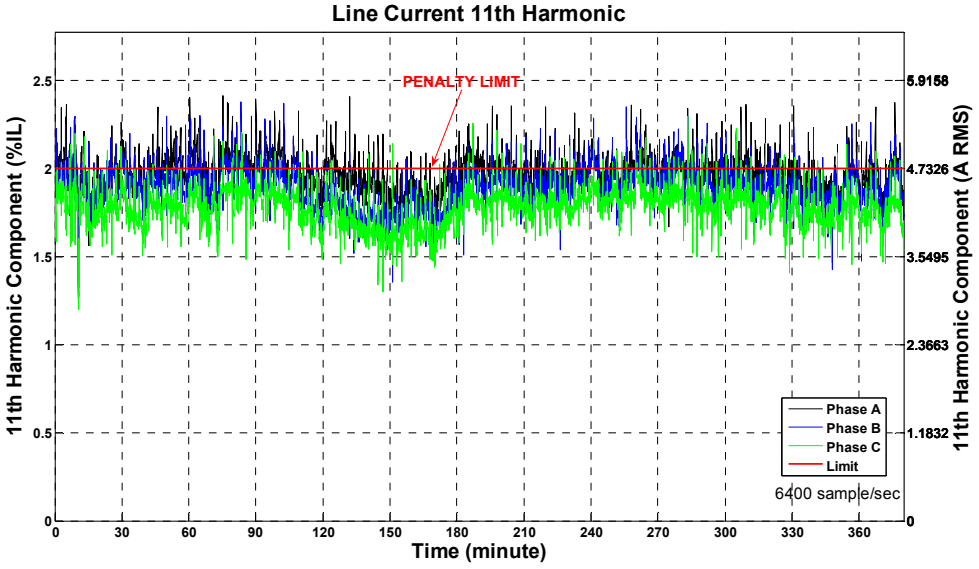

Fig 3.10 11th Harmonic Component of Line Current (3 sec. average, Field Data)

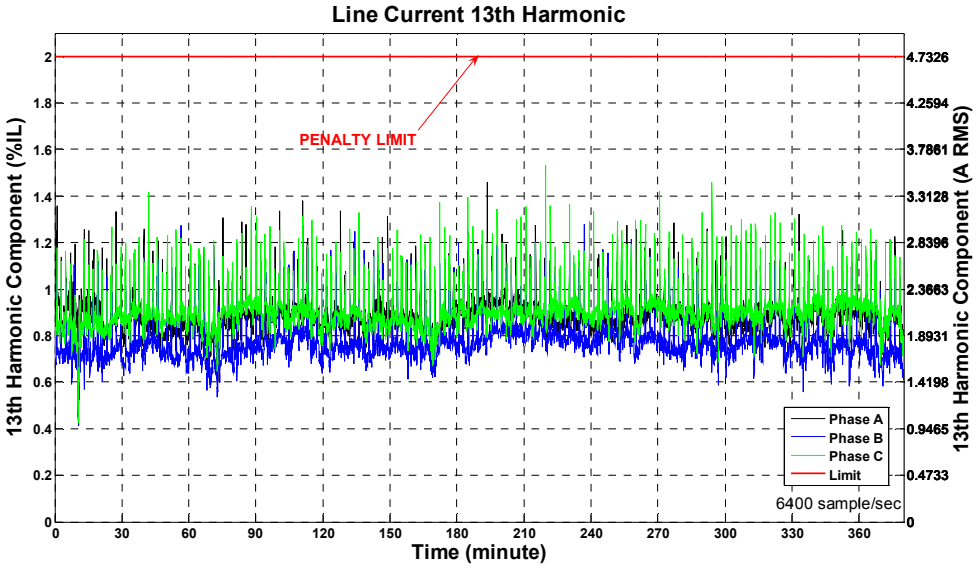

Fig 3.11 13th Harmonic Component of Line Current (3 sec. average, Field Data)

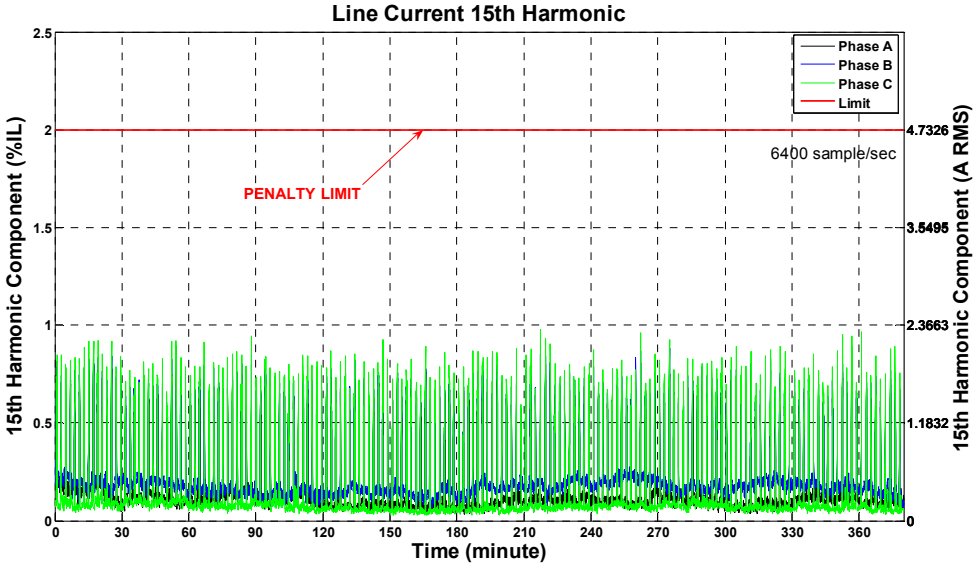

Fig 3.12 15th Harmonic Component of Line Current (3 sec. average, Field Data)

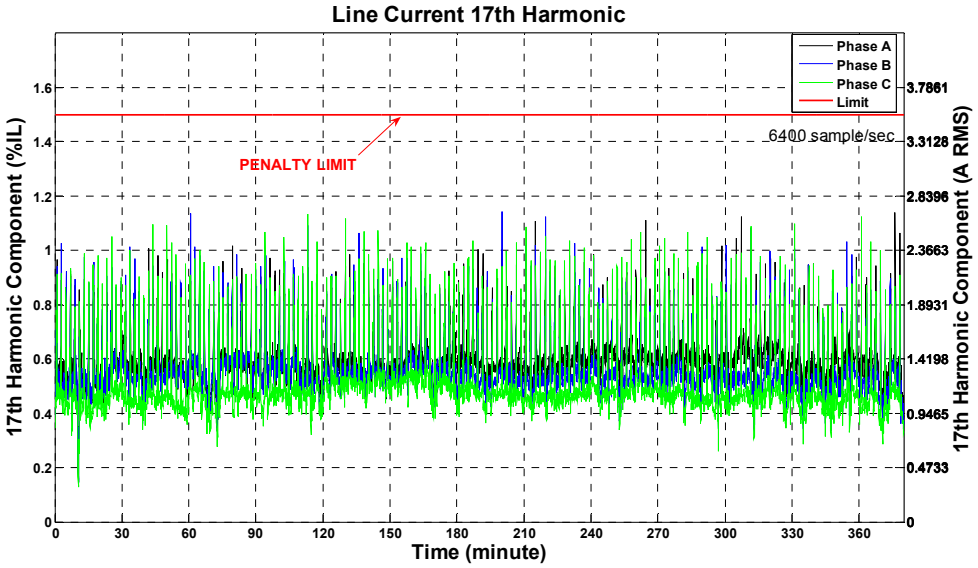

Fig 3.13 17th Harmonic Component of Line Current (3 sec. average, Field Data)

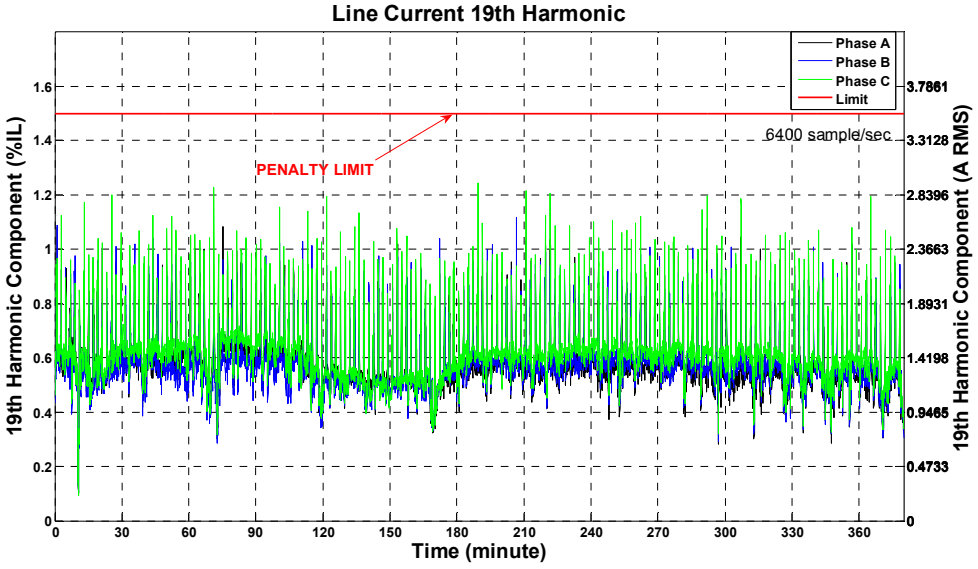

Fig 3.14 19th Harmonic Component of Line Current (3 sec. average, Field Data)

Measurement results have shown that, at TÜBİTAK Space Technologies Institute's 400V bus, 5^{th}, 7^{th} and 11^{th} harmonic components are the most dominant harmonics which are above the limits as expected. In Section 3.2.1, the measurement results are utilized in order to model the non-linear load and the system.

3.2 Simulation Model of the System

In this thesis work, simulation model of the system is formed by using EMTDC/PSCAD 4.2.0 Professional software. The transformerless hybrid power filter system is modeled, simulated and analyzed in PSCAD 4.2.0 environment [53]. Moreover, AC analysis of the passive filter is performed by using Ansoft Simplorer 7.0 software [54].

In order to achieve compatibility with the experimental system, instead of using the available mathematical blocks of PSCAD, the control methods described in Section 2.2.2 are developed in FORTRAN language. Moreover, theoretical results obtained by simulations are evaluated and shown by using MATLAB 6.5 [55].

3.2.1 Load Modeling

The measurement results represented in Section 3.1 indicates that, 5^{th}, 7^{th} and 11^{th} harmonics are the most dominant current harmonics existing at TÜBİTAK Space Technologies Institute. The magnitude of the most dominant harmonics is nearly 30 A_{RMS}. By considering the possibility of new computer loads in future, VSC based Hybrid Active Power Filter is designed to have a 50 A_{RMS} harmonic current filtering capacity.

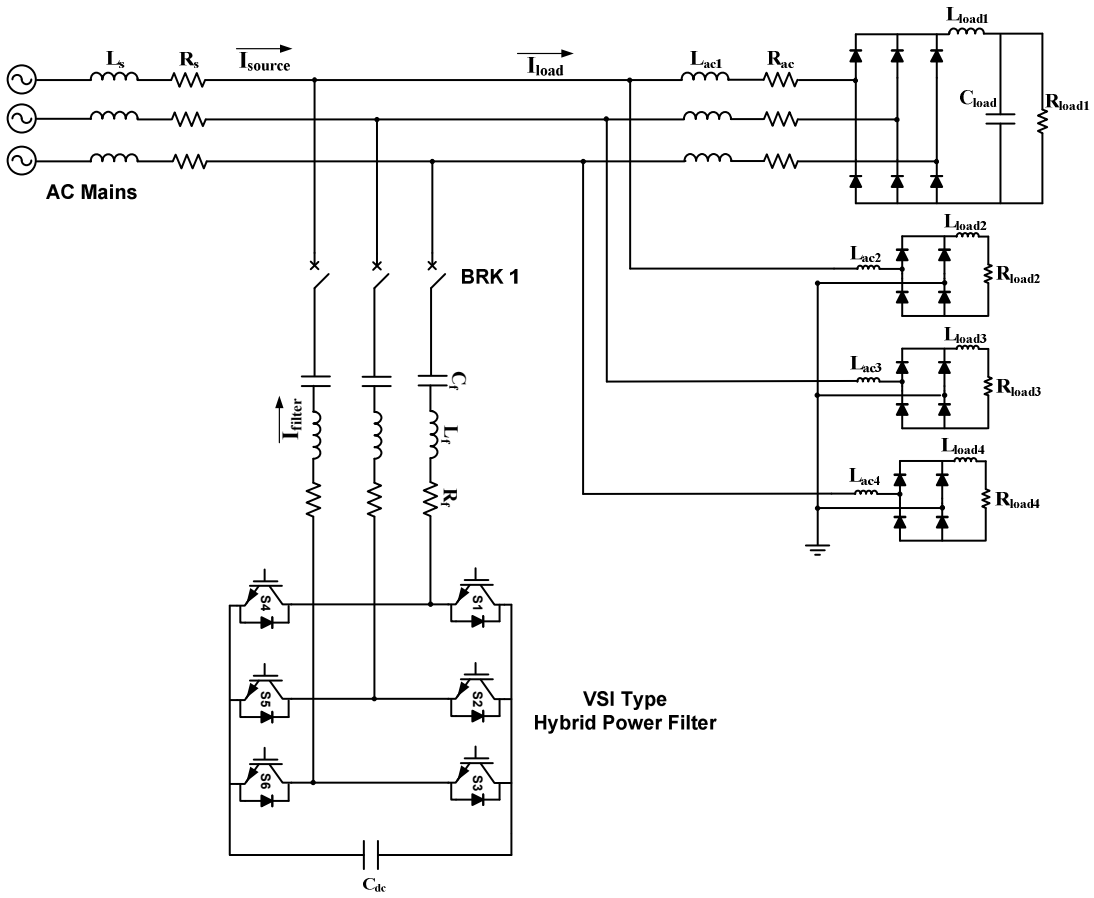

Fig 3.15 Simulation Model of the Transformerless Shunt Hybrid Power Filter

In Fig 3.15, three phase representation of the Hybrid power filter and the non-linear load is represented. In addition to 5^{th}, 7^{th} and 11^{th} harmonics, 3^{rd} harmonics are also observed (Fig 3.6) at the source side due to the fluorescent lamp loads. So, in the non-linear load model, single phase rectifiers with RL load are also used to introduce 3^{rd} harmonic.

The existing system includes a 34.5/0.4kV delta-wye transformer at the AC line. In simulation work, it is modeled as an AC voltage source ($400V_{line}$, 50Hz) in series with the transformer's leakage reactance. The parameters L_s and R_s are calculated as given below:

S=1.25MVA (VA rating of the transformer)

$U_k = 6\%$

So, the 400V secondary side of the transformer is referred as follows;

$$L_s = \frac{V^2}{S} \times U_k \times \frac{1}{2\pi 50} \cong 25\text{uH} \tag{3.1}$$

$$R_s = \frac{2\pi 50}{10} \times L_s \cong 0.77\text{m}\Omega \tag{3.2}$$

Table 3.1 System Parameters

Line Voltage	400 V-rms
Line frequency	50 Hz
Supply inductance (L_s)	25 uH
Filter Capacitor (C_f)	0.6 mF
Filter Inductance (L_f)	365 uH
Tuned freq. of series filter	340 Hz
DC link capacitor (C_{dc})	7 mF
Load Inductances(L_{ac1}, L_{ac2}, L_{ac3}, L_{ac4})	0.5mH, 2.5mH, 1.5mH, 2.5mH
Load Inductances(L_{load1}, L_{load2}, L_{load3}, L_{load4})	2mH, 3mH, 3.5mH, 3mH
Load Resistances(R_{load1}, R_{load2}, R_{load3}, R_{load4})	3Ω, 2Ω, 1.5Ω, 1.8Ω
Load Capacitor (C_{load})	2mF

When the system is simulated under the non-linear load condition given in Fig 3.15 and Table 3.1, the harmonic spectrum of the load current which is similar to measurement results is shown in Table 3.2. The distorted current waveform of the source current and mains voltage are shown in Fig 3.16 and Fig 3.17 respectively.

Table 3.2 Harmonic Spectrum of Actual Load and Simulation Load Model

A_{RMS}	Fund.	3rd	5th	7th	11th	13th	17th	19th
Measurement Results	200-250.0	~9.5	~23.0	~11.0	~4.7	~2.0	~1.4	~1.4
Simulation Load Model	225-247.0	~10.7	~23.6	~12.5	~4.86	~3.24	~1.9	~1.4

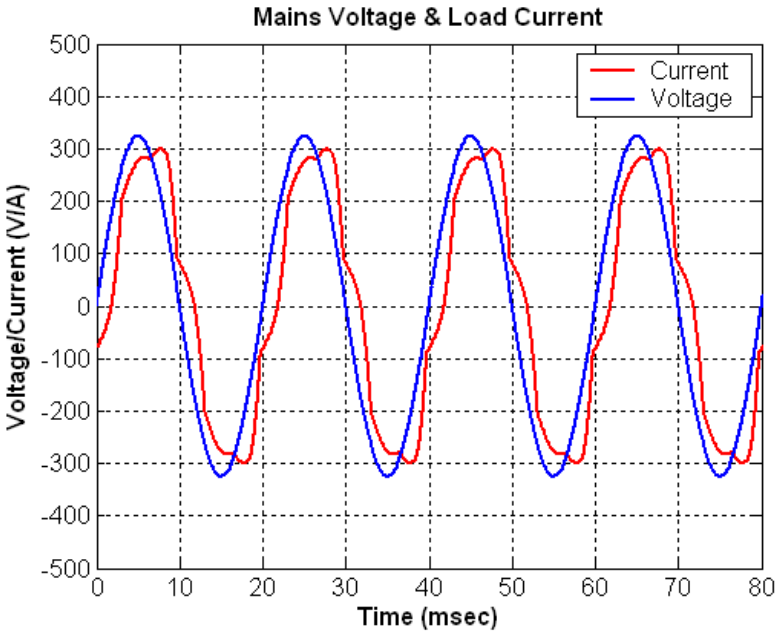

Fig 3.16 Mains Voltage and Load Current

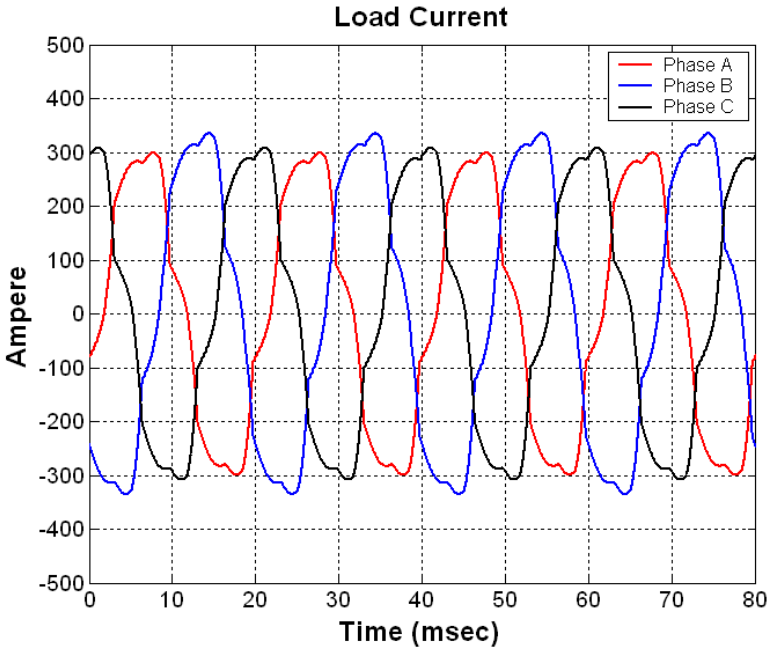

Fig 3.17 Load Current

3.3 Design of Circuit Elements

3.3.1 Passive Filter Capacitor and Reactor

The series connected capacitor (C_F) and the filter reactor (L_F) forms a LC passive filter. So that, the LC filters should be chosen to eliminate the most dominant 5^{th} or 7^{th} harmonic of the diode rectifier load. Although the 5^{th} harmonic component of the non-linear load is the most dominant component, it is reasonable to tune the LC filter at seventh harmonic frequency. The passive filter tuned to 350 Hz shows lower impedance at 550 Hz and 650 Hz than a passive filter tuned to 250 Hz. Moreover, the passive filter tuned to 7^{th} harmonic frequency is less bulky than a 5^{th} harmonic filter for the same filter capacitor (C_F) [56].

The characteristic impedance of the passive filter (Z) is defined as given in (3.3). The filtering performance of the passive filter is determined by this impedance except for

resonant frequency. Therefore, the capacitance value should be as high as possible and inductance value should be as low as possible to obtain low characteristic impedance.

$$Z = \sqrt{\frac{L_F}{C_F}} \tag{3.3}$$

However large capacitance value makes the passive filter bulky and results in a high reactive current. Selecting a low inductance value also increases the switching ripples. By considering all these criteria and to minimize the initial cost of the system, a 30 kVAR passive filter at 400V line voltage tuned around 340Hz is decided to used in the hybrid power system. L_F, C_F parameters are calculated as follows:

$$Q = \frac{V^2}{|Z_c|} \Rightarrow 30kVAR = \frac{400^2}{|Z_c|} \Rightarrow |Z_c| = 5.33 \tag{3.4}$$

$$|Z_c| = \frac{1}{2\pi fC} \Rightarrow 5.33 = \frac{1}{100\pi C} \Rightarrow C \cong 0.6\ mF \tag{3.5}$$

$$f_{tuned} = \frac{1}{2\pi\sqrt{LC}} \Rightarrow 340 = \frac{1}{2\pi\sqrt{L \times 0.6m}} \Rightarrow L \cong 365\ uH \tag{3.6}$$

LC passive filter tuned to 350 Hz shows low impedance at 7th harmonic frequency but it amplifies the harmonic components around 250 Hz. The amplification phenomenon and the damping of the active power filter are shown in this part by single phase analysis of the passive filter.

In (Section 2.1, Fig 2.2) single phase and harmonic equivalent circuit of the hybrid filter with the feedback control is presented. If the active power filter is not connected to the system (K=0), the relationship between the source and the load harmonic currents are obtained as follows:

$$I_{sh} = \frac{Z_{fh}}{Z_{fh} + Z_{sh}} \tag{3.7}$$

By using the single phase equivalent circuit given in Section 2.1, the load is modeled as an ideal current source. AC analysis results of the passive filter specified above shows that, the current components between 230 Hz and 320 are amplified when only the passive filter is connected to the system (Fig 3.18). However, when active power filter is joined with the feedback control, the feedback gain K acts as a damping resistor which suppresses the resonance between the supply and the passive filter. As shown in Fig 3.19, if the feedback gain is increased, the harmonic content of the source current decreases significantly. However, feedback gain is limited to certain values in order to avoid stability problems in the control loop of the active power filter.

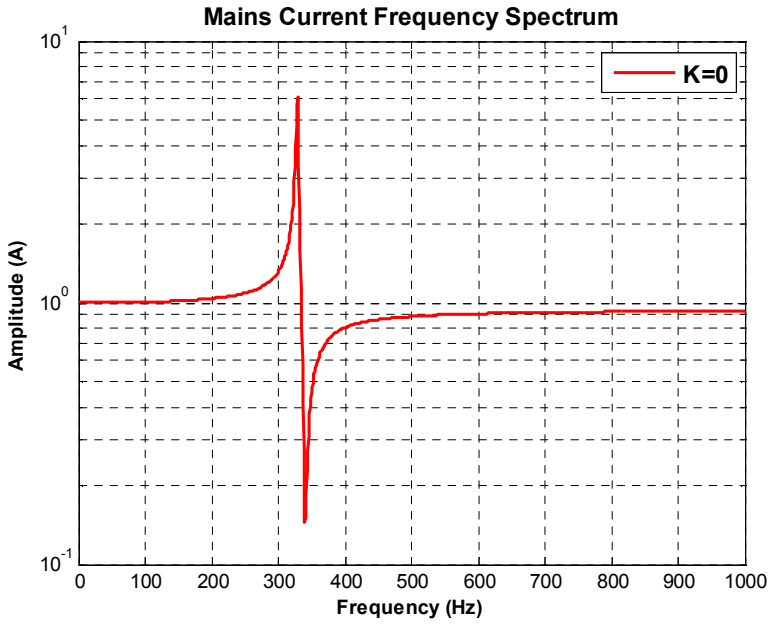

Fig 3.18 Mains Current Frequency Spectrum (Passive Filter)

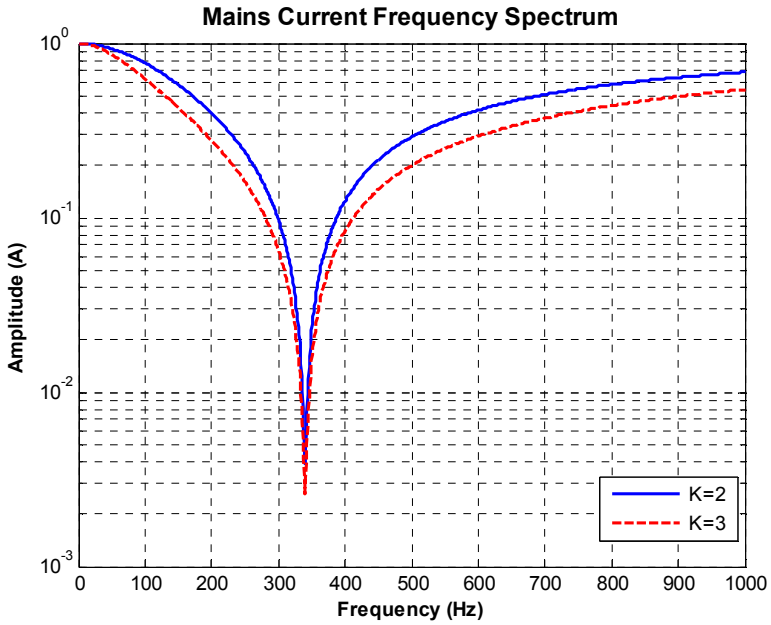

Fig 3.19 Mains Current Frequency Spectrum (Hybrid Power Filter)

3.3.2 Power Converter

The power converter of the hybrid power filter is a three phase voltage source PWM converter. It is composed of six semiconductor switches (IGBTs) with their antiparalel diodes, and DC link capacitor (Fig 3.20). Each IGBT is directly subjected to hybrid filter current and DC link voltage. The harmonic current capacity of the hybrid power filter is decided to be $50A_{RMS}$ by considering the load condition of system (Section 3.1). Moreover, the selected passive filter capacitor also introduces nearly $45A_{RMS}$ leading current component at fundamental frequency. Therefore, at steady state operation, the nominal current passing through at each line is about $70A_{RMS}$.

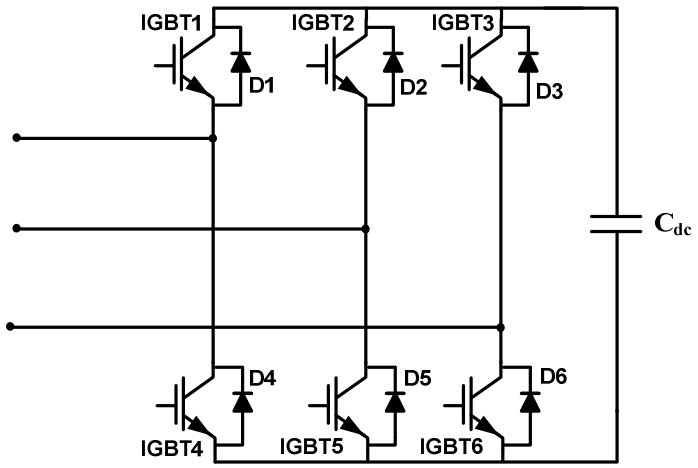

Fig 3.20 Voltage Source Converter

However, the DC link voltage is not as crucial as the current specification of the semiconductor device because the DC link voltage is quite below when compared with a pure shunt connected active power filter [52, 57]. 250V to 6.6kV IGBT modules are commercially available on the market. However, for a low rated converter topology, it is not reasonable to form the inverter with single IGBT packages due to the design complexity of the busbar and higher cost. Therefore, 6-pack intelligent power modules (IPM) with their high speed, low loss and optimized gate drives are seem to be an appropriate solution for this application.

3.3.3 DC Link

In conventional pure shunt connected voltage source active power filters, DC link voltage is required to be higher than the peak value of the utility voltage; otherwise, the generated compensation currents cannot be injected to the mains [57]. However, transformerless hybrid power filter provides a reduced DC link voltage.

So, the DC link voltage is kept as low as possible while observing the filtering performance of the system. The optimum DC link voltage is found by means of

simulation as shown in Section 3.4.1, 3.4.2 and 3.4.3. The selection of the DC link capacitor is also based on simulation analysis to minimize the voltage ripple. As can be seen from theoretical results, 7mF DC link capacitor is complying with the minimum voltage ripple criteria of the DC link voltage. However, ripple current rating, power loss, temperature rise of the capacitor and the life time of the component should also be analyzed for the experimental set up. In Section 4.1.2, the design guide is also provided for the experimentally utilized DC link capacitor.

3.4 Theoretical Results

Theoretical results are obtained for the system given in Fig 3.15, using PSCAD software in a way to minimize the DC link voltage and the rating of the APF, while keeping the filtering performance satisfactory. In this part of the thesis, firstly the theoretical results obtained with the conventional control method are represented. Then, the proposed control methods are investigated. The startup procedure of the system for both control methods is as follows:

- Initially, three upper IGBTs (S1, S2, S3) are turned ON and three lower IGBTs (S4, S5, S6) are turned OFF. During this time interval, active filter is not operating, and DC side of the active filter is seen as a short circuit by the mains side.
- When circuit breaker (BRK1) is closed, the system operates only as a passive LC filter
- After DC link voltage is built up to the specified reference value, the compensation current references are activated in the control loop of the system and hybrid power filter totally operates.

3.4.1 Theoretical Results Obtained by Conventional Control Method

In this part, the single phase rectifiers given in Fig 3.15 are replaced with single RL loads in order to exclude 3rd harmonics and the harmonic content of the load is increased to nearly $50A_{RMS}$. The effects of the 3rd current harmonics on the conventional control method are shown in Section 3.4.3. The simulation model and the parameters of the system are given in Fig 3.21 and Table 3.3 respectively.

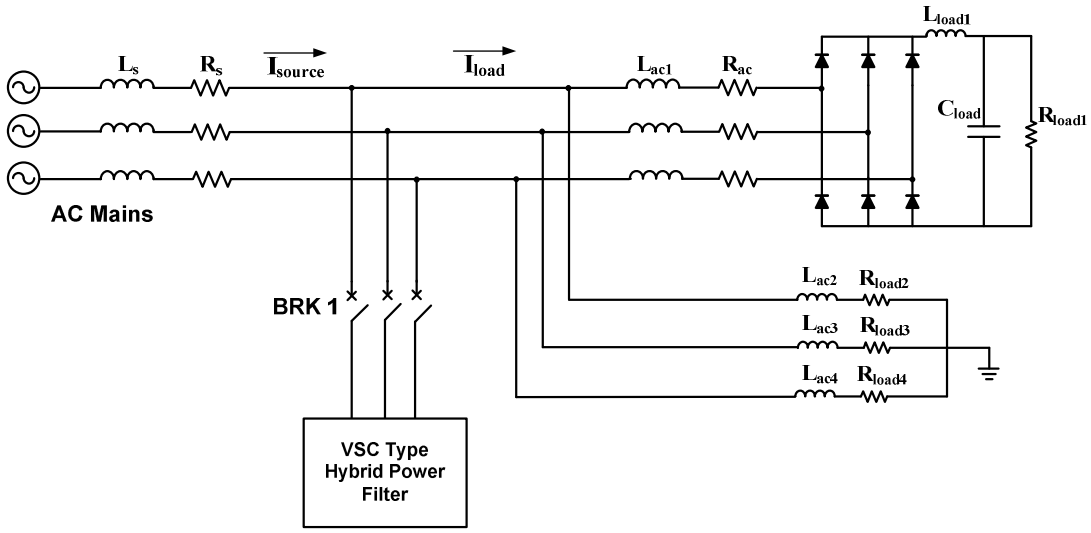

Fig 3.21 Simulation Model Used for Conventional Control Method

Table 3.3 Simulation Parameters

Line Voltage	400 V-rms
Line frequency	50 Hz
Supply inductance (L_s)	25 uH
Rectifier inductance (L_l)	0.1 mH
Filter Capacitor (C_F)	0.6 mF
Filter Inductance (L_F)	365 uH
Tuned freq. of series filter (f_{tuned})	340 Hz
DC link capacitor (C_{DC})	7.05 mF
Load Resistances(R_{load1}, R_{load2}, R_{load3}, R_{load4})	2.1Ω, 2Ω, 2 Ω
Load Inductances(L_{load1}, L_{load2}, L_{load3}, L_{load4})	2mH, 10uH, 10uH, 10uH
Load Inductances(L_{ac1})	0.15mH
Load Capacitor (C_{load})	2mF

"Table 3.3 Cont'd"

Switching frequency ($f_{switching}$)	10kHz
Simulation Step Time	10usec
Feedback Gain (K)	2

Harmonic content of the supply current is obtained by Synchronous Reference Frame method as described previously. The phase information of the supply voltage is obtained by a PLL system, as given in Section 2.2.2.1.1. As can be seen from Fig 3.22, the phase angle information (w_1t) is locked to the supply voltage between 0-2π which is utilized in the transformation matrices.

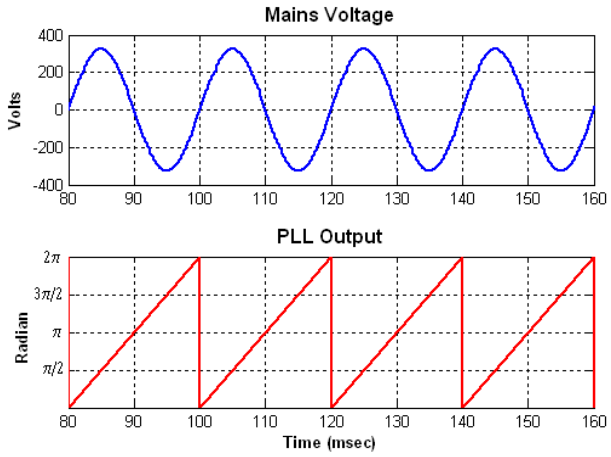

Fig 3.22 Phase Locked Loop (PLL) Output at Steady State

In Fig 3.23 and Fig 3.24 simulation results obtained during the start up procedure are shown. At t=80 ms, circuit breaker (BRK1) is turned on and 7th tuned LC passive filter starts to operate. The performance of the filter is similar to the results of the single phase analysis with zero feedback gain described in Section 3.3.1 (Fig 3.18). After several cycles (t=300 ms), the voltage reference (ΔI_{d1}) required to built up the DC link voltage to 120V is activated. Filter current and DC link voltage response during this interval is represented in Fig 3.24.

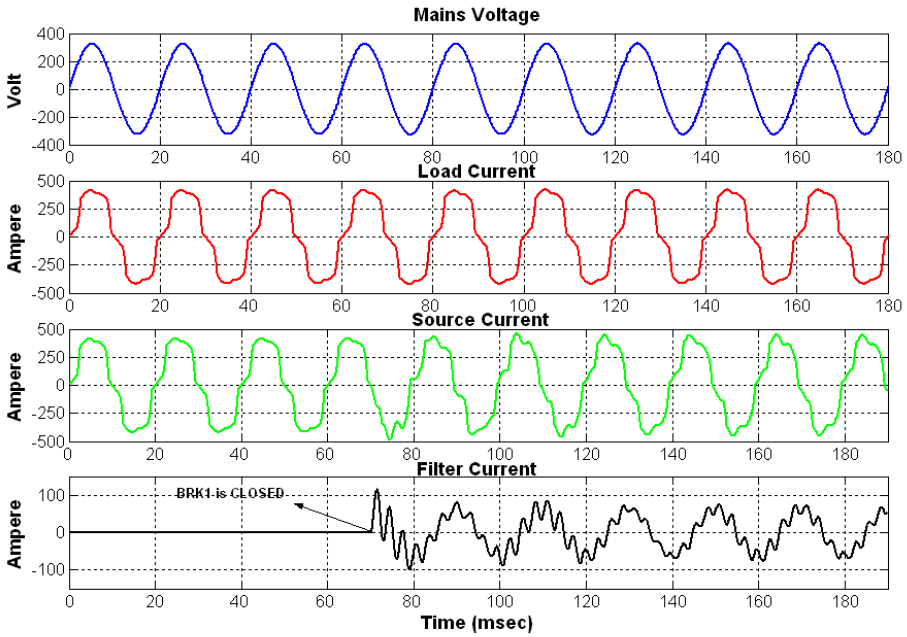

Fig 3.23 During Start Up, Mains Voltage (200V/div), Load Current (250A/div), Source Current (250A/div), Filter Current (100A/div)

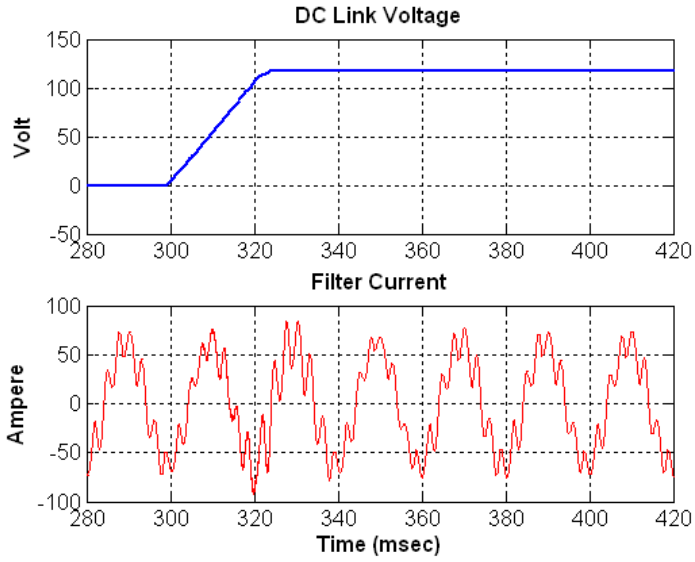

Fig 3.24 DC Link Voltage Built Up,
DC Link Voltage (50V/div), Filter Current (50A/div)

When DC link capacitor voltage is set to 120V, the voltage references (V_{afb}^{*}, V_{bfb}^{*}, V_{cfb}^{*}) obtained in the feedback control loop are activated (Fig 3.25). The mains current becomes a sinusoidal waveform, DC link voltage is kept constant at 120V and filter current is ripple free (Fig 3.26, Fig 3.27). The filtering performance of the system is as expected with the single phase analysis obtained in Section 3.3.1 (Fig 3.19). The hybrid power filter damps the resonance and the amplification phenomenon at fifth harmonic frequency disappears.

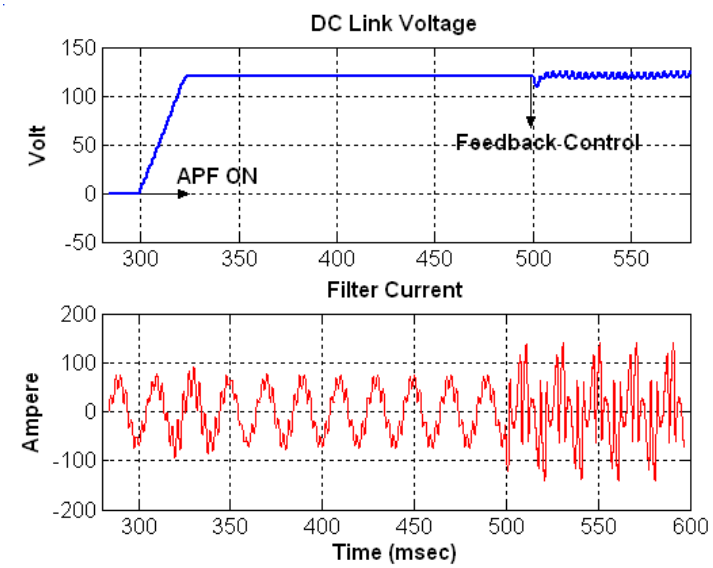

Fig 3.25 DC Link Voltage (50V/div), Filter Current (100A/div)

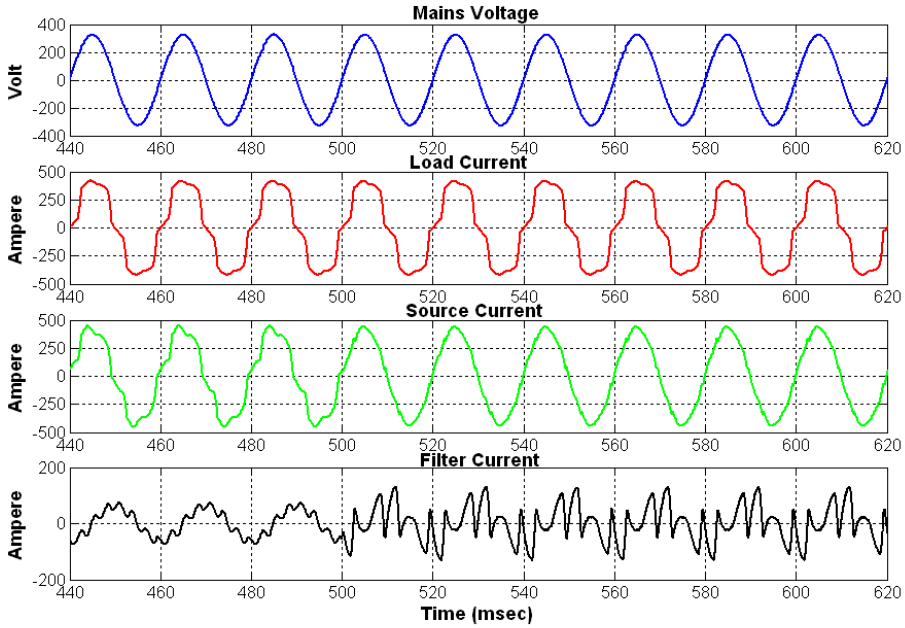

Fig 3.26 Hybrid Power Filter Steady State Results with Feedback Control
Mains Voltage (200V/div), Load Current (250A/div),
Source Current (250A/div), Filter Current (200A/div)

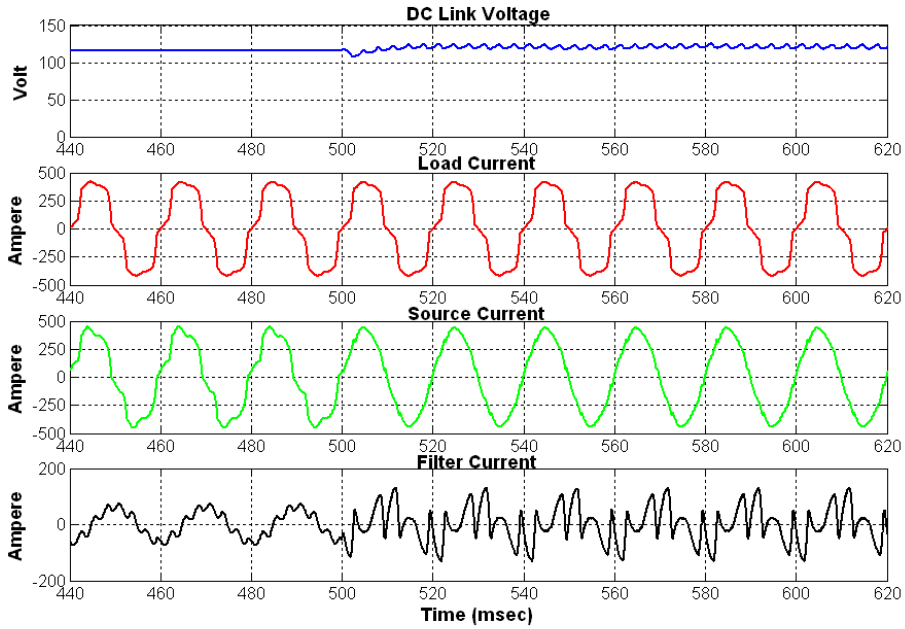

Fig 3.27 Hybrid Power Filter Steady State Results with Feedback Control
DC Link Voltage (50V/div), Load Current (250A/div),
Source Current (250A/div), Filter Current (200A/div)

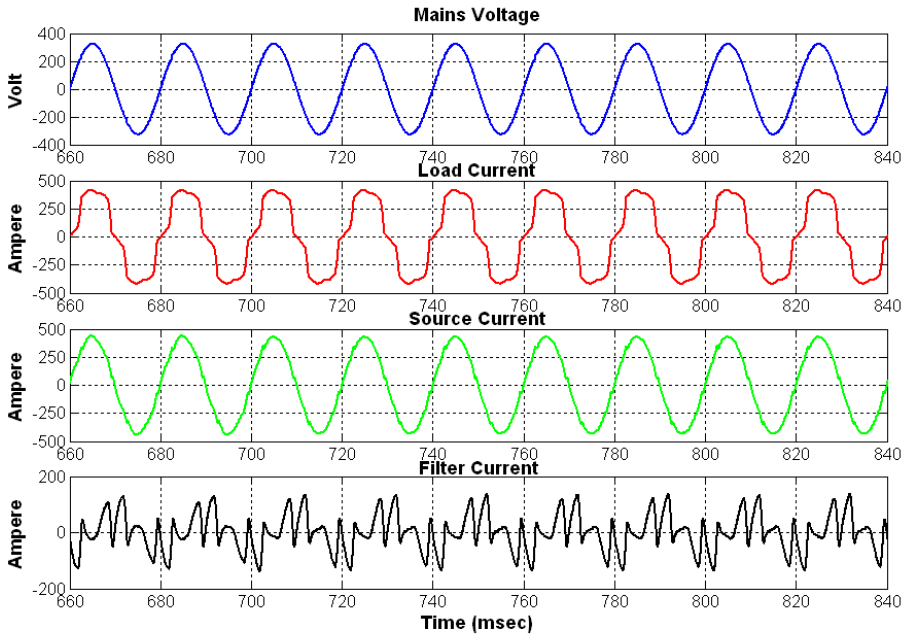

Fig 3.28 Hybrid Power Filter Steady State Results with Feedback and Feedforward Control, Mains Voltage (200V/div), Load Current (250A/div), Source Current (250A/div), Filter Current (200A/div)

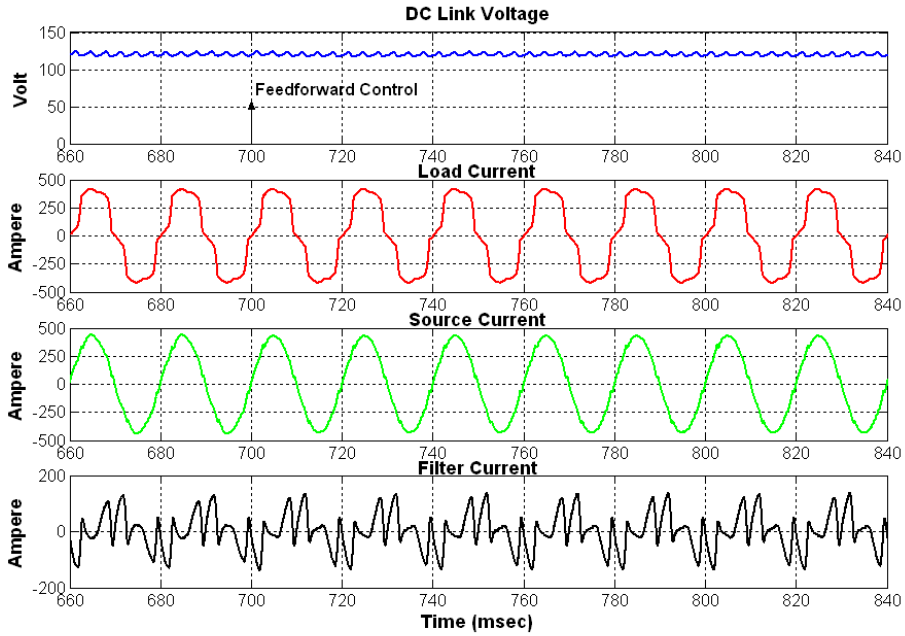

Fig 3.29 Hybrid Power Filter Steady State Results with Feedback and Feedforward Control, DC Link Voltage (50V/div), Load Current (250A/div), Source Current (250A/div), Filter Current (200A/div)

In order to increase the filtering performance of the system at fifth harmonic frequency, the voltage references (V_{aff}^{*}, V_{bff}^{*}, V_{cff}^{*}) obtained from feedforward control are combined to the control loop (Fig 3.28, Fig 3.29). After the addition of Feedforward control, the mains current nearly becomes a pure sinusoidal waveform.

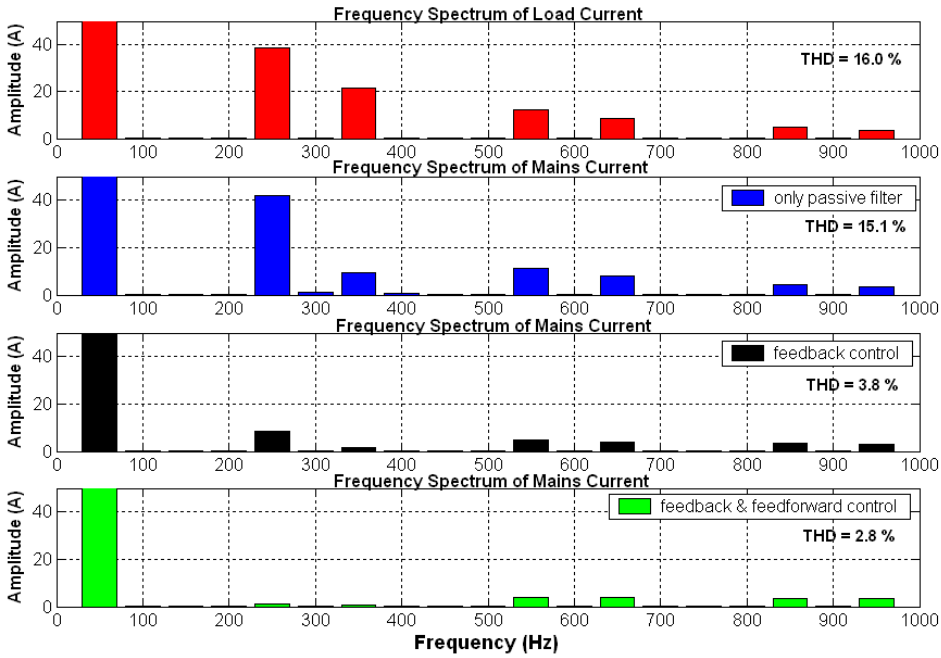

Fig 3.30 Frequency Spectrum of Load and Source Current (Fundamental=305A_{RMS})

The frequency spectrum of the mains current, under different control schemes shows the effectiveness of the feedback and feedforward control applied for the VSC based hybrid power filter (Fig 3.30). Resonance problem occurs at fifth harmonic frequency when passive filter operates alone. However when active power filter is turned on with the feedback control, the most dominant harmonics of the load are greatly reduced. Total harmonic distortion (THD) is reduced from 16.0% to 3.8%. When feedforward control is also included in the system, 9A_{RMS} reduction on the 5^{th} harmonic current component and nearly 1 % reduction on THD is obtained.

The series LC filter of the simulated hybrid filter topology results in an additional fundamental current flow through the inverter. However, the required DC link voltage is much less when compared with a standard voltage source type APF [56]. In the simulated system, the DC link voltage is kept constant at 120 VDC.

Moreover, in voltage source active power filter applications, an additional switching filter is required to isolate the mains side from high frequency ripple currents of the filter current. Although no additional switching filter is used, high frequency current ripples are also minimized with the applied system. The main disadvantage of the hybrid power filter is that, the reactive power compensation capability is limited with capacity of the used passive filter. Thus, installing hybrid power filter to PCC where reactive power compensation is critical will not be a good solution.

3.4.2 Theoretical Results Obtained by Proposed Voltage Feedforward Control Method

In this part, the effect of the existing voltage harmonics on the system which is controlled by the conventional control method (Section 2.2.2.1) is represented. The simulation parameters used in this part is similar to given in Table 3.3, except for the addition of voltage harmonics at the mains side. Then, 3% of the line voltage at 250Hz is added as voltage harmonic and the variation on the supply current is observed. Firstly, the system is simulated under different voltage harmonic conditions and only the passive filter is turned on. As can be seen from Table 3.4, the resultant effect between the existing voltage harmonics and current harmonics of the load can be either additive or subtractive according to the phase angle of the voltage harmonics.

Table 3.4 Supply Current under different supply voltage conditions

Cases	Voltage Harm.	THD %	Mains Current (A_{RMS})				
			I_1	I_5	I_7	I_{11}	I_{13}
Load	-	**16.0**	304.0	**39.0**	22.5	12.3	8.8
PF	-	**15.1**	304.0	**41.5**	11.8	11.1	8.1
PF	$7V\angle 50^\circ$	**20.0**	302	**56.0**	11.9	11.2	8.2
PF	$7V\ \angle -130^\circ$	**10.5**	305	**26.6**	11.8	11.1	8.1

(PF: only passive filter is operating)

Secondly, considering the resultant effect of the voltage harmonics given in Table 3.4, system is simulated for the worst case condition. THD values given in Table 3.5 shows that, addition of voltage harmonic significantly reduce the filtering performance.

Table 3.5 Supply Current under different control schemes

Control Scheme	Voltage Harm.	THD %	Mains Current (A_{RMS})				
			I_1	I_5	I_7	I_{11}	I_{13}
FB	-	**3.8**	305.0	**8.1**	0.7	4.4	4.1
FB + FF	-	**2.8**	305.0	**0.8**	0.7	4.4	4.1
FB	$7V\angle 50^\circ$	**4.9**	303.3	**12.0**	0.8	4.5	4.7
FB + FF	$7V\angle 50^\circ$	**3.6**	303.0	**3.5A**	0.8	4.5	4.7
FB + FF + VFF	$7V\angle 50^\circ$	**2.9**	303.0	**0.5A**	0.8	4.5	4.7

(FB: feedback control, FF: feedforward control, VFF: voltage feedforward control)

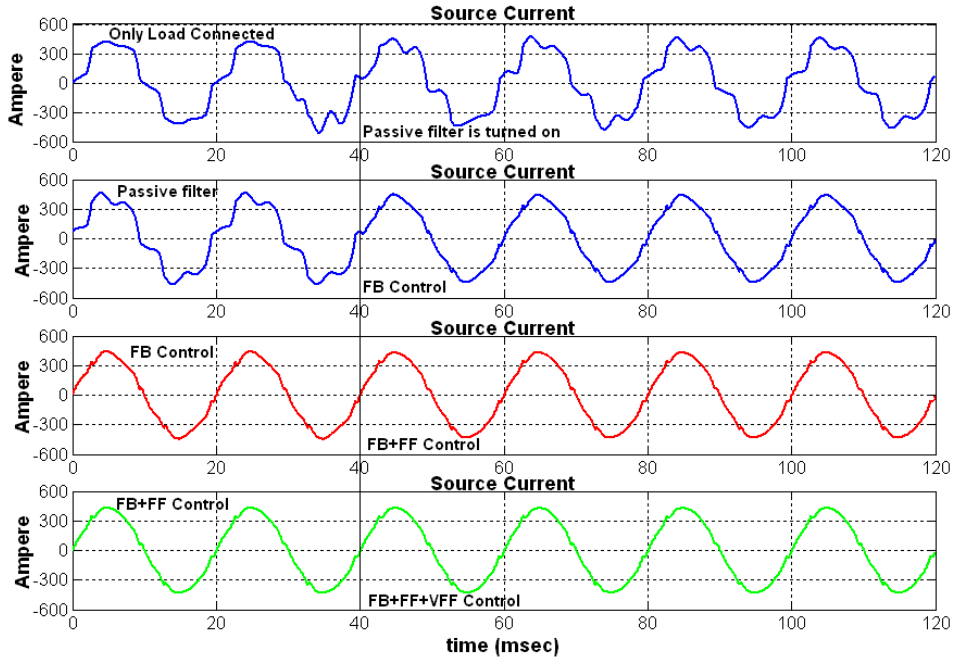

Fig 3.31 Supply Current under Different Control Schemes (FB: Feedback Control, FF: Feedforward Control, VFF: proposed Voltage Feedforward Control)

Moreover, in Fig 3.31, the variation on the source current is represented. Highly distorted current is transformed into a nearly pure sinusoidal waveform by applying feedback, feedforward and the proposed voltage feedforward control methods respectively. It is shown that, when both the conventional feedforward and the proposed voltage feedforward controls are applied with the feedback control; the filtering performance is comparable with the non voltage harmonic case (Table 3.5).

3.4.3 Theoretical Results Obtained by Proposed Voltage Reference Generation Method

Theoretical results in Section 3.4.1 show that the filtering performance of the hybrid power filter is satisfactory under the three phase diode rectifier load. However, the actual load also contains unbalanced 3rd harmonic components due to the fluorescent

lamp loads (Section 3.1, Fig 3.6). Therefore, in the conventional control method, the calculated current references [29] also include 3rd harmonic. However, the designed hybrid active power filter topology is not capable of suppressing these 150Hz components with a three phase three wire connection. Therefore, a method which excludes the third harmonic components during the reference current calculation is proposed in Section 2.2.2.2.2. Moreover, in this part the non-linear load model given in Fig 3.21 is used to obtain a harmonic content similar to that of the actual load and the parameters given in Table 3.1 are utilized in this Section.

The harmonic content of the load is lower than the previous load model used in Section 3.4.1. So that, it is not surprising to obtain a DC link voltage lower than the previous results obtained in Section 3.4.1. The filtering performance of the hybrid power filter is analyzed for various DC link voltage levels. It is observed that, 60VDC is the optimum and sufficient voltage level to greatly reduce the harmonic content of the actual load.

Similar to previous theoretical results, firstly only the passive filter is operated by closing BRK1. Then the DC link voltage reference and current references are included in the control method respectively. In Fig 3.32, the rising of DC link voltage is represented. When the DC link voltage reaches its reference 60V, the PWM converter is modulated with the error signals obtained in the proposed voltage reference generation method (Section 2.2.2.2.2, Fig 2.12) while keeping the DC link voltage constant. Fig 3.33 and Fig 3.34 shows that the after t=800ms, hybrid power filter is totally operating with the proposed control method. The harmonic content of the supply current is greatly suppressed for each phase, while keeping the DC link voltage at very low level (Fig 3.35, Fig 3.36).

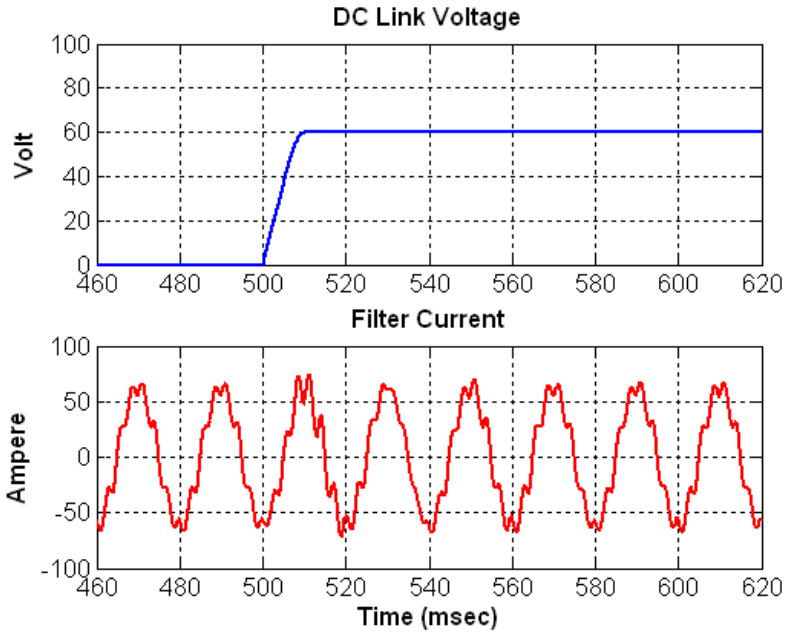

Fig 3.32 DC Link Voltage Built Up
DC Link Voltage (20V/div), Filter Current (50A/div)

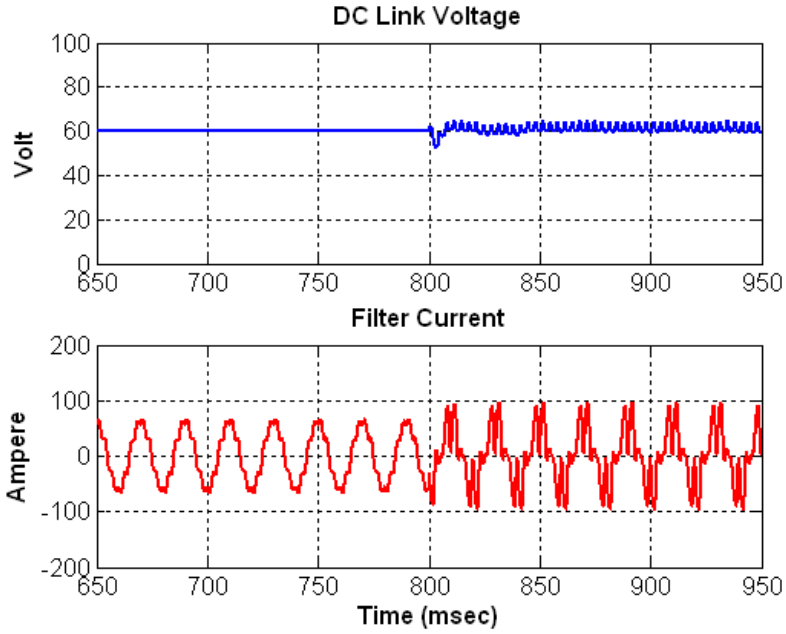

Fig 3.33 DC Link Voltage (20V/div), Filter Current (100A/div)

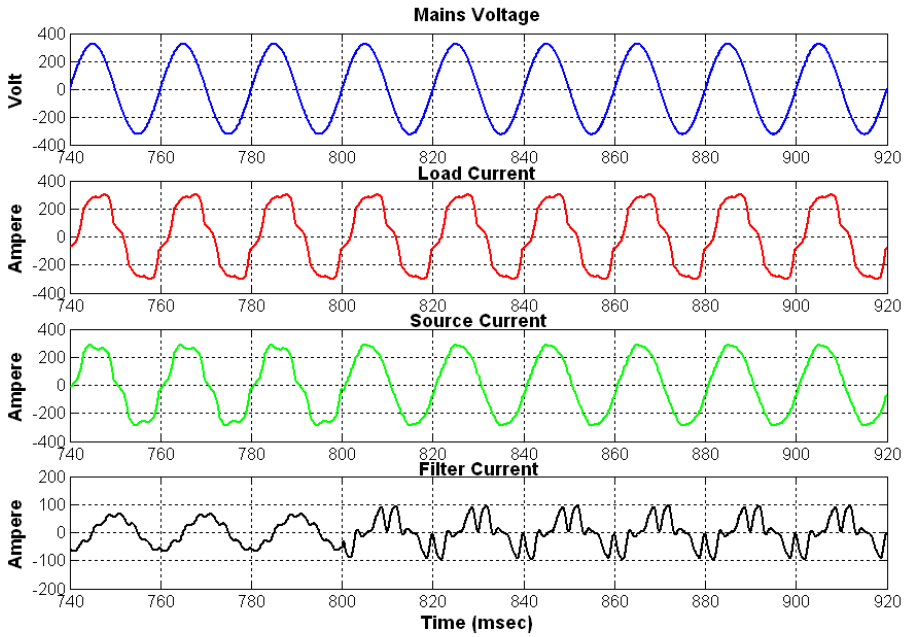

Fig 3.34 Hybrid Power Filter Steady State Results with Proposed Control
Mains Voltage (200V/div), Load Current (200A/div),
Source Current (200A/div), Filter Current (100A/div)

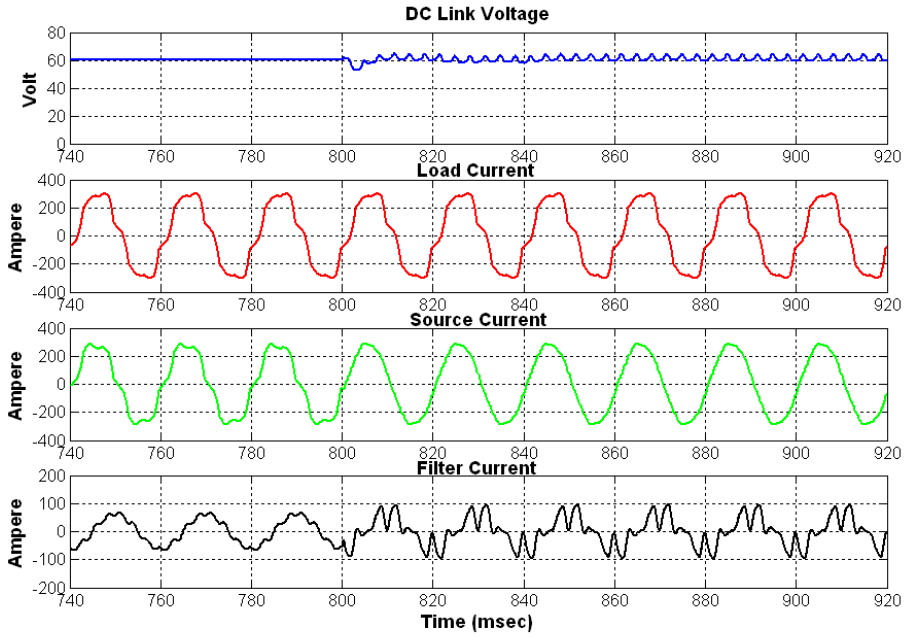

Fig 3.35 Hybrid Power Filter Steady State Results with Proposed Control
DC Link Voltage (20V/div), Load Current (200A/div),
Source Current (200A/div), Filter Current (100A/div)

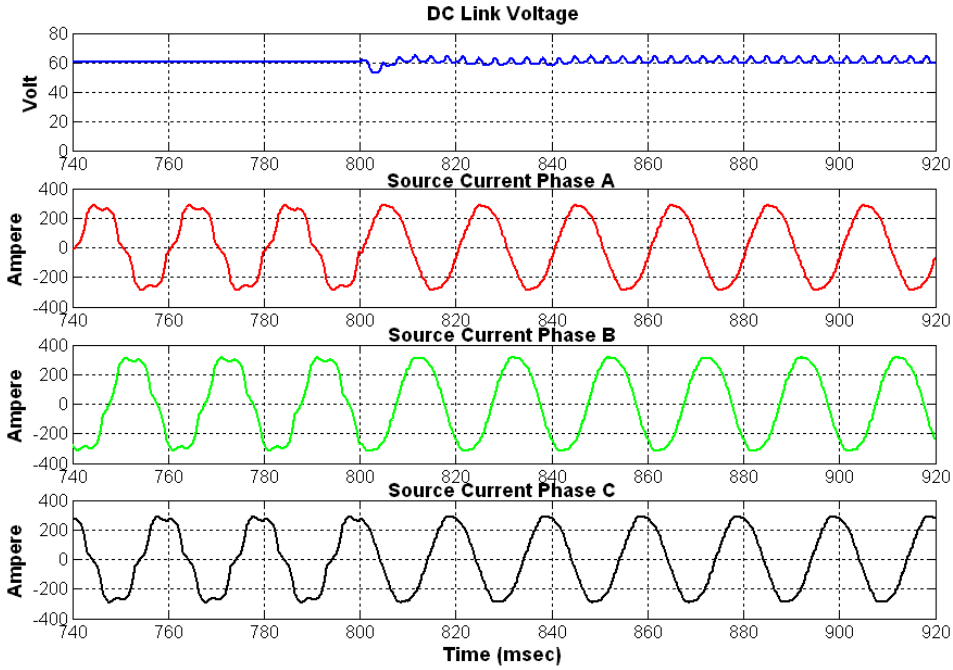

Fig 3.36 Hybrid Power Filter Steady State Results with Proposed Control Source Current Phase A,B,C (200A/div)

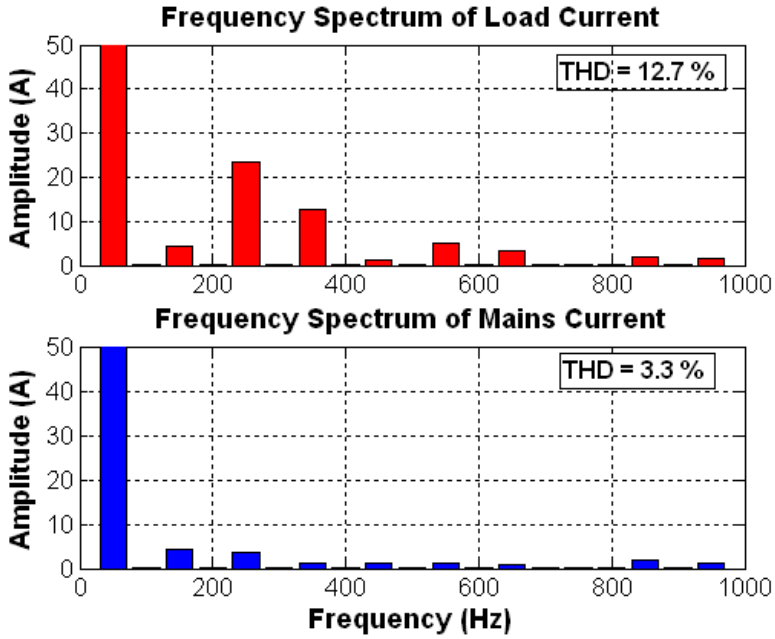

Fig 3.37 Frequency Spectrum of Load and Mains Current

The effectiveness of the proposed control method can be seen from the frequency spectrum of load and the mains current given in Fig 3.37. Since the 3rd harmonic is isolated from the current references, it remains at the same level when the hybrid filter is operating. However, 5th, 7th, 11th and 13th harmonics are filtered in 85%, above 90%, 75%, 65% percentages respectively.

In order to show the effects of 3rd harmonics on the conventional control method, the system is also simulated with the same system parameters and the load configuration given in Table 3.3 and Fig 3.21. In the proposed control method, it is shown that 60VDC is sufficient to generate the required compensation voltage references. However, in the conventional method, the generated voltage reference exceeds the carrier peaks which cause an over modulation. In Fig 3.38, the voltage reference obtained for unity feedback gain is represented. The source current and the DC link voltage for unity feedback gain and 60VDC link are also given in Fig 3.40.

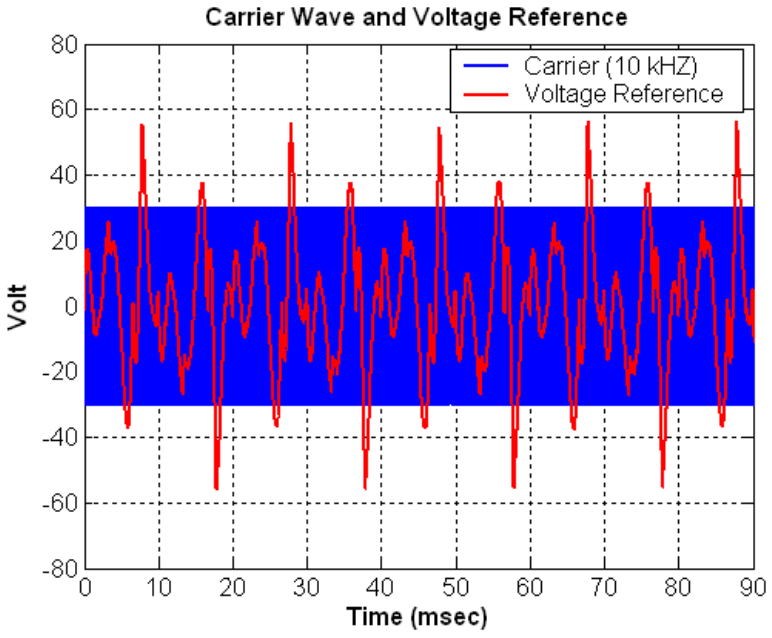

Fig 3.38 Carrier Wave and Calculated Voltage Reference

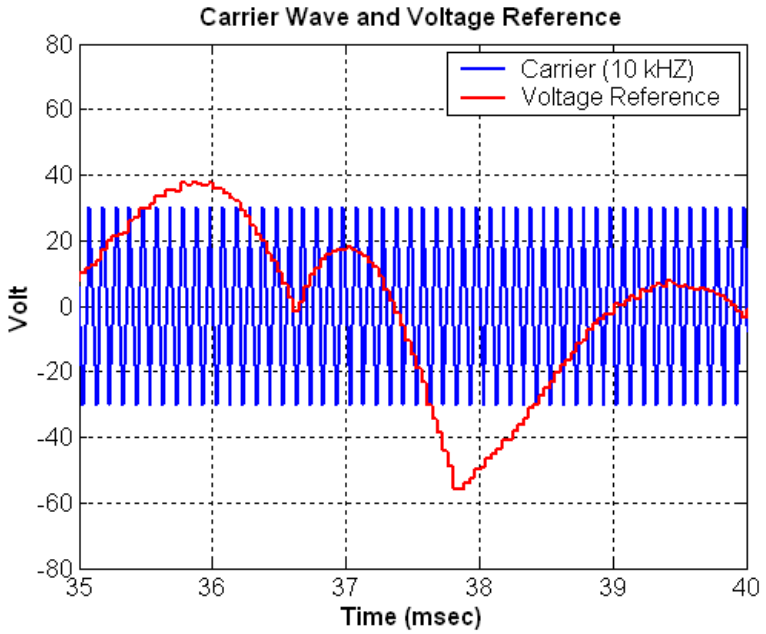

Fig 3.39 Carrier Wave and Calculated Voltage Reference

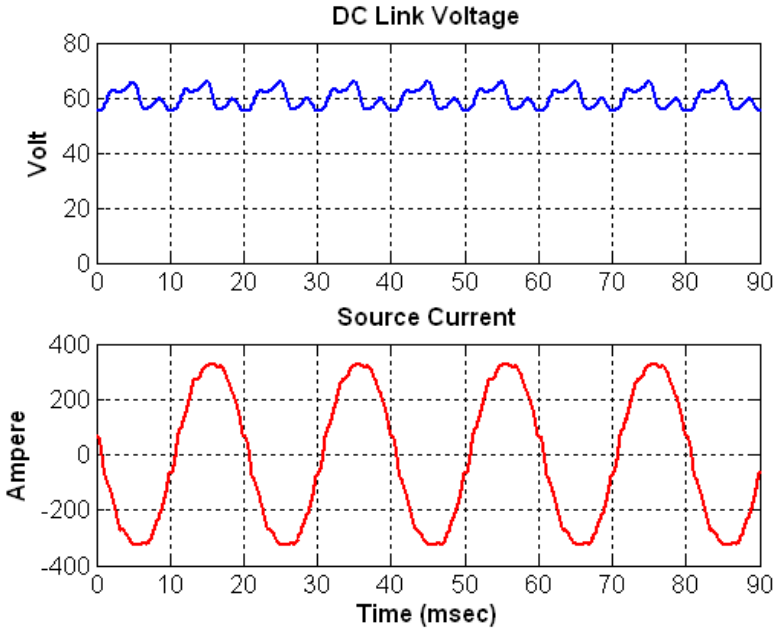

Fig 3.40 Hybrid Power Filter Steady State Results with Conventional Control Method, DC Link Voltage (20V/div), Source Current (200A/div)

In proper operation of the active power filter, occurrence of 300 Hz ripple at the DC link side is acceptable. However, it is shown in Fig 3.40 that, when the hybrid power filter operates with the conventional control method, 100 Hz ripple voltage is observed at the DC link which is an unusual case.

Fig 3.39 and Fig 3.40 given above are obtained by including the conventional feedback and feedforward control together. The 5^{th} and 7^{th} harmonics are greatly reduced and source current seems to be sinusoidal whereas, filtering performance at 550 Hz and 650 Hz is not satisfactory as shown in Fig 3.41. 11^{th} harmonic is filtered in only 30% percentage and almost the entire 13^{th} harmonic is still remaining on the source current. Moreover, in order to avoid over modulation, the feedback gain should be decreased which will also reduce the filtering performance.

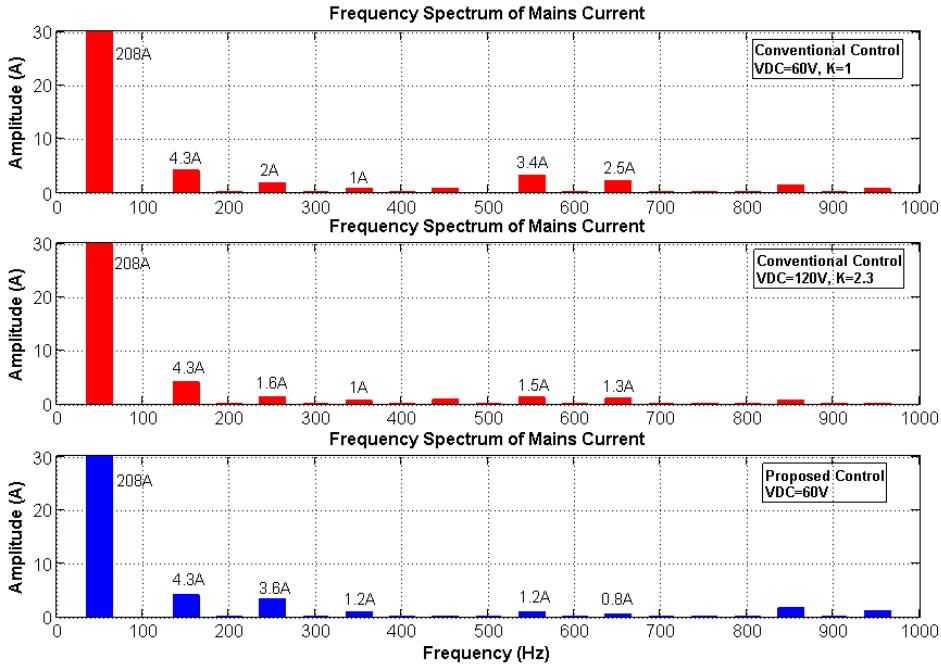

Fig 3.41 Frequency Spectrum of the Source Current with Conventional Control Method (for different DC link Voltage levels and Feedback Gains) and with Proposed Control

It is concluded that, in the case of a 3rd harmonic, the filtering performance given for the proposed method cannot be obtained with the conventional control method at the same DC link voltage level. By simulation analysis it was observed that, if the DC link voltage is set to 120VDC, it is possible to increase the feedback gain up to 2.3 without causing an over modulation (Fig 3.41). The filtering performance is compatible with the proposed voltage reference generation method at the expense of doubled DC link voltage (Fig 3.41). Thus, the hybrid power filter prototype is developed by implementing the proposed control method to isolate the 3rd harmonic content of the load.

CHAPTER 4

HYBRID POWER FILTER IMPLEMENTATION and EXPERIMENTAL RESULTS

The laboratory prototype of Hybrid Power Filter system connected to 400V bus of TÜBİTAK-Space Technologies Institute is composed of mainly, design of power stage, control and protection circuits, and system software. The power stage comprises the three phase inverter, DC link capacitor, a series connected filter capacitors and reactor. The electronic control system hardware includes the measurement circuits, digital signal processor and the protective circuits. The system configuration of the prototype is given in Fig 4.1.

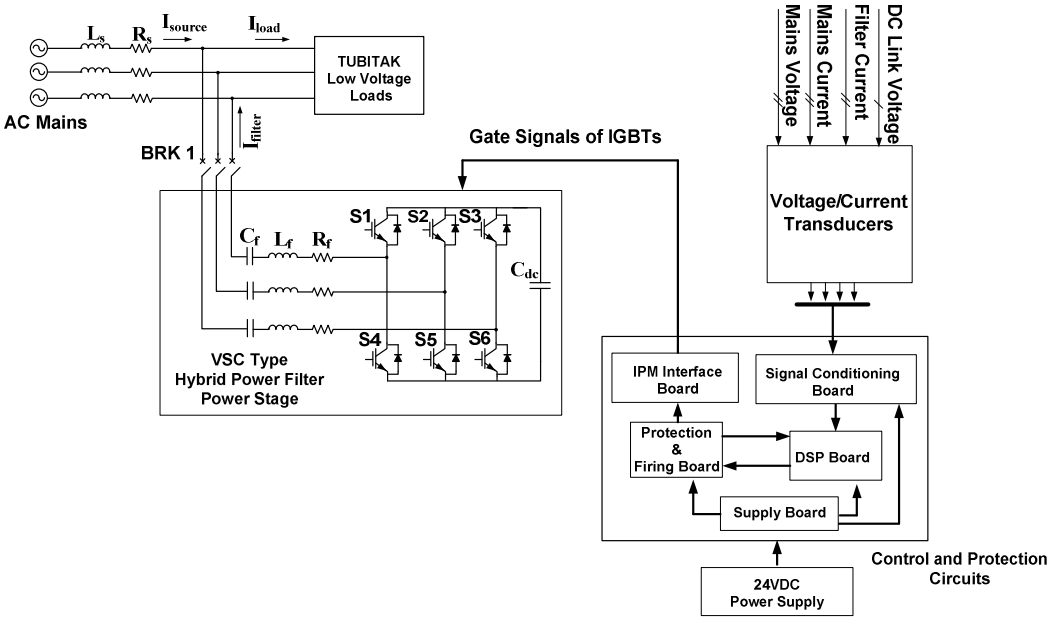

Fig 4.1 System Configuration of Hybrid Active Power Filter Prototype

4.1 Power Stage

The components used in the power stage of the prototype including power converter, DC link capacitor and passive filter components are supplied by considering the design criteria given in Section 3.3.

4.1.1 Power Converter

Three phase converter of the voltage source hybrid power filter is formed by using a six pack Intelligent Power Module (IPM). Six pack IPM modules contain all six IGBTs and their antiparalel diodes in a single package which simplifies the complexity of the three phase converter.

Mitsubishi [58], Semikron [59], Infineon [60], Toshiba [22] and Fuji [24] are the leading IGBT suppliers on the market, manufacturing six-pack IPM modules for various applications such as compressors, fans/blowers, pumps, general purpose drives, washing machines, etc. In the laboratory prototype, a flat base type 300A-1200V IPM (Intelligent Power Module) of Mitsubishi Electric (PM300CLA120) allowing a PWM switching frequency up to 20 kHz is used. Volt-Ampere rating of the selected module is well above the current and voltage requirements indicated in Section 3.3.2. The illustration of the module and inner connections are represented in Fig 4.2. Technical details of the IPM are shown in Appendix A.

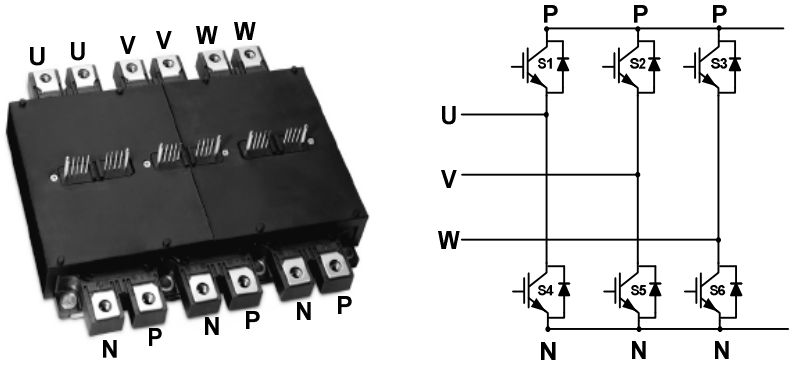

Fig 4.2 PM300CLA1200 IPM Module

4.1.2 DC Link Capacitor

The DC link capacitor used in simulation process is 7mF which results in a low voltage ripple at DC link side. In the experimental set up, 7.05mF capacity is formed by the parallel connection of 2.35 mF branches (Fig 4.3). Each 2.35 mF branch is obtained by the series connection of 4700uF 400V aluminium electrolytic DC link capacitors (ALS30A472NP400) to obtain a voltage rating of 800 VDC for a safe operation in case of any fault. Moreover, the ripple current seen at the DC link is shared by each 2.35mF branch, which reduces the power loss of each capacitor. As indicated in Section 4.1.1, the voltage rating of the selected IPM is also above the required voltage level. As a result, it is also possible to implement a conventional voltage source Active Power Filter with the selected power converter and the designed DC link configuration.

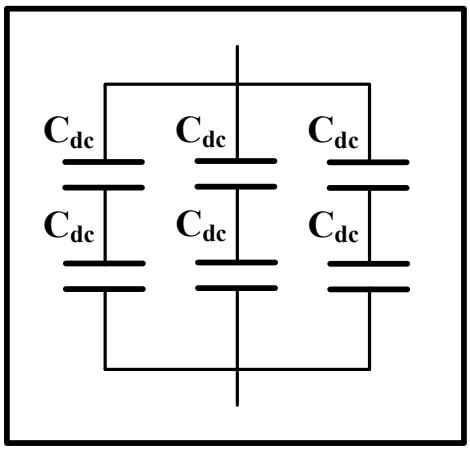

Fig 4.3 Experimental DC Link Capacitor Configuration

In active power filter applications, DC link capacitor is exposed to a ripple current which is the most important parameter for the expected life time of the capacitor. Therefore, by using the theoretical results obtained in Section 3.4, the life time analysis of the specified capacitor is performed as given below.

Typically, the equivalent series resistance (ESR) of the capacitor slowly increases throughout its life time which causes an increase in power loss and core temperature. So, producers define the end of life of the capacitor when its core temperature is higher than its defined limit value or when the ESR value becomes 2 times higher than its initial value [61]. The capacitor power loss (P) definition is given in (4.1).

$$P = \sum I_k^{\,2} \times R_k \tag{4.1}$$

Where, I_k is the ripple current passing through the capacitor, R_k is the initial typical ESR at the corresponding frequency and k stands for each frequency component. Core temperature rise (T_r) and the core temperature (T_c) is calculated as follows:

$$T_r(^0C) = R_{ha} \times P$$
$$T_c(^0C) = T_a + T_c \quad (4.2)$$

Where, R_{ha} (°C/Watt) is the thermal resistance of the capacitor, and T_a is the ambient temperature. In Table 4.1, the ripple current of the DC link capacitor and the corresponding ESR values obtained for 120V DC link is given (Section 3.4). The core temperature and the core temperature rise are calculated by applying (4.1) and (4.2).

Table 4.1 Ripple Current and Corresponding ESR Values

Frequency	ESR	Ripple Current
100Hz	11.6mΩ	I_1=0.1A
200Hz	8.5 mΩ	I_2=0.1A
300Hz	7.5 mΩ	I_3=10.5A
600Hz	6.5 mΩ	I_1=7.0A

$$P = 0.1^2 \times 11.6m + 0.1^2 \times 8.5m + 10.5^2 \times 7.5m + 7.0^2 \times 6.5m \cong 1.15 \text{ W}$$

$$T_r(^0C) = 2.3 \times 1.15 = 2.645 \ ^0C$$

$$T_c(^0C) = 45 + 2.645 = 47.645 \ ^0C$$

The above calculations are made by assuming the following conditions:

Ambient Temperature (T_a): 45 °C

Forced Air Rate: 0 m/sec, and R_{ha} = 2.3 °C/W

Although the power loss of the capacitor is so low, the life time of the capacitor is also checked. At this ambient temperature and core temperature rise, the L_e (Life expectancy) is nearly 400 khrs and voltage factor K_V is 1.21 which is given in [61]. So life expectancy of the capacitor is:

$$\text{Life Expectancy} = 450 \times 1.21 = 484000 \text{ hours}$$

During the switching instants of IGBTs, voltage overshoots are observed due to the stray inductances present in the power circuit. These voltage overshoots appear on the DC link and seen across the power semiconductor. Thus, it should be checked that, the maximum permissible blocking voltage of the semiconductor is not exceeded. In order to limit these improper over voltages, the stray inductance between the DC link capacitor and the power devices should be minimized by using a laminated bus bar [62].

Thus, after selecting the voltage source inverter components properly, the laminated copper busbar is designed for the connection of the DC link capacitors and IPM terminals by using AutoCAD 2007 [63] (Fig A.1). 3D design of the laminated busbar and the technical data of the aluminum electrolytic DC link capacitors capacitor are provided in Appendix A.

4.1.3 Passive Filter Capacitor and Reactor

In Section 3.3.1 the filter capacitors are designed to have a 30kVAR capacity theoretically. The filter capacitor is connected in series with the power converter for each phase. Thus, it should withstand all the compensation current of the hybrid power filter. However, the nominal current of the commercially available 30 kVAR 400 V low voltage AC capacitor units are not satisfying the required $70A_{RMS}$ current rating. As a result, AC filter capacitors shown in Fig 4.4 are provided from ABB. Each capacitor (C) shown in Fig 4.4 is 48uF 400V rated AC filter capacitors. So equivalent capacitance of one module can be obtained as follows:

$$C_{module} = 6 \times C = 288\,uF$$

Then the total capacity obtained by parallel connection of the two modules is:

$$C_{total} = C_{module1} + C_{module2} = 576\,uF$$

As a result; 29kVAR capacity at 400V is obtained by the parallel connection of two 14.5 kVAR capacitor modules for each phase.

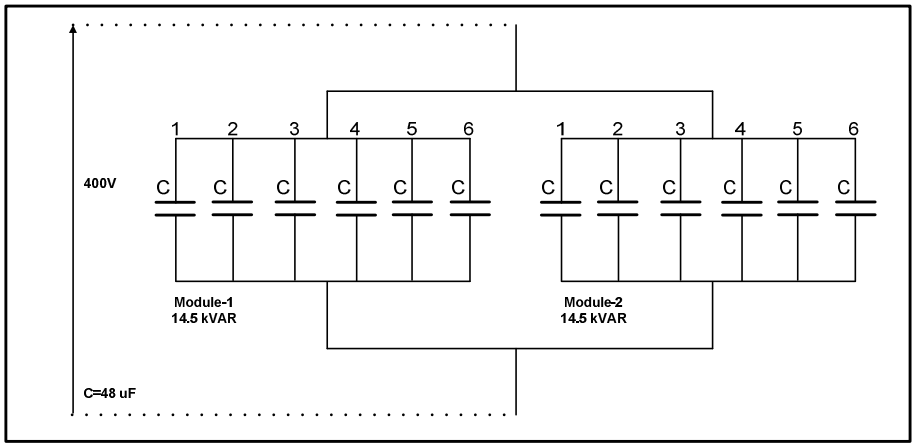

Fig 4.4 Experimental Passive Filter Capacitor Configuration

Moreover, 365uH three phase passive filter reactor, which meets the 340Hz tuning frequency, is provided. The current specification and the technical data of the AC filter reactor are given in Appendix A. Power stage of the laboratory prototype is represented below (Fig 4.5)

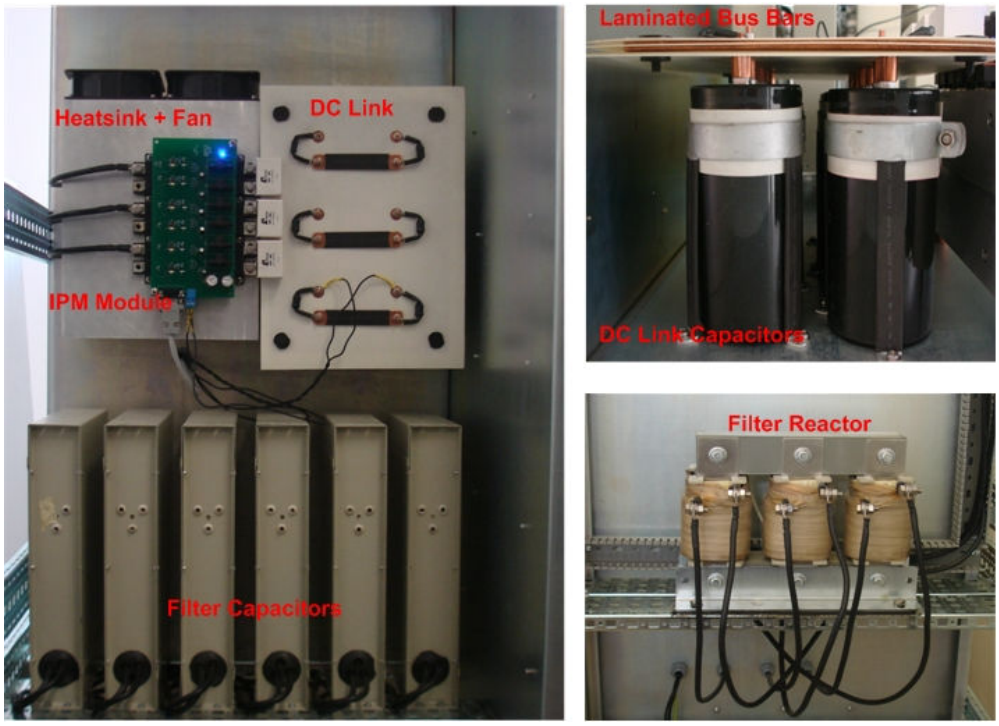

Fig 4.5 Power Stage of the Implemented Hybrid Power Filter Prototype

4.2 Control and Protection Circuits

The design criteria of control and protection circuits of the hybrid power filter are as follows:

- To perform accurate measurement of the signals which are used in the control system (Mains Voltage, Mains Current, Filter Current and DC Link Voltage)
- To generate the appropriate switching signals of the IPM module
- To protect system from unexpected faults (overvoltage at DC link, IPM fault, emergency stop, etc.)

Control and protection circuits of the laboratory system can be divided into 4 groups: measurement and signal conditioning boards, supply board, signal processing (DSP) board, protection and firing boards (Fig 4.6).

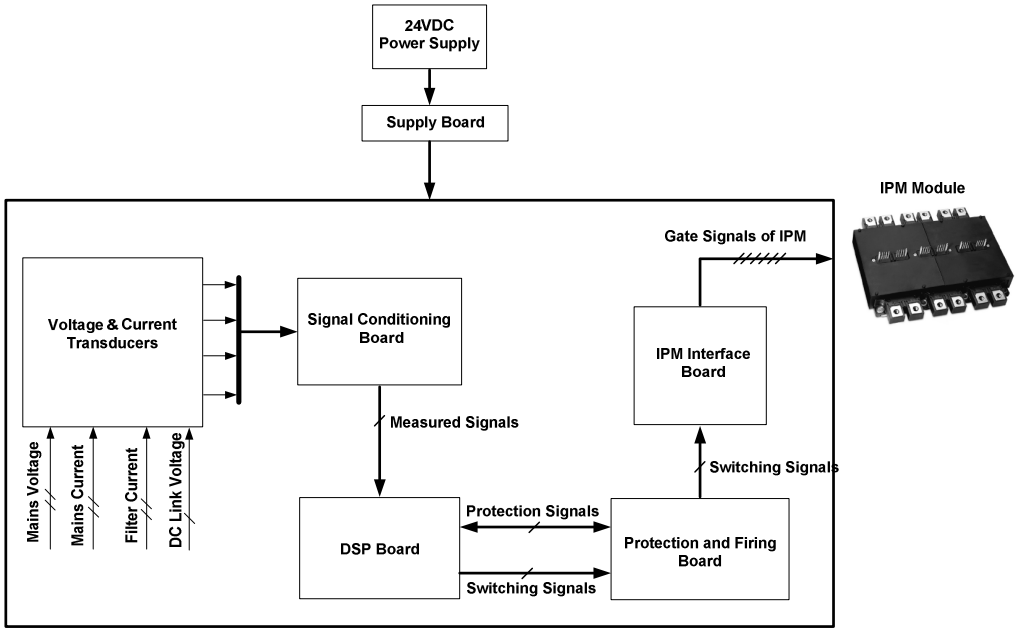

Fig 4.6 Block Diagram of Implemented Control and Protection Circuits

4.2.1 Measurement and Signal Conditioning Boards

As shown, mains voltage, mains current, hybrid power filter current and DC link voltage are the measured signals that are utilized in the control method of the system. Measurement circuits can be divided into two subgroups as: current measurement boards and voltage measurement boards. In Fig 4.7 , the measurement points of both currents and voltages in the system are represented.

Two phase source currents (I_{sa}, I_{sb}) are firstly reduced with a ratio of 2000/5 by the conventional current transformer (CT-1), and filter currents are (I_{fa}, I_{fb}) reduced with a ratio of 100/5 by the conventional current transformer (CT-2). Then, the current between 0-5A_{RMS} scale is measured with split type AC current sensors which can perform measurement up to 5 kHz (CT-3). Technical data of the AC current sensor shown in Fig 4.8 is given in Appendix B.

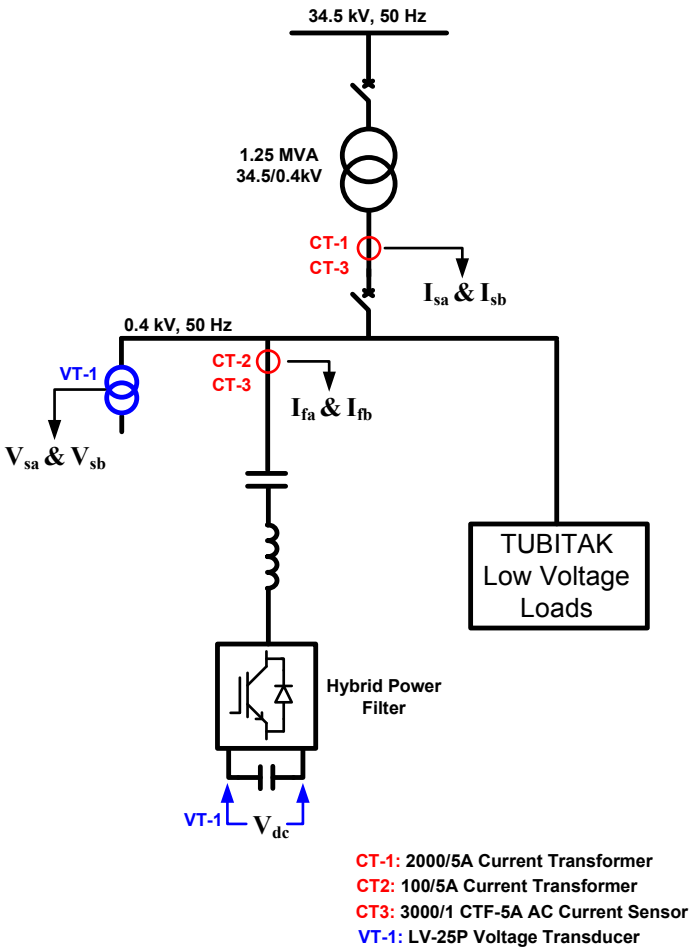

Fig 4.7 Signal Measurement Points of Hybrid Power Filter System

Fig 4.8 CTF-5A AC Current Sensor

Two phase supply voltages (V_{sa}, V_{sb}) used in the PLL of the control method and the DC link voltage are measured with a voltage transducer (LV25-P) which has a measurement capability of DC, AC and pulsed signals. Technical data of the employed voltage transducer is given in the Appendix B. The measured voltage signals are transformed into a current signal between 0-25mA by the LEM board. By signal conditioning board the current signals are transformed into voltage signals which are processed in DSP board. The supply voltage is filtered digitally by a second order low pass filter with a cut off frequency of 50Hz, and the DC link voltage is filtered digitally by a first order low pass filter with a cut off frequency of 30Hz in digital signal processor. Moreover, the measured current signals are also differentially amplified on the same signal conditioning board and transmitted to the DSP board.

4.2.2 Supply Board

Supply board is designed by considering the supply requirements of the other electronic boards. As a result the supply board is designed to produce the $+15V_{DC}$, $-15V_{DC}$, $+5V_{DC}$ and $+3.3V_{DC}$ to provide the supply of DSP board, Signal Conditioning and Measurement boards, IPM Interface board, Protection and Firing Boards. The supply board is composed of DC-DC converters (LAMBDA PXF40-24D15, PXE30-24S05, PXD20-24S3P3) which reduce $24V_{DC}$ to the required DC voltage levels. The $24V_{DC}$ supply for the supply board is provided with a 100W $230V_{AC}/24V_{DC}$ DC power supply (LAMBDA HWS100-24/A). The detailed technical data of the DC power supply is given in Appendix B.

4.2.3 Signal Processing (DSP) Board

In this thesis, the proposed control method is implemented on a 32 bit floating point digital signal processor (DSP) of Texas Instruments. For this purpose, the evaluation

board of TMSF28335 is provided [64]. As shown in Fig 4.9 the evaluation board is located on the designed DSP board. The DSP board includes the offset and buffer circuits for analog/digital inputs to convert the input signals into 0-3V scale which can be recognized by DSP itself. Digital outputs of the DSP are converted from 0-3V to 0-5V scale which is processed by the protection and firing board.

The 150 MHz processor, single precision floating point unit, 12.5MHz 16 channel-12 Bit Analog/Digital Converter unit, prepared sine table in ROM, enhanced PWM module are the main advantages of the used TMSF28335 DSP. The main properties of the floating point digital signal processor are also given in Appendix B.

4.2.4 Protection and Firing Boards

In order to operate the system in a safe manner, some analog and digital faults are produced in the system. If the DC link voltage exceeds the predefined limit value, DC link voltage fault is produced. It is the most probable fault that may occur in the initial tests of the system. In the vicinity of a control supply under voltage, over temperature, over current and short circuit, IPM fault signal is produced by the IPM internal gate control circuits. Furthermore, if one of the voltage level produced by the supply board goes below the required voltage level a Supply fault is produced. All of the produced fault signals are latched and passed through an AND logic to produce a global fault called as System Fault. When the system produces a system fault, the upper IGBTs of the IPM are forced to turn on and lower IGBTs of the IPM are forced to turn OFF by the protection board. As shown in Fig 4.6, switching signals are produced by DSP and transferred to the protection and firing board for protection purposes as described above. However another electronic board called IPM interface board is needed to meet the IPM logic level requirements. Therefore, IPM interface board which is directly mounted on IPM pins is designed to provide opto-coupled isolation for control signals and to assure isolated power supplies for the IPM's built-in gate drive and protection circuits [65]. Implemented control and protection circuits

of the hybrid power filter prototype are given in Fig 4.9. The power stage and the control system of the hybrid power filter are mounted on the same panel by separating them with a divider panel. The overall configuration of the system is represented in Fig 4.10.

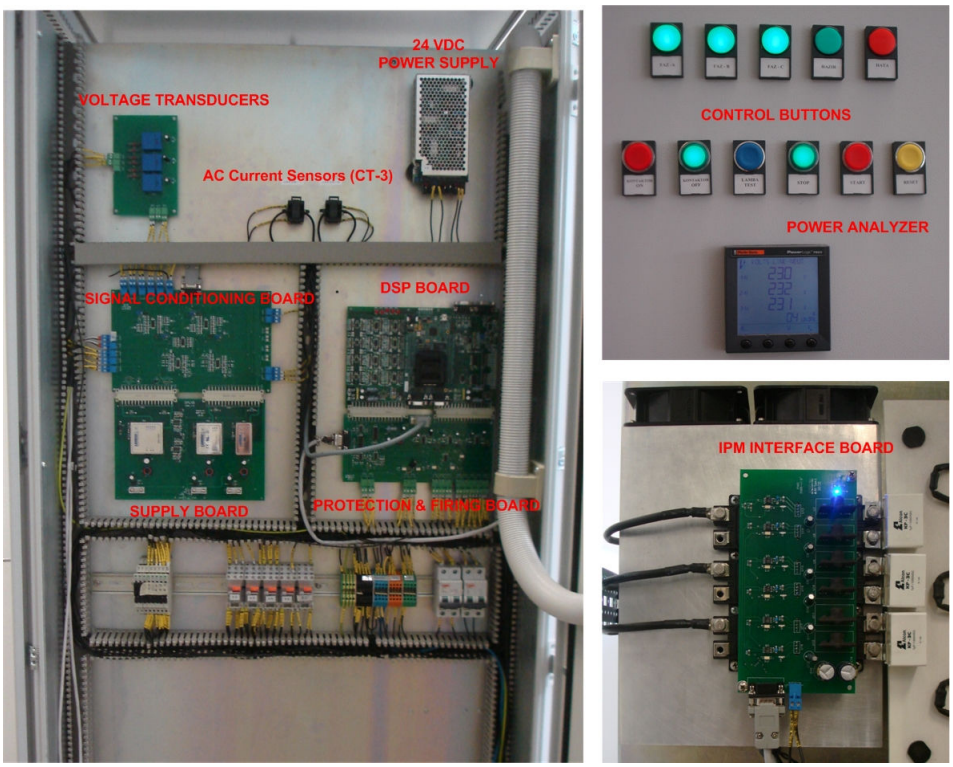

Fig 4.9 Control and Protection Circuits of the Implemented Hybrid Power Filter Prototype

Fig 4.10 Implemented Hybrid Power Filter Prototype

4.3 Software of the Prototype

As described above, the proposed control method is implemented on DSP TMSF28335. The software is developed by Code Composer Studio IDE of Texas Instruments (ANSI C/C++). The flowchart of the software developed by code composer studio is given in Appendix C.

If DSP senses the hardware RESET, firstly the initialization procedure is completed. Initialization procedure includes the initialization of constants, definition of functions, definition of variables, configuration of DSP registers, configuration of peripherals (PWM module) and initial value assignment of variables.

After initializations are completed, the DSP waits for the START signal. During this time period, offset of the ADC channels is calculated and calibration of the signals is

done to obtain the original signal magnitudes. When the START signal is sent to the DSP, the program branches to the main part. All the calculations represented in the proposed voltage reference generation method (Section 2.2.2.2.2) and PLL are implemented in the main part. LPFs used to extract the harmonic component are implemented digitally in terms of mean calculation.

The sampling period of the digital controller is chosen as 40us. The ePWM feature of the TMSF28335 also allows user to implement Sinusoidal Pulse Width Modulation easily at 10 kHz switching frequency [66].

4.4 Experimental Results

In this part of the thesis, the experimental results obtained for Hybrid Active Power Filter which is implemented with the proposed control method (Section 2.2.2.2.2) are given. Moreover, a method which is used to compensate the phase errors of the current measurement devices (CT-1) is investigated. The startup procedure of the laboratory prototype is same with the simulation model of the system (Section 3.4).

When hybrid power filter is OFF, the distorted current waveform of the source side is as shown in Fig 4.11. The frequency spectrum of the source current (Fig 4.12) shows that the harmonic content is slightly higher than the measurement results given in Section 3.1 which is an expected result due to a possible increase in computer loads. As expected 3^{rd}, 5^{th}, 7^{th} and 11^{th} are the most dominant harmonic components to be eliminated. However, 3rd harmonic component is out of the scope of the designed hybrid power filter system due to its 3 phase-3 wire connection topology. Initially, the circuit breaker (BRK1) is turned ON and only the passive filter is operated (Fig 4.13, Fig 4.14).

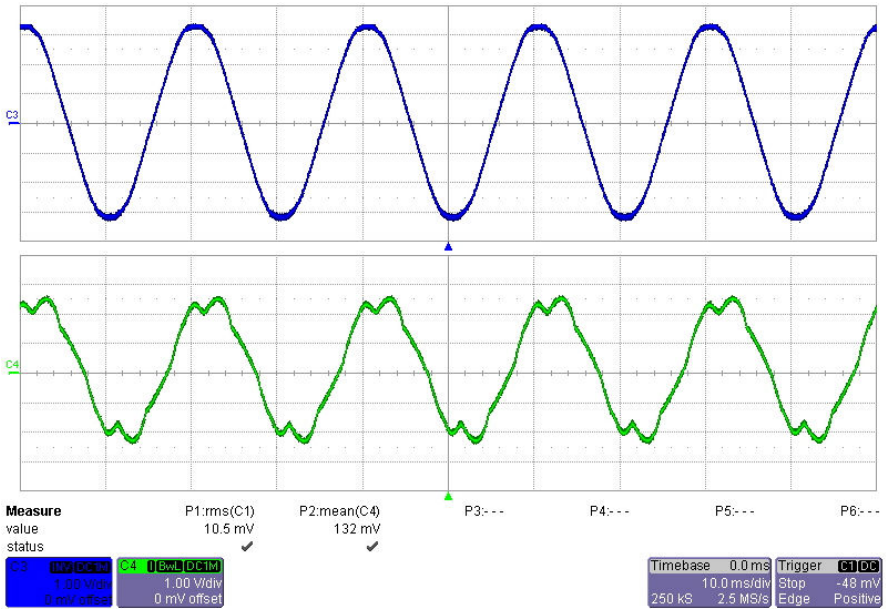

Fig 4.11 Experimental Waveforms when Hybrid Power Filter is OFF
C3: Supply Voltage (100V/div), C4: Supply Current (200A/div)

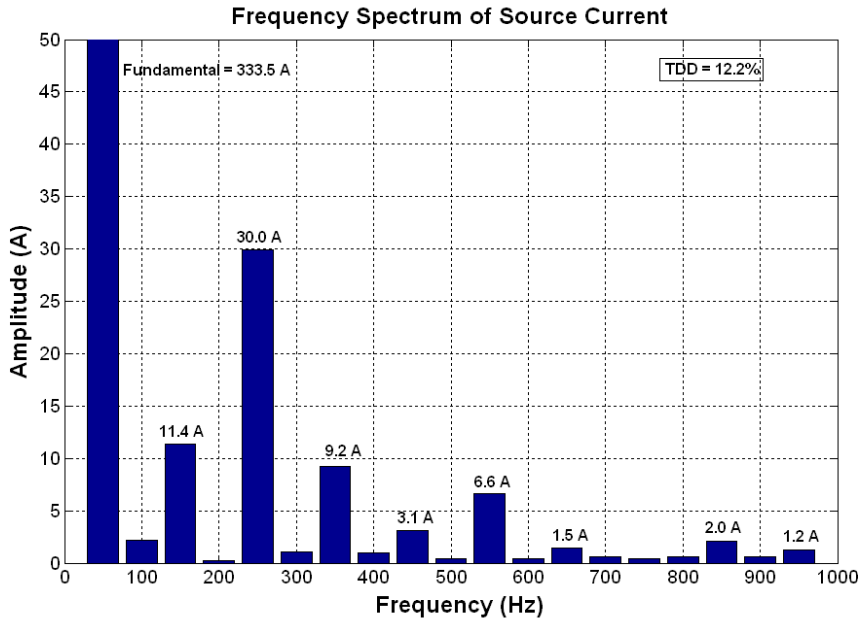

Fig 4.12 Frequency Spectrum of Source Current
When Hybrid Power Filter is OFF

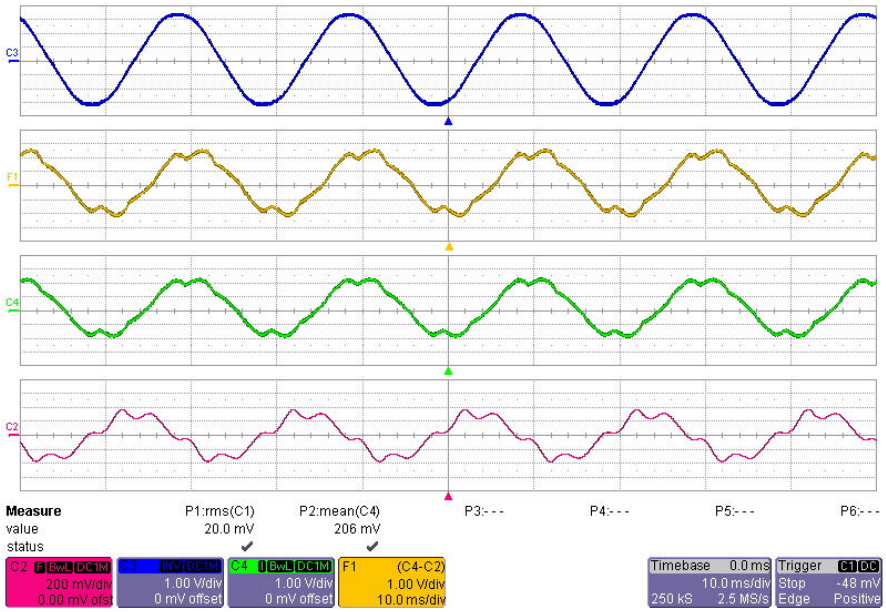

Fig 4.13 Experimental Waveforms when only Passive Filter is ON
C2: Filter Current (40A/div), C3: Supply Voltage (100V/div)
C4: Source Current (200A/div), F1: Load Current (200A/div)

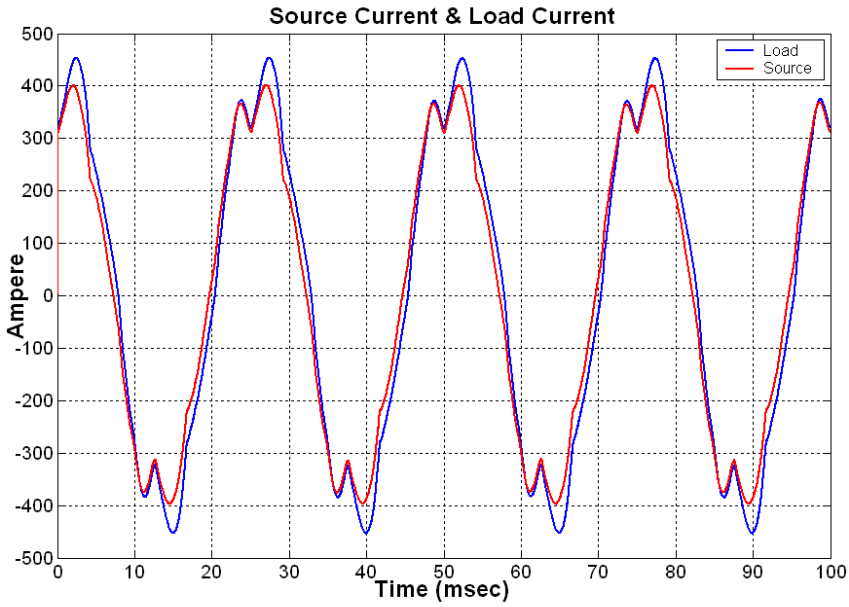

Fig 4.14 Load Current and Source Current when only Passive Filter is ON

Then the DC link capacitor voltage is built up and set to its reference 60V. The transient response of the system shows that, DC link voltage reaches to 60V with an overshoot of nearly 20V and kept constant at its reference value. The experimental waveforms obtained, as the hybrid power filter is turned on are given below.

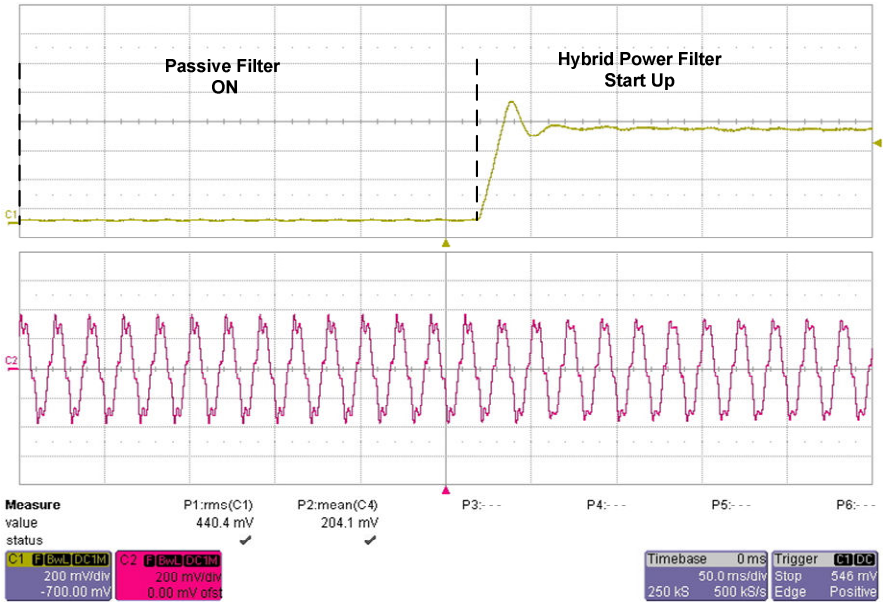

Fig 4.15 C1: DC Link Voltage (20V/div), C2: Filter Current (40A/div)

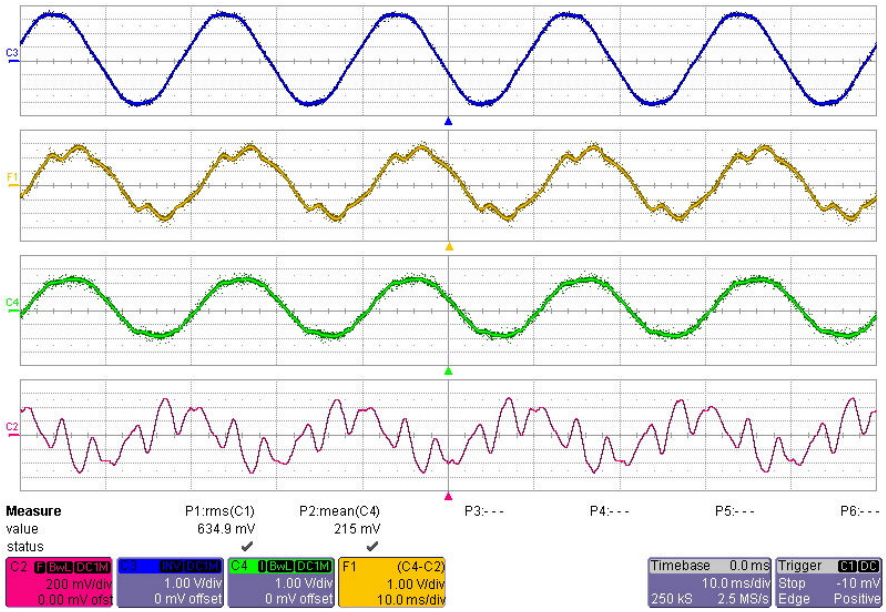

Fig 4.16 F1: Load Current (200A/div), C2: Filter Current (40A/div) C3: Supply Voltage (100V/div), C4: Source Current (200A/div)

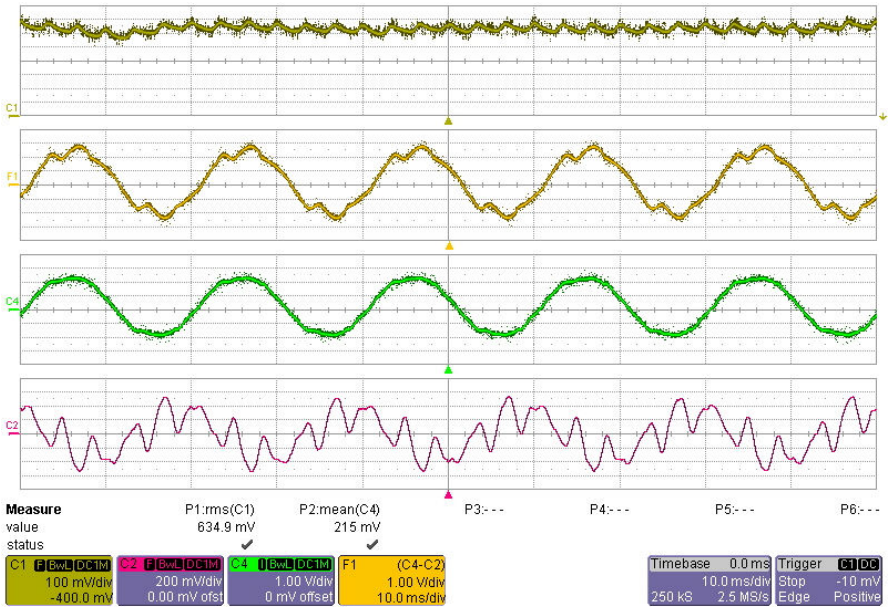

Fig 4.17 C1: DC Link Voltage (10V/div), C2: Filter Current (40A/div) C4: Source Current (200A/div), F1: Load Current (200A/div)

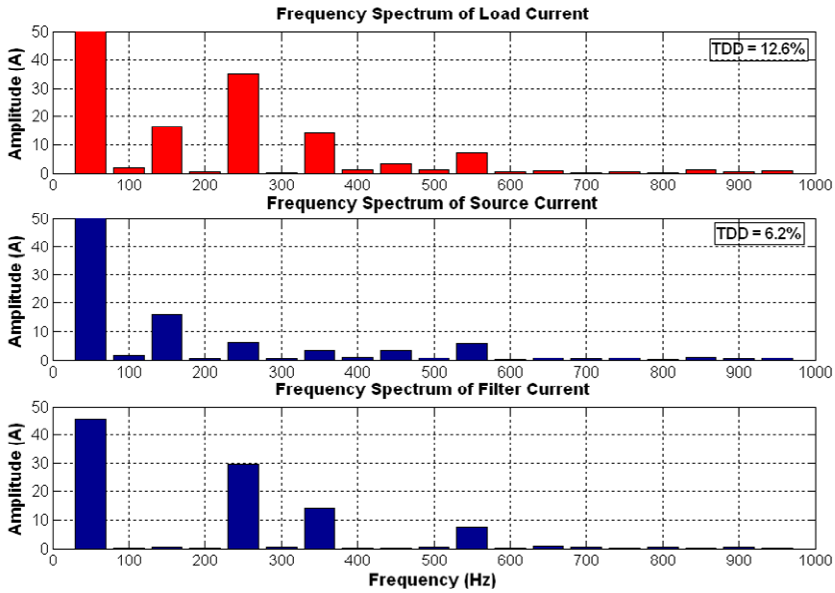

Currents	I_1	I_3	I_5	I_7	I_9	I_{11}	I_{13}	I_{17}
Load	330.4A	16.2A	34.9A	13.9A	3.3A	7.4A	0.8A	1.24A
Source	302.3A	16.0A	6.4A	3.54A	3.4A	5.8A	0.7A	1.22A
Filter	45.4A	-	29.7A	13.8A	-	7.5A	0.7A	0.2A

Fig 4.18 Frequency Spectrum of Load, Source and Filter Current

When hybrid power filter is turned on with the proposed control method, the most dominant 5th, 7th and 11th harmonics are reduced and source current seems to be sinusoidal as shown in Fig 4.16 and Fig 4.17. However, the frequency spectrum of the load, source and filter current shows that, the performance of the system is not satisfactory. Theoretically, hybrid power filter should inject the calculated harmonic content of the load current in same magnitude but with opposite phase. However, the experimental results obtained in Fig 4.18 show that, the injected filter current (I_{Fh}) is not completely in opposite phase with the load current harmonic content (I_{Lh}). After analyzing the obtained data for various cycles, it is observed that the conventional 2000:5A current transformer (CT-1 in Fig 4.7) used for the measurement of the source current results in a phase difference Ø which also increases with increasing harmonic order. In order to compensate the indicated phase error (Ø), a phase compensation method is introduced and digitally implemented as given below. The

operation principle of the hybrid power filter and the experimental result can be represented as given in Fig 4.19.

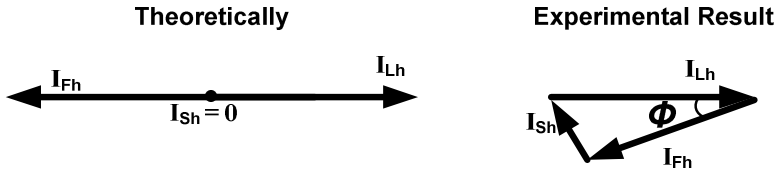

Fig 4.19 Vector Representation of Currents

Theoretically, current harmonic vector of the load (I_{Lh}) and the current harmonic vector of the filter (I_{Fh}) should be in opposite phase to obtain a zero current harmonic vector at the source side (I_{Sh}). However, in the experimental results, Ø is different from zero and the cosine theorem is applicable to obtain the phase difference for each harmonic frequency.

$$I_{Sh}^{\ 2} = I_{Lh}^{\ 2} + I_{Fh}^{\ 2} - 2 \times I_{Lh} \times I_{Fh} \times \cos(\phi_h) \tag{4.3}$$

Where "h" represents the harmonic order.

Inserting the experimental results indicated in Fig 4.18, phase errors for each harmonic frequencies are obtained ($Ø_5 = 6°$, $Ø_7 = 13°$, $Ø_{11} = 38°$, $Ø_{13} = 56°$).

The compensating current references of the hybrid power filter are calculated in d-q reference frame (Fig 2.5). In the implemented control method, as mentioned in Section 2.2.2.2.2, three phase current vectors are mapped into d-q rotating reference frame by applying Clarke and Park transformations respectively.

Current vectors I_α and I_β are orthogonal vectors and assume $I_{\alpha,}$ I_β:

$$\begin{aligned} I_\alpha &= \cos(\theta) \\ I_\beta &= \sin(\theta) \end{aligned} \tag{4.4}$$

Applying Park transformation matrices to unity current vectors as given in (2.22);

$$\begin{aligned} I_d &= \cos(wt) \times I_\alpha - \sin(wt) \times I_\beta \\ I_q &= \sin(wt) \times I_\alpha + \cos(wt) \times I_\beta \end{aligned} \tag{4.5}$$

So;

$$\begin{aligned} I_d &= \cos(wt) \times \cos(\theta) - \sin(wt) \times \sin(\theta) \\ I_q &= \sin(wt) \times \cos(\theta) + \cos(wt) \times \sin(\theta) \end{aligned} \tag{4.6}$$

Rearranging (4.6);

$$\begin{aligned} I_d &= \cos(\theta + wt) \\ I_q &= \sin(\theta + wt) \end{aligned} \tag{4.7}$$

I_d and I_q vectors can be shifted on the same reference frame by adding the phase delay Ø and new shifted vectors I_d' and I_q' are obtained as shown in (4.8).

$$\begin{aligned} I_d' &= \cos(\theta + wt + \phi) = \cos(\theta + wt) \times \cos(\phi) - \sin(\theta + wt) \times \sin(\phi) \\ I_q' &= \sin(\theta + wt + \phi) = \sin(\theta + wt) \times \cos(\phi) + \cos(\theta + wt) \times \sin(\phi) \end{aligned} \tag{4.8}$$

Where; $\begin{aligned} I_d &= \cos(\theta + wt) \\ I_q &= \sin(\theta + wt) \end{aligned}$

So, shifted new vectors I_d' and I_q' can be obtained in terms of I_d and I_q.

$$\begin{aligned} I_d' &= \cos(\theta + wt + \phi) = I_d \times \cos(\phi) - I_q \times \sin(\phi) \\ I_q' &= \sin(\theta + wt + \phi) = I_q \times \cos(\phi) + I_d \times \sin(\phi) \end{aligned} \tag{4.9}$$

Therefore the phase errors of each harmonic component (I_{d5}, I_{q5}, I_{d7}, I_{q7}, I_{d11}, I_{q11}, I_{d13}, I_{q13}) on d-q reference frame (Fig 2.12) can be compensated by applying a simple phase delay calculation represented in (4.9). After utilizing the phase compensation method, the following waveforms are observed experimentally.

Fig 4.20 and Fig 4.22 shows that the DC link voltage of the Hybrid power filter is kept constant at 60VDC and the source current becomes nearly a pure sinusoidal. It is clear from Fig 4.23 that, the supply voltage and current is not in phase. The reactive power compensation capacity is limited (30kVAR) with the capacity of the utilized passive filter. In order to obtain a unity power factor, the passive filter capacitor should be increased which will increase the size and the cost of the system. Moreover, the hybrid active power filter is designed and implemented mainly for the elimination of the most dominant current harmonics.

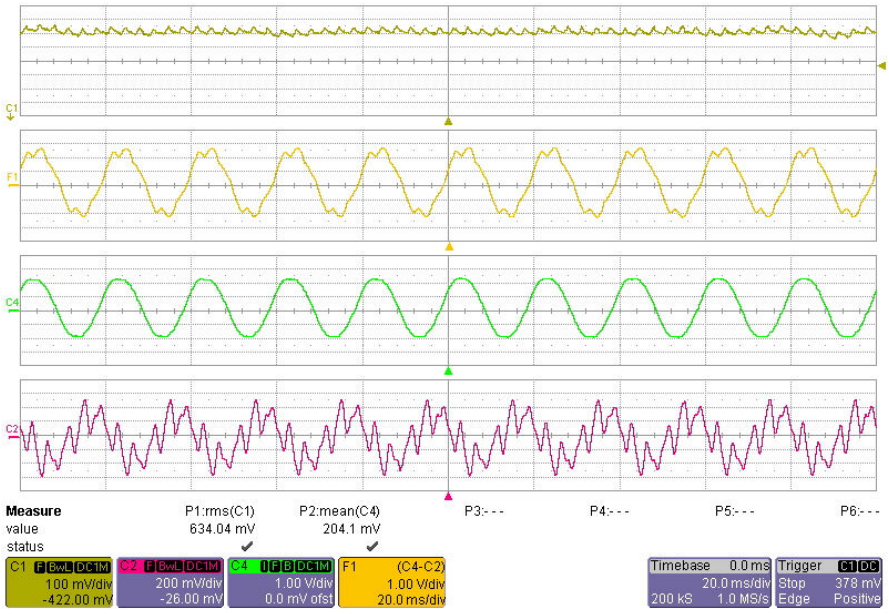

Fig 4.20 DC Link Voltage (10V/div), C2: Filter Current (40A/div) C4: Source Current (200A/div), F1: Load Current (200A/div)

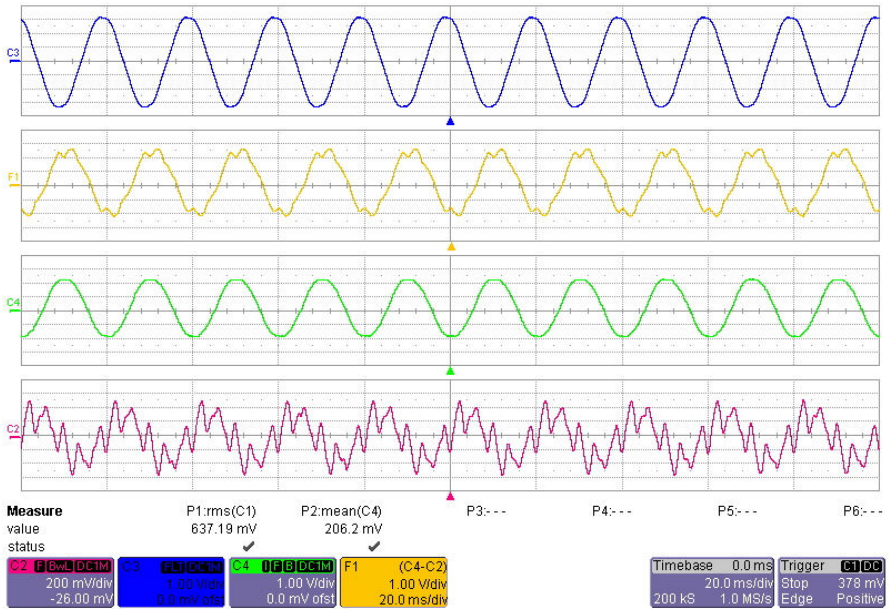

Fig 4.21 C2: Filter Current (40A/div), C3: Supply Voltage (100V/div) C4: Source Current (200A/div), F1: Load Current (200A/div)

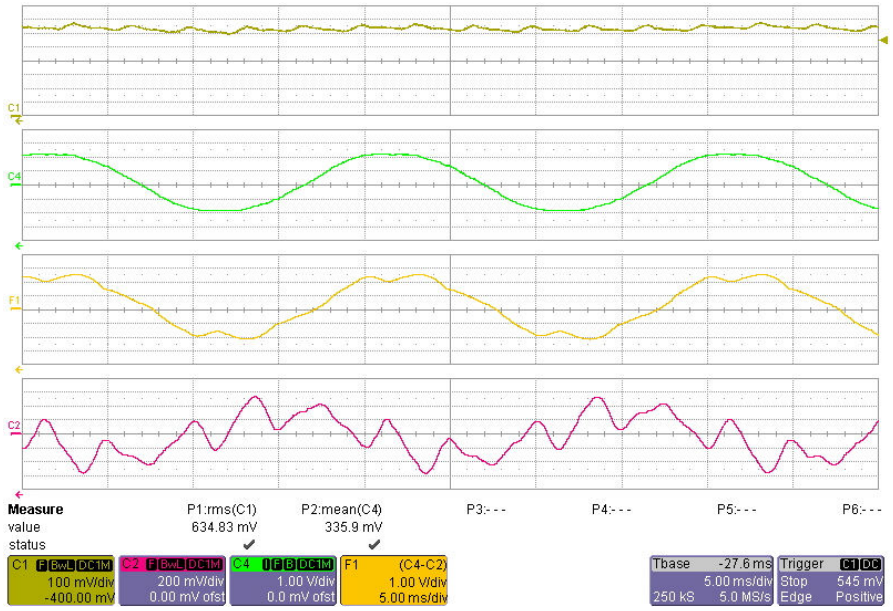

Fig 4.22 C1: DC Link Voltage (10V/div), C2: Filter Current (40A/div) C4: Source Current (200A/div), F1: Load Current (200A/div)

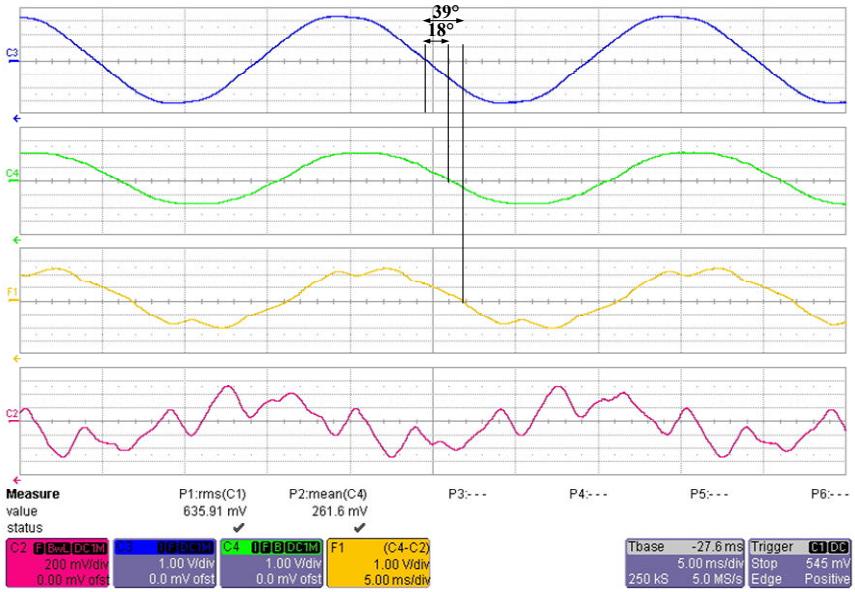

Fig 4.23 C2: Filter Current (40A/div), C3: Supply Voltage (100V/div) C4: Source Current (200A/div), F1: Load Current (200A/div)

Addition of phase error compensation greatly improves the filtering performance of the system. The frequency spectrum of the source current proves that (Fig 4.24) the most dominant 5^{th}, 7^{th} and 11^{th} harmonics are suppressed to satisfy the current distortion limits indicated in Table 1.2. The 13^{th} harmonic component is already below the limit value, so that it is excluded in the current reference calculation.

The DC link voltage of the hybrid power filter is quite low when compared with a conventional voltage source Active Power Filter. In the implemented system, DC link voltage is kept constant at 60VDC. As a result, the rating of the power converter is greatly reduced. In fact, two definitions ($S_{VSC,max}$, $S_{VSC,installed}$) can be made for the volt-ampere rating of the power converter. $S_{VSC,max}$ is the maximum converter capacity which shows the capability of the power converter for the specified DC link voltage level. Whereas, $S_{VSC,installed}$ is used to indicate the amount of power occupied while compensating the harmonic content of the experimental load given in Fig 4.24.

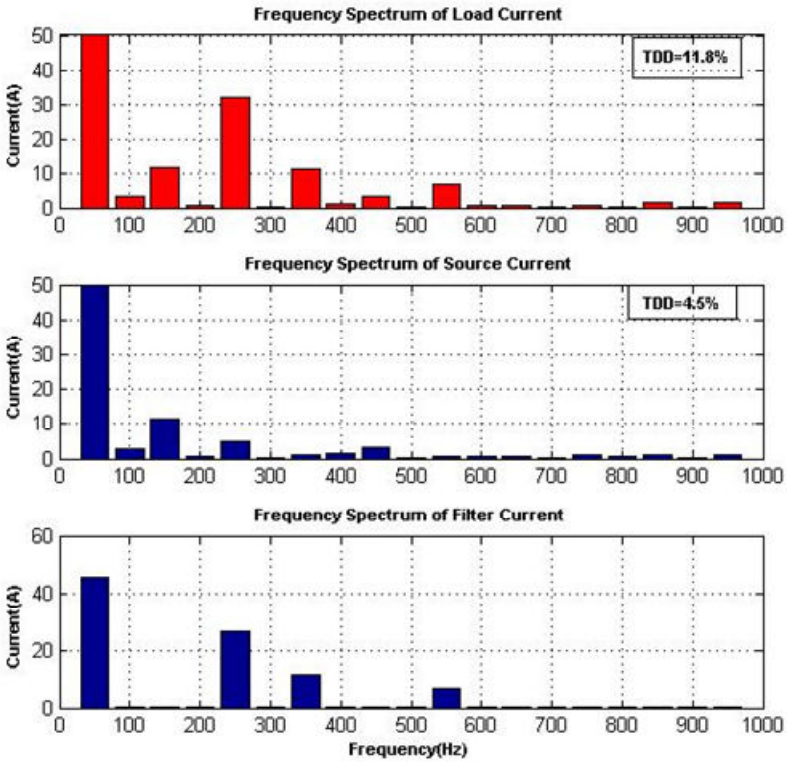

Currents	I_1	I_3	I_5	I_7	I_9	I_{11}	I_{13}	I_{17}
Load	311.7A	11.4A	32.1A	11.3A	3.2A	7.0A	0.8A	1.5A
Source	289.4A	11.5A	5.1A	1.2A	3.1A	0.5A	0.8A	1.5A
Filter	45.8A	-	27.1A	11.4A	-	7.2A	-	-

Fig 4.24 Frequency Spectrum of Load, Source and Filter Current

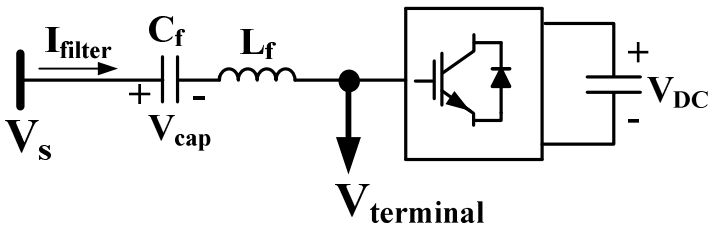

Fig 4.25 Single Line Diagram of the Hybrid Power Filter

The maximum converter capacity is defined as below:

$$S_{VSC,max} = \sqrt{3} \times V_{terminal,max} \times I_{filter,max} \tag{4.10}$$

However, to determine the maximum terminal voltage of the converter and the maximum filter current the following constraints should be satisfied. Firstly, the voltage appearing across the capacitor (V_{cap}) should not exceed the nominal voltage of the selected AC capacitors (4.11). Then, the nominal current rating of the filter reactor should be met (4.12). Finally, in order to generate the required compensation currents, (4.13) should be satisfied.

$$\sum_{h=1}^{n} (I_{filter,h} \times Z_{C,h}) < V_{Cap,nominal} \tag{4.11}$$

$$\sqrt{\sum_{h=1}^{n} (I_{filter,h})^2} < I_{L,nominal} \tag{4.12}$$

$$\sum_{h\neq 1}^{n} Z_{F,h} \times \hat{I}_{Filter,h} < V_{DC} \tag{4.13}$$

In (4.11), (4.12), and (4.13) h represents the order of the harmonic, $I_{filter,h}$ is the filter current, $Z_{C,h}$ is the impedance of the capacitor and $Z_{F,h}$ is the impedance of the LC filter at the corresponding harmonic frequency. As explained in Section 4.1.3, the filter reactor is selected to have a $70A_{RMS}$ nominal current rating. $45A_{RMS}$ of this current is the fundamental current flow due to the filter capacitor. So, the maximum harmonic current that the hybrid filter can withstand is limited by the filter reactor as $50A_{RMS}$ (4.14).

$$I_{Filter,h(max)} = \sqrt{70^2 - 45^2} = 50 A_{RMS} \tag{4.14}$$

In the implement system, the most dominant 5^{th}, 7^{th}, and 11^{th} current harmonics are eliminated. The impedances of the experimentally used passive filter (Section 4.1.3)

at 50 Hz, 250 Hz, 350 Hz and 550 Hz are given in (4.15). Then, the terminal voltage can be expressed as given in (4.16), by assuming zero fundamental voltage at the terminal of the voltage source converter. So, the maximum terminal voltage can be obtained by assuming the all harmonic content ($50A_{RMS}$) appearing at 550Hz as a worst case.

$$\begin{aligned} \left|Z_{F,1}\right| &= 5.19\ \Omega \\ \left|Z_{F,5}\right| &= 0.487\ \Omega \\ \left|Z_{F,7}\right| &= 0.044\ \Omega \\ \left|Z_{F,11}\right| &= 0.78\ \Omega \end{aligned} \tag{4.15}$$

So, the constraint given in (4.13) is checked with $I_{filter,11}=50A_{RMS}$ and $Z_{F,11}=0.78\Omega$.

$$Z_{F,11} \times I_{Filter,11} = 0.78 \times 50 \times \sqrt{2} = 55V < V_{DC} = 60V$$

$$V_{terminal} = \sqrt{\sum_{h\neq 1}^{n} (Z_{F,h} \times I_{Filter,h})^2} \tag{4.16}$$

$$V_{terminal,max} = Z_{F,11} \times I_{Filter,max} = 0.78 \times 50 = 39V \tag{4.17}$$

By using equation (4.10) the maximum converter rating at 60VDC link is obtained as given below:

$$S_{VSC,max} = \sqrt{3} \times 39 \times 70 \cong 4.7\ kVA$$

Then, by using the current spectrum given in Fig 4.24 and the impedances shown in (4.15), the installed rating of the voltage source converter can be easily found as below:

$$\sqrt{\sum_{h=1}^{n} (I_{filter,h})^2} = \sqrt{45^2 + 27.1^2 + 11.4^2 + 7.2^2} = 54.23A_{RMS}$$

$$V_{terminal} = \sqrt{(27.1 \times 0.487)^2 + (11.4 \times 0.044)^2 + (7.2 \times 0.78)^2} = 14.35 V_{RMS}$$

$$S_{VSC,installed} = \sqrt{3} \times V_{terminal} \times I_{filter,RMS} = \sqrt{3} \times 14.35 \times 54.23 \cong 1.35 kVA$$

If the harmonics of the load indicated in Fig 4.24 were filtered by a conventional VSC type APF, the required DC link would be around 700 VDC which increases the losses and the rating of the power converter [56]. However, the total rating of the hybrid power filter (S_{HPF}) by including the passive filter is higher than the rating of the conventional VSC type active power filter (S_{APF}), due to the unavoidable fundamental current flow as shown in (4.18) and (4.19)

$$S_{HPF} = \sqrt{3} \times V_S \times I_{filter,RMS} = \sqrt{3} \times 400 \times 70 \cong 48.5 \text{ kVA} \quad (4.18)$$

$$S_{APF} = \sqrt{3} \times V_S \times I_{filter,RMS} = \sqrt{3} \times 400 \times 50 \cong 34.6 \text{ kVA} \quad (4.19)$$

Although the overall rating of the hybrid power filter is higher, the reduction in the converter rating is a significant benefit in terms of losses. Moreover, it provides the opportunity of employing low rated IGBTs or even MOSFETs in the converter design. Even though no additional switching filter is used, high frequency current ripples are also minimized with the applied system. Moreover, experimental results have shown the effectiveness of the proposed control method which is also simple to implement. As a result, the advantages listed above show that especially for large power applications, Hybrid active power filters are seem to be an appropriate solution with their reduced DC link voltages.

CHAPTER 5

CONCLUSIONS & FURTHER WORK

In this research work, the design and implementation of a three phase shunt connected Hybrid Active Power Filter has been carried out. The prototype has been designed and developed to eliminate most dominant harmonics existing at TÜBİTAK-Space Technologies Institute 400V low voltage line.

The developed prototype is composed of a three phase voltage source converter with PWM modulation and a series connected LC passive filter tuned at 340Hz. The amplification phenomenon of the shunt connected passive filter is suppressed by the applied hybrid filter topology. The 5^{th}, 7^{th} and 11^{th} harmonics are greatly reduced and the line currents have become to comply with IEEE Std. 519-1992. The DC link voltage of the VSC is also significantly decreased as compared with a conventional shunt connected VSC Active Power Filter. The reduction of the DC link voltage also assures low rated converter and lower losses.

Moreover, the conventional control method applied for transformerless hybrid power filters are analyzed [29, 33, 35]. The feedback and the feedforward control methods are effective to eliminate the current harmonics of a three phase diode rectifier load. However, the existence of voltage harmonics at the source side affects the performance. Hence, a voltage feedforward method is introduced and verified by simulation results to isolate the supply side voltage harmonics.

The developed laboratory prototype is designed to eliminate the most dominant harmonics of the distorted line current of TÜBİTAK. It is observed by measurement results that unbalanced 3^{rd} harmonic components are also available at the source side.

However, the developed hybrid active power filter topology cannot eliminate these 150Hz components with a three phase three wire connection. Hence, a voltage reference generation method is proposed to exclude the third harmonic components during the reference current calculation. The proposed method is digitally implemented and verified by both simulation and experimental results.

Furthermore, it is observed that, conventional current transformers perform accurate measurement in terms of magnitude but not in terms of phase. Therefore, the proposed control method is updated to compensate the phase error of the conventional current transformers which are used to measure the source current.

Following conclusions can be drawn from the results of theoretical and experimental work of this research work:

- The DC link voltage and the volt-ampere rating of the power converter of VSC based Active Power Filter is greatly reduced with the developed Hybrid Power Filter topology.
- The reduced DC link voltage allows designers to use lower rated IGBTs, or MOSFETs at lower costs.
- Although the switching frequency is 10 kHz in the implemented system, the hybrid power filter current is ripple free, and no additional switching ripple filter is required.
- The reactive power compensation capability is limited with the capacity of the employed passive filter capacitor. This criterion may limit the application of hybrid power filters where, both current harmonic elimination and reactive power compensation are crucial.
- The resonance risk of the existing passive filters can be damped by utilizing hybrid power filter topology with reduced converter ratings.

- The applied topology provides direct connection of Active Power Filters to the mains side in high power applications without using a coupling transformer.

In this research work, the experimental results of the implemented hybrid power filter prototype are given for the proposed voltage reference generation method to exclude the 3rd harmonic current components. However, theoretically proposed voltage feedforward method has not been verified by experimental results yet. The implemented system can be operated to filter the harmonics of a thyristor controlled rectifier load. By utilizing a thyristor rectifier load, the phase angle of the load can be changed with respect to the voltage harmonics phase. Therefore, the experimental verification of the proposed voltage feedforward method can be stated as a future work.

The developed hybrid power filter prototype assures satisfactory filtering results with a reduced DC link voltage. Nevertheless, a complete comparison between a conventional VSC type active power filter and the hybrid power filter is not included. The ratings of the IPM module and DC link capacitors are suitable to be operated as a conventional VSC type APF; by only changing the series LC filter with an appropriate filter reactor. Therefore, an exact analysis can be performed between these two topologies in terms of loss, cost and filtering performance.

REFERENCES

[1] IEEE Std. 519-1992, "IEEE Recommended Practices and Requirements for Harmonic Control in Electrical Power Systems"

[2] IEEE Std. 519-1981, "Guide for Harmonic Control and Reactive Power Compensation of Static Power Converters"

[3] B. Singh, K. Al-Haddad, A. Chandra, "A Review of Active Power Filters for Power Quality Improvements," IEEE Trans. on Industrial Electronics, Vol. 46, No. 5, pp. 960-971, Oct. 1999

[4] R. D. Henderson, P. J. Rose, "Harmonics: The effects on power quality and transformers," IEEE Transactions on Industry Applications, vol. 30, no. 3, pp. 528-532, May/June 1994

[5] A. Elmoudi, M. Lehtonen, H. Nordman "Effect of harmonics on transformers loss of life," Conference Record of the IEEE International Symposium on Electrical Insulation, pp. 408-411, 2006

[6] IEC Norm 555-3 prepared by the International Electrical Commission

[7] Elektrik Piyasasında Dağıtım Sisteminde Sunulan Elektrik Enerjisinin Tedarik Sürekliliği, Ticari Ve Teknik Kalitesi Hakkında Yönetmelik,EMRA, 2006 (in Turkish)

[8] Elektrik İletim Sistemi Arz Güvenilirliği veKalitesi Yönetmeliği, EMRA, 2007 (in Turkish)

[9] S. N. AL. Yousif, M. Z. C. Wanik, A. Mohammed, "Implementation of Different Passive Filter Designs for Harmonic Mitigation", National Power & Energy Conference (PECon) Proceedings, Malaysia, pp. 229-234, 2004

[10] Damian A. Gonzalez, John C. Mccal, “Design of Filters to Reduce Harmonic Distortion in Industrial Power Systems”, IEEE Trans. On Industry Applications, Vol. IA-23, No. 3, pp. 504-511, May/June 1987

[11] J. C. Das, “Passive Filters, Potentialities and Limitations”, IEEE Trans. On Industry Applications, Vol. 40, No. 1, pp. 232-241, Jan/Feb 2004

[12] H. Sasaki, T. Machida, “A New Method to Eliminate AC Harmonic Currents by Magnetic Flux Compensation-Consideration on Basic Design,” IEEE Trans. Power App. Syst., Vol. 90, No. 5, pp. 2009-2019, Sep./Oct. 1971

[13] H. Kawahira, T. Nakamura, S. Nakazawa, “Active Power Filters”, IEEJ IPEC-Tokyo, pp. 981-992, 1983

[14] H. Akagi, H. Fujita, “A New Power Line Conditioner for Harmonic Compensation in Power Systems”, IEEE Trans. On Power Delivery, Vol. 10, No. 3, pp. 1570-1575, July 1995

[15] D. Chen, S. Xie, “Review of the Control Strategies Applied to Active Power Filters,” IEEE International Conf. on Electric Utility Deregulation, Restructuring and Power Tech., pp. 666-670, April 2004

[16] Y. Hayachi, N. Sato, K. Takahashi, “A Novel Control of a Current Source Active Filter for AC power system harmonic compensation,” IEEE Trans. on Industry App., Vol. 27, No. 2, pp. 380-384, 1991

[17] H. Akagi, “Active Harmonic Filters,” Proceedings of the IEEE, Vol. 93, No. 12, pp. 2128-2141, Dec. 2005

[18] H. Özkaya, “Parallel Active Filter Design, Control, and Implementation”, M.S. Thesis Electrical and Electronics Engineering Middle East Technical University, June 2007

[19] L. Benchaita, S. Saadate, A. Salemnia, “A comparison of voltage source and current source shunt active filter by simulation and experimentation,” IEEE Trans. on Power Systems, Vol. 14, No. 2, pp. 642-647, May 1999

[20] V. B. Bhavaraju, P. Enjeti, “A novel active line conditioner for a three-phase system,” in Proc. IEEE IECON’93, Vol. 2, pp. 979-985, Oct. 1993

[21] A. D. le Roux, Hd. T. Mouton, H. Akagi “Digital control of an integrated series active filter and diode rectifier with voltage regulation,” IEEE Trans. On Industry Applications, Vol. 39, Iss. 6, pp. 1814-1820, Nov. /Dec. 2003

[22] “TOSHIBA [Online],” http//www.toshiba.co.jp, last visited on 25/08/2009

[23] “ABB [Online],” http//www.abb.com, last visited on 25/08/2009

[24] “Fuji Electric Group [Online],” http//www.fujielectric.com, last visited on 25/08/2009

[25] L. A. Moran, J. W. Dixon, J. R. Espinoza and R. R. Wallace, “Using Active Filters To Improve Power Quality”, 5th Brazilian Power Electronics Conference, COBEP’99

[26] F. Z. Peng, H. Akagi, A. Nabae “A new approach to harmonic compensation in power systems,” in Conf. Rec. IEEE-IAS Annu Meeting, Vol. 1, pp. 874-880, Oct. 1988

[27] H. Fujita, H. Akagi “A practical approach to harmonic compensation in power systems-series connection of passive and active filters,” in Conf. Rec. IEEE-IAS Annu Meeting, Vol. 2, pp. 1107-1112, Oct. 1990

[28] L.Chen, A.V.Jouanne “A Comparison and Assessment of Hybrid Filter Topologies and Control Algorithms” IEEE Power Electronics Specialists Conference, Vol. 2, pp 565-570, 2001

[29] H. Akagi “A medium voltage transformerless AC/DC Power Conversion System Consisting of a Diode Rectifier and a Shunt Hybrid Filter” IAS annual meeting, Vol. 1, pp 78-85, Oct. 2002

[30] C. A. Quinn, N. Mohan, “Active filtering of harmonic currents in three-phase, four-wire systems with three-phase, single-phase nonlinear loads,” in Proc. IEEE APEC’92, pp. 829–836, 1992

[31] P. Enjeti, W. Shireen, P. Packebush, and I. Pitel, “Analysis, design of a new active power filter to cancel neutral current harmonics in three phase four-wire electric distribution systems,” in Conf. Rec. IEEE-IAS Annu. Meeting, Vol. 30, pp. 939–946, Feb.1993

[32] H. Özkaya, O.S. Şentürk, A.M. Hava, “Üç fazlı paralel etkin süzgecin akım denetim yöntemleri” ELECO 2006, Elektrik-Elektronik-Bilgisayar Mühendisliği Sempozyumu, 6-10 Aralık 2006, Bursa, sayfa 121-125

[33] H. Özkaya, O.S. Şentürk, A.M. Hava, “Performance enhancement of discrete time hysteresis current regulators and comparison with linear current regulators for parallel active filters,” IEEE-IEMDC 2007 Conference, Antalya, Turkey, Vol.2, pp. 1282-1287, May 2007

[34] W. Tangtheerajaroonwong, T. Hatada, K. Wada, H. Akagi, “Design of a Transformerless Shunt Hybrid Filter Integrated into a Three Phase Diode Rectifier”, PESC’06, pp. 1-7, June 2006

[35] R. Inzunza, H. Akagi, “A 6.6 kV Transformerless Shunt Hybrid Active Filter for Installation on a Power Distribution System”, IEEE Trans. On Power Electronics, Vol. 20, No. 4, pp. 893-900, July 2005

[36] G. D. Marques, “A Comparison of Active Power Filter Control Methods in Unbalanced and Non-sinusoidal Conditions”, Proceedings of IECON, Vol. 1, pp. 444-449, 1998

[37] S: D. Round, D. M. E. Ingram, “An Evaluation of Techniques for Determining Active Filter Compensating Currents in Unbalanced Systems”, Proc. European Conf. on Power Electronics and Applications, Vol. 4, pp. 767-772, Trondheim, 1997

[38] S. Rechka, E. Ngandui, J. Xu, P. Sicard, “A comparative Study of Harmonic Detection Algorithms for Active Filters and Hybrid Active Filters”, Power Elects. Specialists Conf., Vol. 1, pp. 357-363, 2002

[39] G. W. Chang, T. C. Shee, “A Comparative Study of Active Power Filter Reference Compensation Approaches”, Power Engineering Society Summer Meeting, Vol. 2, pp. 1017-1021, 2002

[40] L. Asiminoaei, F. Blaabjerg, S. Hansen, “Evaluation of Harmonic Detection Methods for Active Power Filter Applications”, Applied Power Elects. Conf. and Expo., Vol. 1, pp. 635-641, 2005

[41] A. M. Massoud, S. J. Finney, B. W. Williams, “Review of Harmonic Current Extraction Techniques for an Active Power Filter”, International Conf. on Harmonics and Quality of Power, Vol. 1, pp. 154-159, 2004

[42] J. M. M. Ortega, M. P. Esteve, M. B. Payan, A. G. Exposito, L. G. Franguelo, “Reference Current Computation Methods for Active Power Filters: Accuracy Assessment in the Frequency Domain”, IEEE Trans. on Power Electronics, Vol. 20, No. 2, pp. 446-456, 2005

[43] H. Akagi, Y. Kanazawa, A. Nabae, “Generalized theory of instantaneous reactive power and its applications,” Transactions of the IEEE Japan, Part B, Vol. 103, No. 7, pp. 483-490, 1983

[44] H. Akagi, Y. Kanazawa, A. Nabae, “Generalized theory of the instantaneous reactive power in three phase circuits,” IPEC’83 International Power Electronics Conference, Tokyo, Japan, pp. 1375-1386, 1983

[45] H. Akagi, Y. Kanazawa, A. Nabae, “Instantaneous reactive power compensator comprising switching devices without energy storage components,” IEEE Trans. Ind. Appl., Vol. 1A-20, No. 3, pp. 625-630, 1984

[46] H. Akagi, E. H. Watanabe, M. Aredes, “Instantaneous Power Theory and Applications to Power Conditioning”, Book IEEE Press, pp. 41-102, 2007

[47] S.Bhattacharya, T.M. Frank, D.M. Divan, and B. Banerjee “Active Filter System Implementation” IEEE Industry Applications Magazine, Vol. 4, pp. 47- 63, 1998

[48] A. Altintas, O. Bingol, “The Evaluation and Comparison of Mathematical Models Utilized in Active Power Filters” Suleyman Demirel Üniversitesi Fen Bilimleri Enstitüsü Dergisi pp 145-150, 2004 (Originally in Turkish)

[49] S. K. Chung, “A Phase Tracking System for Three Phase Utility Interface Inverters”, IEEE Trans. On Power Electronics, Vol. 15, pp. 431-438, May 2000

[50] V. Kaura, V. Blasko, “Operation of a Phase Locked Loop System Under Distorted Utility Conditions”, IEEE Trans. On Industry Applications, Vol. 33, pp. 58-63, Jan./Feb. 1997

[51] L. R. Limongi, R. Bojoi, “New Control Strategy for Hybrid Power Filters Using Sinusoidal Signal Integrators for Current Reference Generation”, IAS Annual Meeting Conference Record, pp. 1636-1643, Sept. 2007

[52] O.Ucak, İ.Kocabas, A.Terciyanlı “Design and Application of a Hybrid Active Power filter with Supply Side Harmonics Isolation”, PCIM Conference, pp. 2008

[53] EMTDC/PSCAD 4.2.0 Professional. A Power System and Power Electronics time domain transient simulation software, MONITOBA-HVDC Research Centre, 2005

[54] Ansoft-Simplorer V7.0. A power electronics simulation software, Ansoft Corporation, 2004

[55] Matlab 6.5. A numerical computation software, Mathworks Inc., 2002

[56] H. Akagi, S. Srianthumrong, Y. Tamai, “Comparisons in Circuit Configuration and Filtering Performance between Hybrid and Pure Shunt Active Filters”, Industry Applications Conference, Vol. 2, pp. 1195-1202, 2003

[57] İ.Kocabas, O.Ucak, A.Terciyanlı, “DSP Based Voltage Source Paralel Active Power Filter Implementation”, Eleco, pp 171-175, 2006 (Originally in Turkish)

[58] “POWEREX [Online],” http//www.infineon.com, last visited on 12/08/2009

[59] “SEMIKRON [Online],” http//www.semikron.com, last visited on 12/08/2009

[60] “INFINEON [Online],” http//www.infineon.com, last visited on 12/08/2009

[61] BHC Capacitors Application Notes TD001-003 pp. 16-26

[62] M. C. Caponet, F. Profumo, R. W. D. Doncker, A. Tenconi, “Low Stray Inductance Bus Bar Design and Construction for Good EMC Performance in Power Electronics Circuits”, IEEE Trans. On Power Electronics, Vol. 17, pp. 225-231, March 2002

[63] AutoCAD 2007. A 2D and 3D design and drawing software, Autodesk

[64] “eZdsp™ F28335 Technical Reference”, Spectrum Digital, Inc. September 2007

[65] “BP7A-L-Series IPM Interface Circuit Reference Design”, Powerex, February 2005

[66] TMS320x28xx, 28xxx Enhance Pulse Width Modulator (ePWM) Module Reference Guide

APPENDIX A

TECHNICAL DATA OF THE POWER STAGE OF THE PROTOTYPE

Table A.1: Maximum Ratings of PM300CLA120 Inverter Part

Symbol	Parameter	Condition	Ratings	Unit
V_{CES}	Collector-Emitter Voltage	V_D=15V, V_{CIN}=15V	1200	V
±IC	Collector Current	T_C=25°C	300	A
±ICp	Collector Current (Peak)	T_C=25°C	600	A
P_C	Collector Dissipation	T_C=25°C (Note-1)	1562	W
T_j	Junction Temperature		-20 ~ + 150	°C

Table A.2: Maximum Ratings of PM300CLA120 Control Part

Symbol	Parameter	Ratings	Unit
V_D	Supply Voltage	1200	V
V_{CIN}	Input Voltage	300	V
V_{FO}	Fault Output Supply Voltage	600	V
I_{FO}	Fault Output Current	1562	mA

Table A.3: Maximum Ratings of PM300CLA120 Total System

Symbol	Parameter	Condition	Ratings	Unit
$V_{CC(PROT)}$	Supply Voltage Protected by SC	V_D=13.5~16.5V, Inverter Part T_j=+125°C Start	800	V
$V_{CC(SURGE)}$	Supply Voltage (Surge)	Applied between: P-N, Surge Voltage	1000	V
T_{stg}	Storage Temperatue		-40 ~ + 125	°C
V_{iso}	Isolation Voltage	60Hz Sinusoidal, Charged Part to Base, AC 1 min	2500	V_{rms}

Table A.4: Maximum Ratings of PM300CLA120
Thermal Resistances

Symbol	Parameter	Condition	Limits			Unit
			Min.	Typ.	Max.	
$R_{th(j-c)Q}$	Junction to Case Thermal Resistances	Inverter IGBT (per 1 element) (Note-1)	-	-	0.08	°C/W
$R_{th(j-c)F}$		Inverter FWD_i (per 1 element) (Note-1)	-	-	0.13	
$R_{th(c-f)}$	Contact Thermal Resistances	Case to fin (per 1 module) Thermal grease applied (Note-1)	-	-	0.014	

(Note-1): T_c measurement point is under the chip.
If you use this value $R_{th(f-}$should be measured just under the chips

Table A.5: Electrical Characteristics of PM300CLA120 Inverter Part

Symbol	Parameter	Condition		Limits			Unit
				Min.	Typ.	Max.	
$V_{CE(SAT)}$	Collector-Emitter Saturation Voltage	V_D=15V, I_C=300A V_{CIN}=0V	T_j=25°C	-	1.8	2.3	V
			T_j=125°C	-	1.9	2.4	
V_{EC}	FWD_i Forward Voltage	-I_C=300A,V_D=15V, V_{CIN}=15V		-	2.8	3.9	V
t_{on}	Switching Time	V_D=15V, V_{CIN}=0V-15V,V_{CC}=600V, I_C=300A, T_j=125°C Inductive Load		0.5	1	2.5	us
t_{rr}				-	0.5	0.8	
$t_{c(on)}$				-	0.4	1	
t_{off}				-	2.3	3.5	
$t_{c(off)}$				-	0.7	1.2	
ICES	Collector-Emitter Cutoff Current	V_{CE}= V_{CES}	T_j=25°C	-	-	1	mA
			T_j=125°C	-	-	10	

Table A.6: Recommended Conditions for Use of PM300CLA120

Symbol	Parameter	Recommended Value	Unit
V_{CC}	Supply Voltage	≤ 800	V
V_D	Control Supply Voltage	15 ± 1.5	V
$V_{CIN(ON)}$	Input ON Voltage	≤ 0.8	V
$V_{CIN(OFF)}$	Input OFF Voltage	≥ 9.0	V
f_{PWM}	PWM Input Frequency	≤ 20	kHz
t_{dead}	Arm Shoot-through Blocking Time	≥ 3.0	us

Table A.7 Technical Specifications of the (ALS30A472NP400) DC Link Capacitor

Capacitance	4700uF -20 +20 %
Rated Voltage	400VDC
Surge Voltage	440VDC
Typical ESR	20.0 mΩ @ 100Hz and 20°C
Typical Z	14.2 mΩ @ 10kHz and 20°C
Leakage Current (mA)	6.0 mA (max.) @ 400VDC
Rated Ripple Current	17.0 A_{rms} @100Hz and 85°C
Temperature Range	-40°C to 85°C
Diameter	77mm
Length	146mm

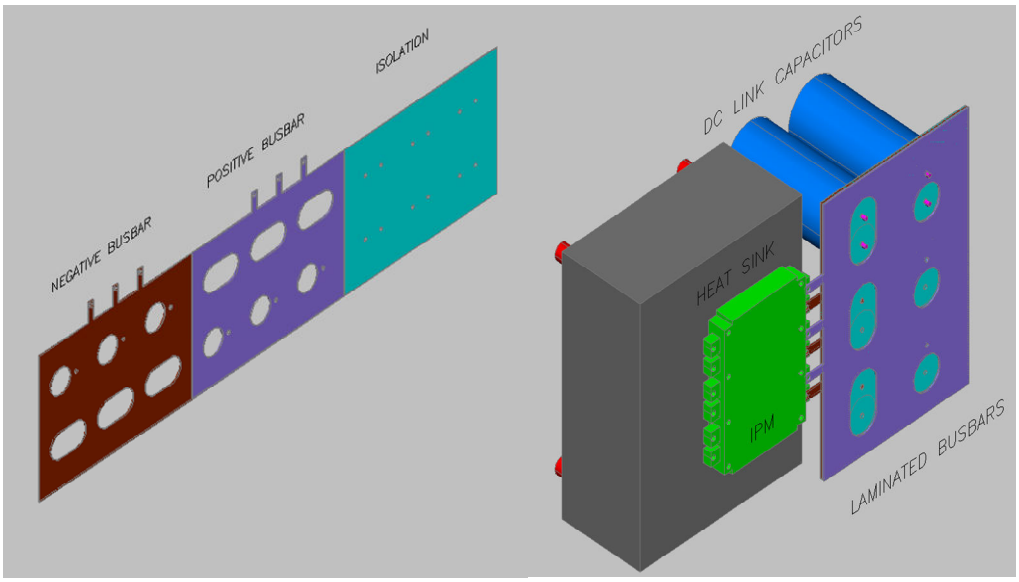

Fig A.1 Laminated Bus Bar Design and the Power Converter

Table A.8: Technical Specifications of the Filter Reactor

Technical Data	
Reactance	365uH
Operating Voltage	400V
Rated Frequency	50 Hz
Design	Iron Core
Insulation Class	F Class
Protection Class	IP00
Phase	3
Operating Current Frequency Spectrum	
50 Hz	45 A
250 Hz	44 A
350 Hz	20 A
550 Hz	15 A
650 Hz	9 A
850 Hz	7 A
950 Hz	4 A
1150 Hz	3 A
1250 Hz	2 A

APPENDIX B

TECHNICAL DATA OF THE COMPONENTS IN THE CONTROL SYSTEM OF THE PROTOTYPE

Table B.1 Technical Data of the CTF-5A AC Current Sensor

Applicable Current	AC 0.01-5Arms
Output Example	AC 1.66mA±1% (5A)
Phase Accuracy	-1.5°±1.0°(5A)
Nominal CT Ratio	3000:1 CT
Inside Diameter	φ10mm Max.
Input Current	100Arms continuous
Open Circuit Protection	7.5V Applicable
Frequency	10Hz-5kHz
Operational Temperature	-10/+50 °C, less than 80%RH
Material of Core	Ferrite
CT Open/Close Capability	Approx. 100 times
Dimension/Weight	26(W)×23(D)×48(H)mm /Approx. 45gs.

Table B.2 Technical Data of the Voltage Transducer LV 25-P

Symbol	Parameter		Value	
I_{PN}	Primary nominal r.m.s. current		10mA	
I_P	Primary current measuring range		0…±14mA	
R_M	Measuring resistance		R_{min}	R_{max}
	with ±12V	@±10mA$_{max}$	30Ω	190 Ω
		@±14mA$_{max}$	30 Ω	100 Ω
	with ±15V	@±10mA$_{max}$	100 Ω	350 Ω
		@±14mA$_{max}$	100 Ω	190 Ω
I_{SN}	Secondary nominal r.m.s current		25mA	
K_N	Convesion ratio		2500:1000	
V_C	Supply voltage (±5%)		±12V..15V	
I_C	Current consumption		10(@±15V)+I_s mA	
V_d	R.m.s. voltage for AC isolation test, 50Hz 1mn		2.5kV	

Table B.3 Technical Specifications of Lambda HWS100-24/A

Nominal Output Voltage	24V
Max. Output Current	4.5 A
Max. Output Power	108W
Efficiency (%)	87
Input Voltage Range	85 ~ 265VAC (47 ~ 63Hz)
Input Current (100/200VAC) (Typ)	1.3/0.65 A
Inrush Current (Typ)	14 A at 100VAC, 28A at 200VAC
PFHC	Built to meet IEC61000-3-2
Power Factor (100/200VAC) (Typ)	0.99/0.95
Output Voltage Range	19.2 ~ 28.8V
Operating Temperature	-10~ +60°C) (-10~ +40°C:100%,+50°C:%60,+60°C:%20)
Operating Humidity	30~90%RH (No dewdrop)
Withstand Voltage	Input- FG : 2kVAC (20mA), Input-Output: 2kVAC (20mA), Output- FG : 500VAC (100mA) for 1min
Isolation Resistance	More than 100MΩ at 25 °C and 70% RH output – FG : 500VDC
Conducted Emission	Built to meet EN55011/EN55022-B, FCC-B, VCCI-B
Radiated Emission	Built to meet EN55011/EN55022-B, FCC-B, VCCI-B
Weight (Typ)	500g
Size (W x H x D)	33 x 82 x 160 (mm)

Table B.4 TMSF28335 Digital Signal Processor Features

Generation	28x Delfino Floating Point Series
CPU	1 C28x
Floating Point Unit (FPU)	Yes
Frequency (MHz)	150
RAM	68 KB
OTP ROM	2 KB
Flash Memory	512 KB
PWM	18 Channel
Analog Digital Conversion (ADC)	16 Channel – 12 Bit
ADC Conversion Time	80 ns
Serial Port Peripherals	3 Serial Communication Interface (SCI) Module 1 SPI Module 2 CAN Module 2 McBSP Module

"Table B.4 Cont'd"

Inter Integrated Circuit (I2C) Bus	1
Timers	3 32Bit CPU Timer, 1 Watchdog Timer
General Purpose Input/Output	88
Core Supply	1.9V
I/O Supply	3.3V
Operating Temperature Range	-40°C to 85°C, -40°C to 125°C
Development Support	ANSI C/C++ Compiler/Assembler/Linker Code Composer Studio IDE DSP/BIOS Digital Motor Control and Digital Power Software Libraries

APPENDIX C

FLOWCHART OF THE DEVELOPED DSP SOFTWARE

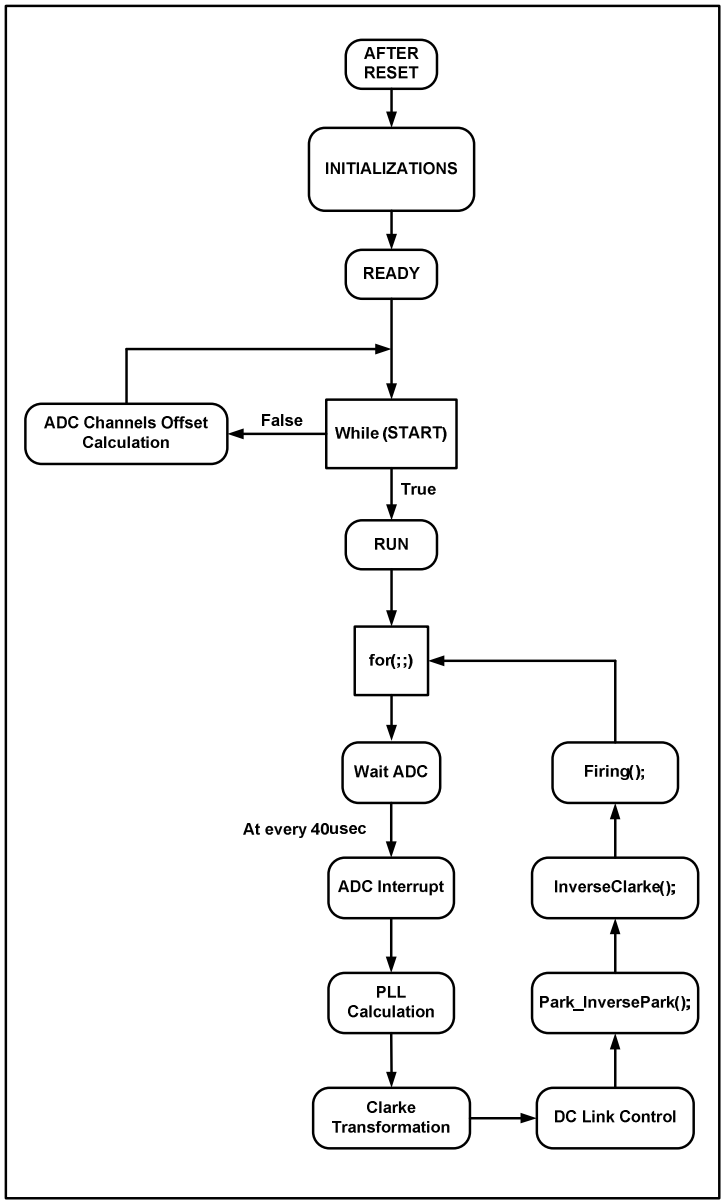

Fig C.1 Flowchart of the Developed DSP Software